March 2019

DEVELOPMENT OF FUNCTIONAL BIOMATERIALS USING PROTEIN BUILDING BLOCKS

Li-Sheng Wang
University of Massachusetts Amherst

DEVELOPMENT OF FUNCTIONAL BIOMATERIALS USING PROTEIN BUILDING BLOCKS

A Dissertation Presented

by

LI-SHENG WANG

Submitted to the Graduate School of the
University of Massachusetts Amherst in partial fulfillment
of the requirements for the degree of

DOCTOR OF PHILOSOPHY

February 2019

Department of Chemistry

DEVELOPMENT OF FUNCTIONAL BIOMATERIALS USING PROTEIN BUILDING BLOCKS

A Dissertation Presented

by

LI-SHENG WANG

Approved as to style and content by:

_____
Vincent M. Rotello, Chair

_____
Michael J. Knapp, Member

_____
Kenneth R. Carter, Member

_____
Alfred J. Crosby, Member

_____
Richard W. Vachet, Department Head
Department of Chemistry

DEDICATION

To my family, friends, Prof. Ming-Yuan Liao, Prof. Ja-An Ho, and mentors whose indispensable guidance and support have helped bring this research to fruition.

ACKNOWLEDGMENTS

First, I would like to thank Professor Vincent M. Rotello for his valuable guidance and mentorship throughout this work. His approach to scientific inquiry and critical thinking have a tremendous influence on my research career. I also would like to acknowledge my committee members, Professor Michael J. Knapp, Professor Kenneth R. Carter, and Professor Alfred J. Crosby for their input and academic support throughout my doctoral studies.

This work could not have been done without the help of the present and past members of the Rotello group. I have truly appreciated the friendly and cooperative environment in the lab. Of particular note, my many thinks go to Bradley Duncan, Brian Creran, Roberto Cao, Ryan Landis, Moumita Ray, Akash Gupta, Yi-Wei Lee, Sanjana Gopalakrishnan, and Rui Huang as you all went above and beyond to ensure our research was a success. I would also want to thank my collaborators, Jiaxin Zhu and Shengkai Li, for their gracious help with our projects. Additionally, I genuinely thank Carol, jms, Bob, Ryan and the rest of the chemistry staff for their support on keep everything going.

Finally, I would like to thank my entire family for their love and support, especially my parents, brother, my girlfriend, as well as my old and new friends. Without your endless understanding and care, I won't be able to finish anything here. Last but not least, I want to express my sincere gratefulness to my previous advisors, Professor Ming-Yuan Liao and Professor Ja-an Annie Ho. I wouldn't even consider pursuing my Ph.D. degree if it wasn't your recommendation and faith in me. Your guidance and supports have and will be a source of continual inspiration for me.

Thank you all.

ABSTRACT

DEVELOPMENT OF FUNCTIONAL BIOMATERIALS USING PROTEIN BUILDING BLOCKS

FEBRUARY 2019

LI-SHENG WANG, B.S., NATIONAL CHI NAN UNIVERSITY

M.S., NATIONAL TSING HUA UNIVERSITY

Ph.D., UNIVERSITY OF MASSACHUSETTS AMHERST

Directed by: Professor Vincent M. Rotello

Proteins have intrinsic molecular properties that are highly useful for materials applications, especially for biomaterials. My research has focused on translating these molecular properties to materials surface behavior. In one approach, I developed a fluorous-based thermal treatment strategy to generate stable thin films from a variety of naturally abundant proteins. The different surface properties generated from the choice of protein were utilized to modulate cell-surface interactions, prevent bacterial adhesions, and control drug loading/release. I have used nanoimprint lithography to generate patterned protein films for cell alignment. Coupling with inkjet printing deposition, I have fabricated mixed protein films with spatial and compositional control. In terms of biomedical applications, I have developed antimicrobial coatings by post-functionalization or loading antibiotics into protein films. Using a high internal phase emulsion template, I have developed a degradable protein-based porous material that showed great versatility for slow release of antimicrobial essential oils. Overall, these examples highlight the potency of using protein building blocks for the development of functional biomaterials.

TABLE OF CONTENTS

Page

LIST OF TABLES

Table Page

LIST OF FIGURES

CHAPTER 1

PROTEIN-BASED MATERIALS

1.1 Introduction

Materials derived from renewable and sustainable resources have gained growing interest due to the rising concerns about the destined depletion of fossil resources and the increasing accumulation of undegradable wastes.[1] Therefore, researchers and scientists have been focusing on exploitation of biomass as an alternative source of energy and raw materials for commercial products.[2,3] Raw materials acquired from agricultural and livestock, such as cellulose, starch, and proteins, are natural polymers with intrinsic and unique properties. Similar to petroleum-based polymers, natural polymers can be employed as sustainable building blocks for constructing functional materials individually or in blends.[4]

Among other natural polymers, proteins have shown great potentials on the development of functional biomaterials due to their structural and functional diversity, biodegradability, and inherent biocompatibility.[5] The development of protein-based materials has been focused on films, adhesives, coatings, plastics, gels, etc.[6] These protein-based materials are especially promising for biomedical applications, such as tissue engineering,[7] drug delivery,[8] and biosensing.[9]

1.2 Proteins

Proteins are nanoscale polyamides, composed of different amino acids that possess a variety of functional groups, including polar, non-polar, aromatic, anionic and cationic.

These functional groups give the amino acids their unique chemical properties. The order in which the amino acids are sequentially arranged is described as the primary structure of the protein. In proteins primary structure, these amino acids are connected through peptide bonds, forming a linear sequence of amino acids with functional groups pointing out from the polyamide backbone (Figure 1). In a protein molecule, secondary structures are formed driven by the supramolecular interactions, including van der Waals, hydrogen bonding, electrostatic, and hydrophobic interaction, of amino acids in the segments of a protein sequence.[10] These individual secondary structures, such as alpha-helix, beta-sheet, and beta-turns, are further assemble into a tertiary structure based on the overall spatial arrangement of the interactions between functional groups that are far apart in the peptide chain, giving the protein an overall structural character such as globular, fibrous, or random coil. These individual protein molecules can further assemble into quaternary structures that are composed of multiple proteins.

Proteins serve a variety of biological functions including cell signaling, enzymatic catalysis, and structural support of tissues. The behavior of the protein is dependent on its tertiary structure. Proteins can be classified into 3 main categories: globular, fibrous, and membrane proteins which correlates with their structures. Globular proteins are primarily water soluble, generally spherical in three-dimensional shape, and can be transporter proteins, antibodies as well as enzymes. Fibrous proteins are stem-like shaped structural biomacromolecules that assemble to form connective tissues which are water insoluble, maintaining tissue integrity, such as muscles, feathers hair and silk. Membrane proteins interact with biological membranes such as the cell's phospholipid bilayer to aid in cellular response to environmental stimuli.

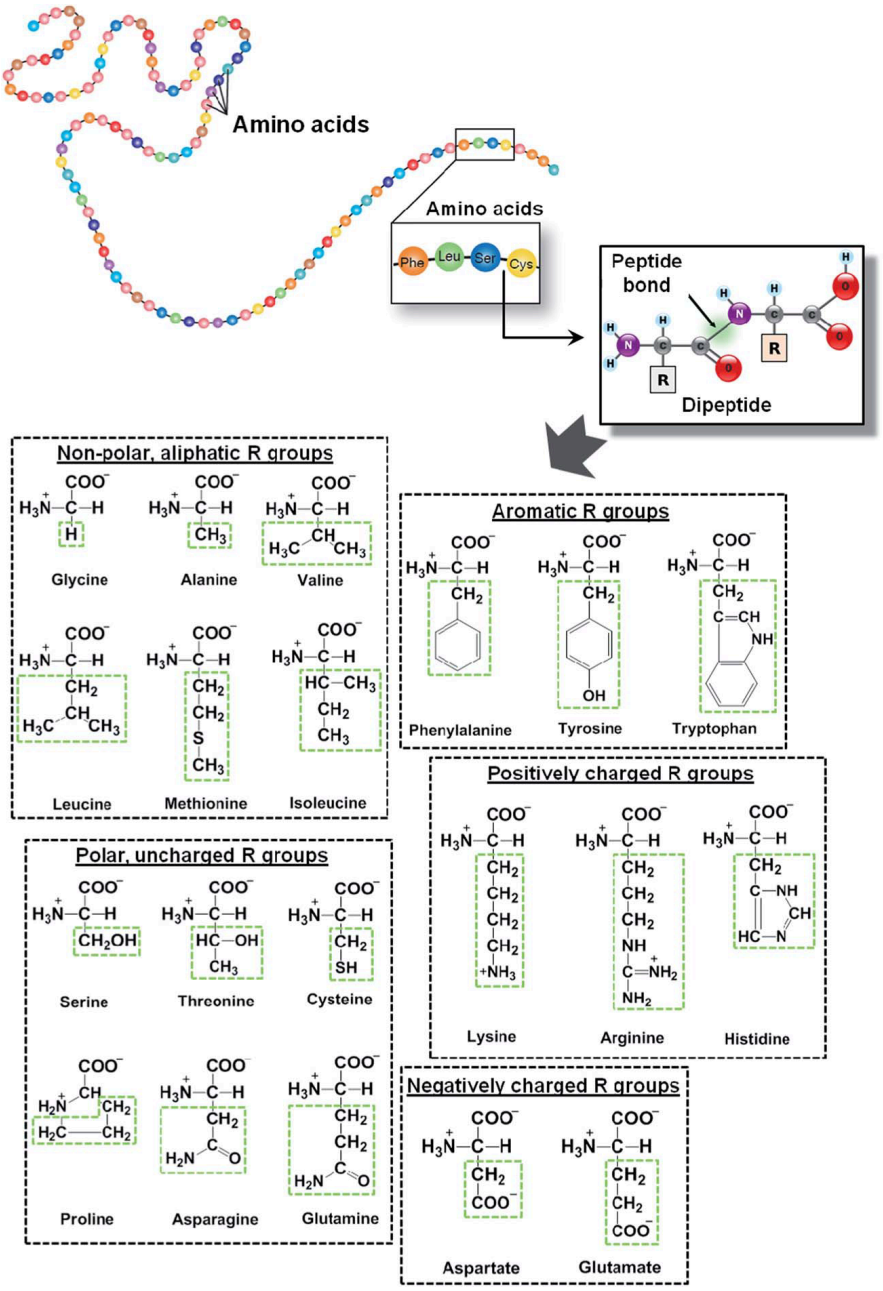

Figure 1.1: Amino acids and peptide bonds. (reproduced from Ref. 9)

1.3 Strategies for constructing protein-based materials

Proteins are Nature's nanoscale building blocks, providing incredible functional and structural diversity.[11] Moreover, proteins are biocompatible and sustainable precursors

for generating functional materials.[12] The vast majority of applications of protein-based materials require stability in aqueous environments.[13] However, current methods for stabilizing protein materials employ either a) denaturing conditions that relinquish the surface properties of the protein;[14] b) use naturally self-assembling proteins that dramatically reduce the variety of proteins that can be used;[15] or c) employ toxic cross-linkers that adversely affect the behavior of protein nanobricks by significantly altering their biocompatibility and/or surface functionality.[16]

1.3.1 Self-assemble protein materials

Proteins that self-assemble in nature (e.g. amyloidogenic,[17] elastin,[18] keratin,[19] silk protein,[20] collagen,[21] and resilin)[22] provide particularly attractive scaffolds, combining biodegradability and biocompatibility in materials comprised entirely of natural precursors. In general, these structural proteins are characterized by long-range ordered molecular secondary structures (e.g. beta-pleated sheets, or triple helices) that arise due to the highly repetitive amino acid sequences within the protein molecule.[23] For example, the primary structure of *B. mori* silk fibroin consists the repeat sequence $[GAGAGS]_n$.[24] The hydrophobic domains of elastin are rich in non-polar amino acids, with common repeating motifs of $[GVGVP]_n$.[25] These structural features promote self-assembly, and mechanical properties, and thus materials-related functions in nature.

The process for preparing structural protein-based materials usually involve extraction/dissolution, following by reprocessing into the desired format (Figure 1.2).[26] For example, the transition of silk fibroin molecules from the solution state to beta sheet crystalline state can be induced with methanol, heat, pH, vortexing or sonication.[27] These

straightforward fabrication process has made self-assemble protein-based materials especially promising materials for constructing scaffolds for interfacing with cells for tissue engineering[28] and wound healing applications.[29] For example, collagen- and gelatin-based scaffolds have been employed for culturing retinal epithelial cells,[30] and cross-weaved silk fibres have been co-cultured with fibroblasts for making artificial skin.[31]

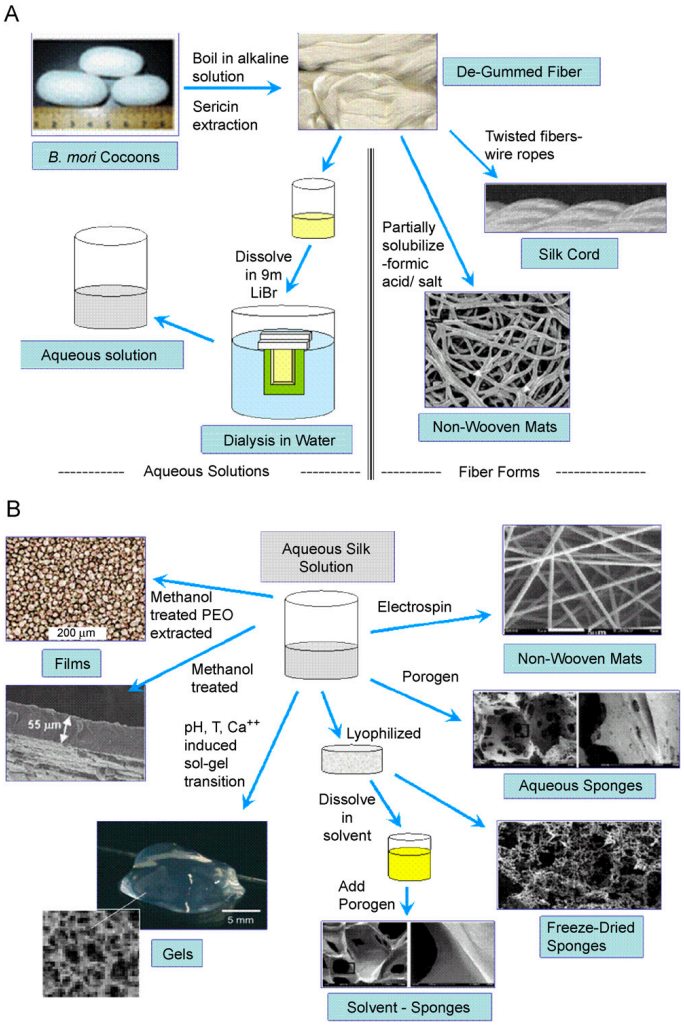

Figure 1.2: Silk fibroin is purified from sericins via boiling in an alkaline solution. The de-gummed or purified silk fibers can be processed for preparation of other material morphologies (reproduced from Ref. 26)

1.3.2 Chemical cross-linked protein materials

While structural proteins naturally self-assemble into stable materials, most proteins-based materials are not stable under aqueous solutions, meaning susceptible to water dissolution. This instability limits the range of precursors and hence the ultimate materials properties for current protein-based materials. One strategy for overcoming this restriction is through use of covalent cross-linkers, including glutaraldehyde, [32] formaldehyde,[33] and glyoxal.[34] These cross-linkers chemically connect individual protein molecules through chemical bonding with protein side chains, resulting in stable protein-based materials. For example, formaldehyde is the simplest of crosslinking agents due to its widest reaction specificity toward amino acids, including lysine, cysteine, tyrosine, histidine, tryptophan and arginine.[35]

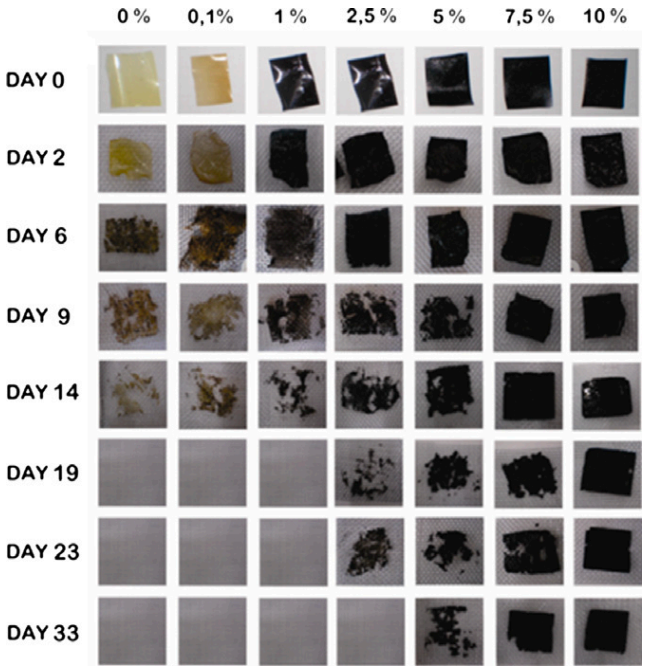

Figure 1.3: Biodegradability of soy protein isolate films crosslinked with different percentage of cross-linkers (reproduced from Ref. 36)

Chemical crosslinking provides stability and mechanical property to protein-based materials (Figure 1.3).[36] For example, Ramakrishna's group demonstrated improved thermal stability and mechanical property of gelatin nanofibers after expose to glutaraldehyde vapor for 3 days.[37] Ustunol and Mert showed that the solubility of whey protein film decreased with increased tensile strength and water vapor permeability after crosslinking.[38] Nevertheless, these treatments can compromise the behavior of protein materials by altering the side chain functionality on protein building blocks. Moreover, the residual crosslinkers or those released from the hydrolysis of film can cause toxic effects.[39]

1.3.3 Heat cured protein materials

Heat curing of proteins is a straightforward technique to generate water-stable materials.[40] For example, Su's group used heat-stabilized albumen film as insulator to fabricate a bio-based memristor.[41] The secondary structure of protein is fairly sensitive to thermal stress,[42] hence increasing temperature can result in protein unfolding, consequently inducing denaturation, aggregation and gelation.[43] This denaturation process facilitates the physical crosslinking of water-soluble protein building blocks, forming complexed interconnecting networks (Figure 1.4).[44] Many approaches have used elevated temperatures to form soy,[45] wheat gluten,[46] and whey protein films.[47] However, the temperature of the treatment greatly affects the stability of the protein films, and can lead to unwanted chemical reactions such as the Maillard reaction.[48] In addition, heat curing often results in significantly denatured protein surfaces, altering the proteins native properties of the final products.

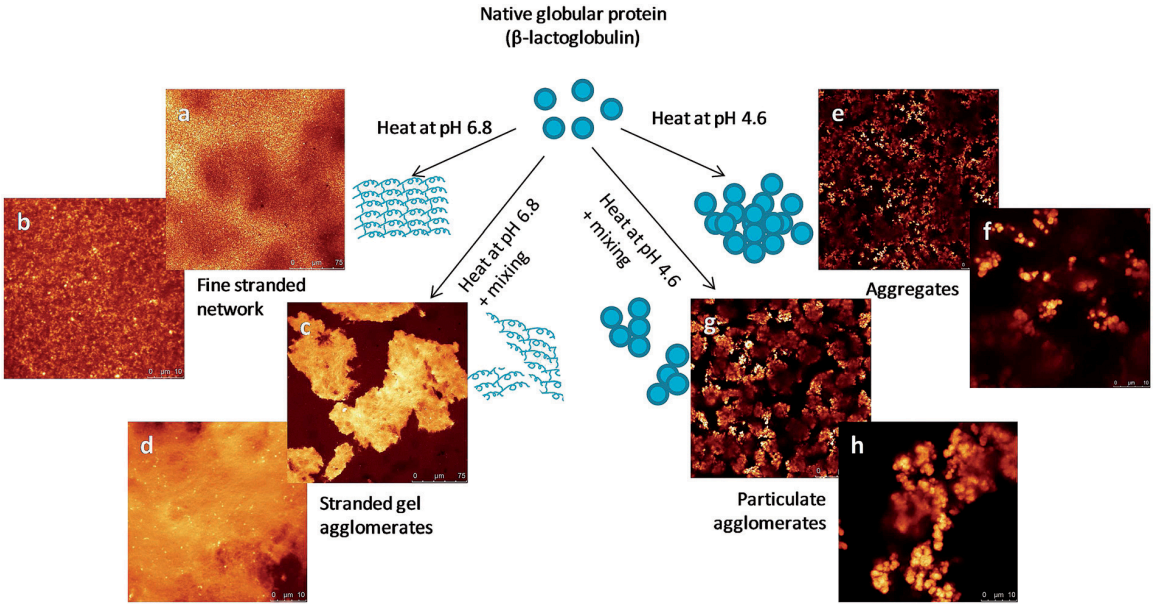

Figure 1.4: Protein unfolding, network formation and aggregation resulting in different structures of gels formed at different pH with or without shear (reproduced from Ref.44)

1.4 Polymerized high internal phase emulsions (PolyHIPEs)

PolyHIPEs are emulsion-templated porous polymers synthesized within high internal phase emulsions (HIPEs).[49] HIPEs are highly concentrated, viscous, paste-like emulsions in which the internal phase constitutes more than 75% of the total volume.[50] By polymerizing the external phase of HIPEs, a hierarchical porous structure can be obtained with voids resulted from the emulsion templates and small interconnecting windows formed between adjacent emulsion droplets (Figure 1.5).[51] The formation of polyHIPEs usually require high quantity of surfactants and monomer/crosslinker in external phase.[52] The most widely investigated polyHIPE material is polystyrene fabricated using water-in-oil (W/O) HIPEs. [53] Other hydrophobic monomers have also been used to create polyHIPEs, such as methacrylate[54] and divinylbenzye.[55] On the other hand, hydrophilic polyHIPEs can be prepared from oil-in-water (O/W) HIPEs.[56] For example, using paraffin

as internal phase and the acrylamide monomer in external phase can be polymerized under UV irradiation with the presence of photoinitiator.[57]

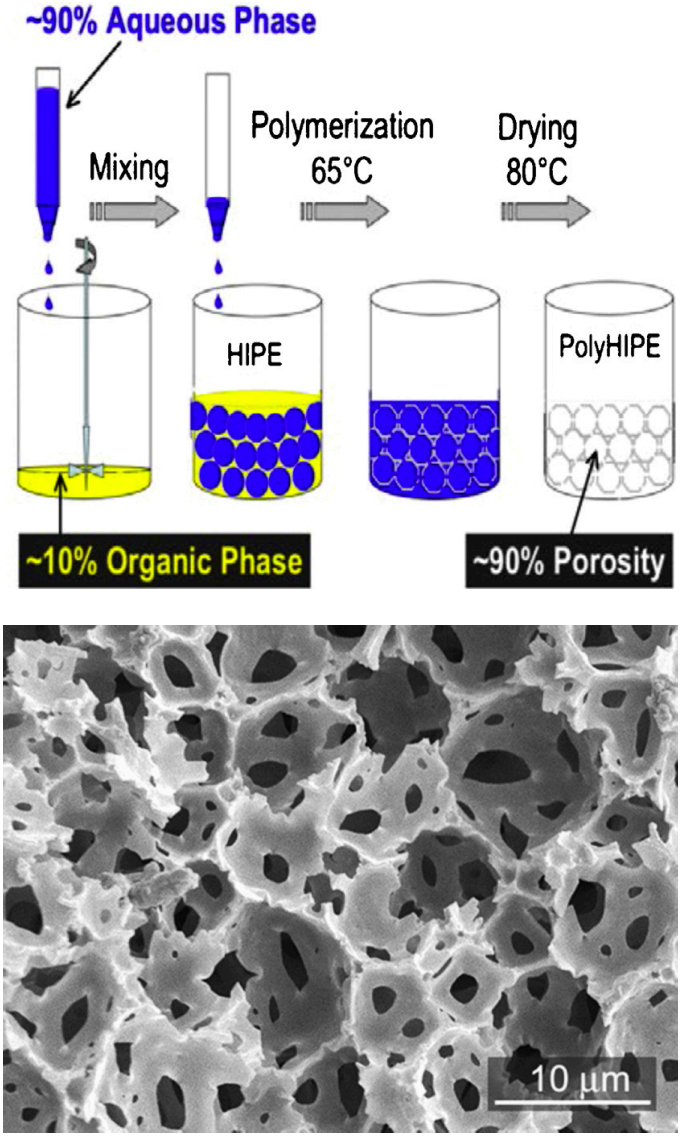

Figure 1.5: (top) Schematic illustration of HIPE formation and polyHIPE synthesis. (bottom) A typical porous polyHIPE structure observed under scanning electron microscopy (reproduced from Ref. 51)

1.5 Dissertation overview

This thesis highlights the strategy of using protein as building blocks to create functional biomaterials. The research described herein will focus on the translating of

proteins unique properties into materials surface functionalities. Chapter 2 describes the development of a universal protein film stabilization strategy using nanoimprint lithography (NIL). The fluorous environment provided by NIL process generated stable patterned protein films that retain the surface functionality of native proteins, including hydrophilicity, degradability, surface charges and zwitterionic properties. Chapter 3 describes a facile approach to generate antimicrobial coatings with both biocidal and antifouling properties using chlorinated protein films. Chapter 4 expands the tunability of cell-surface interactions of the individual protein films by coupling with inkjet printing deposition technique to generate customizable surfaces with spatial and compositional control. Chapter 5 provides an approach to fabricate functional protein films using a fluorous media, which expands the applications of such protein films to 3D substrates. Chapter 6 discusses the electrostatic interaction of charged molecules and protein coatings and their application for the development of antimicrobial drug-eluting coatings. Finally, Chapter 7 describes the generation of a biodegradable porous scaffold via templating polymerization of protein and essential oils.

1.6 References

(1) H. Sardon, A. P. Dove, *Science* **2018**, *360*, 380 LP.

(2) Z. Al-Hamamre, M. Saidan, M. Hararah, K. Rawajfeh, H. E. Alkhasawneh, M. Al-Shannag, *Renew. Sustain. Energy Rev.* **2017**, *67*, 295.

(3) L. Scheiterle, A. Ulmer, R. Birner, A. Pyka, *J. Clean. Prod.* **2018**, *172*, 3851.

(4) A. K. Mohanty, M. Misra, L. T. Drzal, *J. Polym. Environ.* **2002**, *10*, 19.

(5) K. H. Smith, E. Tejeda-Montes, M. Poch, A. Mata, *Chem. Soc. Rev.* **2011**, *40*, 4563.

(6) X. Hu, P. Cebe, A. S. Weiss, F. Omenetto, D. L. Kaplan, *Mater. Today* **2012**, *15*, 208.

(7) M. Li, M. J. Mondrinos, M. R. Gandhi, F. K. Ko, A. S. Weiss, P. I. Lelkes, *Biomaterials* **2005**, *26*, 5999.

(8) S. Hofmann, C. T. Wong Po Foo, F. Rossetti, M. Textor, G. Vunjak-Novakovic, D. L. Kaplan, H. P. Merkle, L. Meinel, *J. Control. Release* **2006**, *111*, 219.

(9) H. Tao, M. A. Brenckle, M. Yang, J. Zhang, M. Liu, S. M. Siebert, R. D. Averitt, M. S. Mannoor, M. C. McAlpine, J. A. Rogers, D. L. Kaplan, F. G. Omenetto, *Adv. Mater.* **2012**, *24*, 1067.

(10) B. Rost, C. Sander, *J. Mol. Biol.* **1993**, *232*, 584.

(11) N. H. C. S. Silva, C. Vilela, I. M. Marrucho, C. S. R. Freire, C. Pascoal Neto, A. J. D. Silvestre, *J. Mater. Chem. B* **2014**, *2*, 3715.

(12) L. Xiao, S. Liu, D. Yao, Z. Ding, Z. Fan, Q. Lu, D. L. Kaplan, *Biomacromolecules* **2017**, *18*, 2073.

(13) M. T. Cicerone, M. J. Pikal, K. K. Qian, *Adv. Drug Deliv. Rev.* **2015**, *93*, 14.

(14) M. B. Pérez-Gago, P. Nadaud, J. M. Krochta, *J. Food Sci.* **2006**, *64*, 1034.

(15) G. H. Altman, F. Diaz, C. Jakuba, T. Calabro, R. L. Horan, J. Chen, H. Lu, J. Richmond, D. L. Kaplan, *Biomaterials* **2003**, *24*, 401.

(16) P. J. Nowatzki, D. A. Tirrell, *Biomaterials* **2004**, *25*, 1261.

(17) T. P. J. Knowles, T. W. Oppenheim, A. K. Buell, D. Y. Chirgadze, M. E. Welland, *Nat. Nanotechnol.* **2010**, *5*, 204.

(18) J. Skopinska-Wisniewska, A. Sionkowska, A. Kaminska, A. Kaznica, R. Jachimiak, T. Drewa, *Appl. Surf. Sci.* **2009**, *255*, 8286.

(19) C. K. Hong, R. P. Wool, *J. Appl. Polym. Sci.* **2005**, *95*, 1524.

(20) J. G. Hardy, T. R. Scheibel, *Prog. Polym. Sci.* **2010**, *35*, 1093.

(21) K. Panduranga Rao, *J. Biomater. Sci. Polym. Ed.* **1996**, *7*, 623.

(22) J. N. Renner, K. M. Cherry, R. S.-C. Su, J. C. Liu, *Biomacromolecules* **2012**, *13*, 3678.

(23) Y. Jang, J. A. Champion, *Acc. Chem. Res.* **2016**, *49*, 2188.

(24) H.-J. Jin, D. L. Kaplan, *Nature* **2003**, *424*, 1057.

(25) J. F. Almine, D. V Bax, S. M. Mithieux, L. Nivison-Smith, J. Rnjak, A. Waterhouse, S. G. Wise, A. S. Weiss, *Chem. Soc. Rev.* **2010**, *39*, 3371.

(26) C. Vepari, D. L. Kaplan, *Prog. Polym. Sci.* **2007**, *32*, 991.

(27) B. Kundu, N. E. Kurland, V. K. Yadavalli, S. C. Kundu, *Int. J. Biol. Macromol.* **2014**, *70*, 70.

(28) J. M. Zuidema, C. J. Rivet, R. J. Gilbert, F. A. Morrison, *J. Biomed. Mater. Res. Part B Appl. Biomater.* **2013**, *102*, 1063.

(29) A. Schneider, X. Y. Wang, D. L. Kaplan, J. A. Garlick, C. Egles, *Acta Biomater.* **2009**, *5*, 2570.

(30) S. R. Hynes, E. B. Lavik, *Graefe's Arch. Clin. Exp. Ophthalmol.* **2010**, *248*, 763.

(31) H. Wendt, A. Hillmer, K. Reimers, J. W. Kuhbier, F. Schäfer-Nolte, C. Allmeling, C. Kasper, P. M. Vogt, *PLoS One* **2011**, *6*, e21833.

(32) Y. Wang, X. Mo, X. S. Sun, D. Wang, *J. Appl. Polym. Sci.* **2007**, *104*, 130.

(33) P. Hernández-Muñoz, A. López-Rubio, J. M. Lagarón, R. Gavara, *Biomacromolecules* **2004**, *5*, 415.

(34) C. Marquié, *J. Agric. Food Chem.* **2001**, *49*, 4676.

(35) J. Zink, T. Wyrobnik, T. Prinz, M. Schmid, *Physical, Chemical and Biochemical Modifications of Protein-Based Films and Coatings: An Extensive Review*, **2016**.

(36) A. González, M. C. Strumia, C. I. Alvarez Igarzabal, *J. Food Eng.* **2011**, *106*, 331.

(37) Y. Z. Zhang, J. Venugopal, Z.-M. Huang, C. T. Lim, S. Ramakrishna, *Polymer* **2006**, *47*, 2911.

(38) Z. Ustunol, B. mert, *J. Food Sci.* **2006**, *69*, FEP129.

(39) S. Matsuda, H. Iwata, N. Se, Y. Ikada, *J. Biomed. Mater. Res.* **1999**, *45*, 20.

(40) A. H. Clark, D. H. P. Sanuderson, A. Suggett, *Int. J. Pept. Protein Res.* **2018**, *17*, 353.

(41) Y.-C. Chen, H.-C. Yu, C.-Y. Huang, W.-L. Chung, S.-L. Wu, Y.-K. Su, *Sci. Rep.* **2015**, *5*, 10022.

(42) X. L. QI, C. HOLT, D. MCNULTY, D. T. CLARKE, S. BROWNLOW, G. R. JONES, *Biochem. J.* **1997**, *324*, 341 LP.

(43) C. Le Bon, T. Nicolai, D. Durand, *Macromolecules* **1999**, *32*, 6120.

(44) T. K. Singh, S. K. Øiseth, L. Lundin, L. Day, *Food Funct.* **2014**, *5*, 2686.

(45) N. Rangavajhyala, V. Ghorpade, M. Hanna, *J. Agric. Food Chem.* **1997**, *45*, 4204.

(46) V. Micard, R. Belamri, M.-H. Morel, S. Guilbert, *J. Agric. Food Chem.* **2000**, *48*, 2948.

(47) K. S. MILLER, M. T. CHIANG, J. M. KROCHTA, *J. Food Sci.* **2006**, *62*, 1189.

(48) P. Hernández-Muñoz, R. Villalobos, A. Chiralt, *Food Hydrocoll.* **2004**, *18*, 647.

(49) M. S. Silverstein, *Polymer* **2014**, *55*, 304.

(50) C. F. Welch, G. D. Rose, D. Malotky, S. T. Eckersley, *Langmuir* **2006**, *22*, 1544.

(51) M. S. Silverstein, *Prog. Polym. Sci.* **2014**, *39*, 199.

(52) L. L. C. Wong, P. M. Baiz Villafranca, A. Menner, A. Bismarck, *Langmuir* **2013**, *29*, 5952.

(53) X. Yang, L. Tan, L. Xia, C. D. Wood, B. Tan, *Macromol. Rapid Commun.* **2015**, *36*, 1553.

(54) N. R. Cameron, D. C. Sherrington, *J. Mater. Chem.* **1997**, *7*, 2209.

(55) A. Barbetta, N. R. Cameron, *Macromolecules* **2004**, *37*, 3188.

(56) P. Krajnc, D. Štefanec, I. Pulko, *Macromol. Rapid Commun.* **2005**, *26*, 1289.

(57) X. Fan, S. Zhang, Y. Zhu, J. Chen, *RSC Adv.* **2018**, *8*, 10141.

CHAPTER 2

FABRICATION OF ROBUST PROTEIN FILMS USING NANOIMPRINT LITHOGRAPHY

2.1 Introduction

Protein-derived materials provide an inherently biocompatible and sustainable platform for the generation of functional materials[1,2]. Thin films comprised of proteins have been used for a variety of applications such as lithographic resists[3], food packaging[4], drug delivery[5,6], sensors[7,8], and tissue engineering[9,10]. Proteins make attractive precursors to manufacture functional surfaces due to their aqueous processability and minimal environmental impact[11]. The intrinsic structural and functional diversity of proteins provides a tool for controlling the properties of protein-based materials [12].

Resistance to aqueous degradation of protein films is crucial for most applications[13]. Methods to produce stable protein films are currently limited to two main strategies: using naturally self-assembling proteins or using crosslinkers. Naturally assembling proteins are promising materials to generate robust films[14,15, 16]. Kaplan *et al.* have used the β-sheet rich silk fibroin protein as a building block to assemble biocompatible structures[17]. By controlling the processing conditions used for the film fabrication, the degradation rates of the subsequent films could be modulated[18]. A recent extension of this work created bio-integrated electronics by tuning the degradation profile of the silk-based construct[19], with post-functionalization providing a potential strategy for diversifying film properties [20]. Covalently crosslinking of proteins into polymeric complexes allows a broader palette of proteins to be employed[21,22]. For example, Taylor *et al.* have used formaldehyde to crosslink kafirin protein microparticles together into water

stable films[23]. These kafirin films demonstrated enhanced structural stability and altered susceptibilities to enzymatic degradation. However, unreacted additives retained in protein films can adversely affect the final behavior of protein films[24,25]. Current methods using extensive heat treatment to crosslink endogenous protein also cause unwanted side reactions[26].

We demonstrate here a facile nanoimprint lithography (NIL) based method for the fabrication of stable, patterned protein films. The thermal NIL process employed in our approach uses precisely controlled temperature and pressure to mold thermoplastic materials[27] in a scalable fashion[28,29]. During the nanoimprinting process, heat and pressure pack exposed peptide side chains into robust interdigitated non-covalent networks. This process is general in terms of protein building block, as demonstrated through the imprinting of proteins with widely differing structures. Significantly, the imprinted proteins retain much of their native structure after the imprinting process. Through parametric variation of temperature and pressure we can further control the stability and biodegradability of the films. The utility of these films as biomaterials is demonstrated through regulation of cellular adhesion through choice of protein precursor, with the nanostructures of these materials dictating cell orientation.

2.2 Results and discussion

Three model proteins featuring widely differing sizes and charges were chosen to demonstrate the versatility of NIL film generation: bovine serum albumin (BSA), hemoglobin (Hemo), and lysozyme (Lyso). Protein films were generated according to the method depicted in Fig. 2.1a. Briefly, 10 % w/w aqueous solutions of protein were filtered and spin cast onto plasma cleaned substrates. The generated films were around 200 nm in

thickness as determined by ellipsometry and confirmed by atomic force microscopy. (Fig. 2.1b,c)

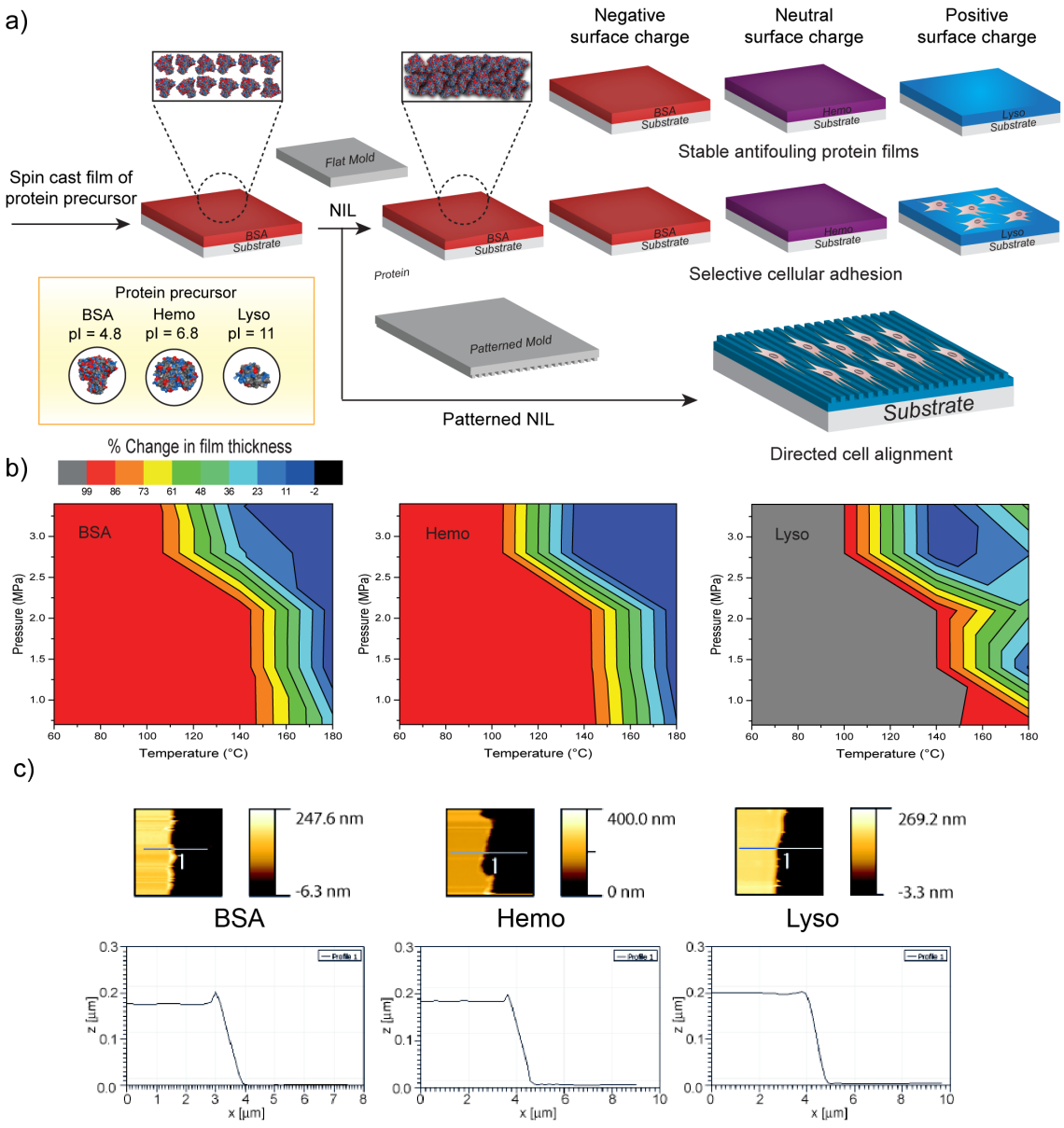

Figure 2.1: Method and conditions used for imprinted protein film fabrication. a) Proteins were spin-cast and then embossed to generate planar and contoured surfaces for different applications. b) Plots showing the effect of pressure and temperature on film stability in water. Films were washed for 1 min with water and the thickness measured by using ellipsometry after drying. c) AFM images and cross-sections of scratched protein films.

NIL conditions were parametrically varied to determine the factors influenced stability of the imprinted protein films. The stabilities of the films were determined by measuring thickness changes after washing with water (Fig. 2.1b). The results indicate that both pressure and heat are required for generating stable protein films. While substantial variation is observed in the heatmaps, stable films can be generated from all three proteins with temperatures greater than 140 °C and pressure of 2.8 MPa.

The secondary structure of the individual protein components within the films was characterized before and after processing using circular dichroism (CD) spectroscopy (Fig. 2.2).[30] From the spectra it is clear that there is substantial retention of secondary structure, indicating the absence of gross structural changes upon imprinting. Given the general retention of protein structure, we next explored the mechanism of film stabilization. Treatment of the films with 2-mercaptoethanol did not disrupt the films, ruling out interprotein disulfide as the stabilizing factor. In contrast, treatment with detergent dissolved the films, indicating that interprotein hydrophobic interactions between exposed side chains provide the observed stability of the film to aqueous media (Fig. 2.3a).

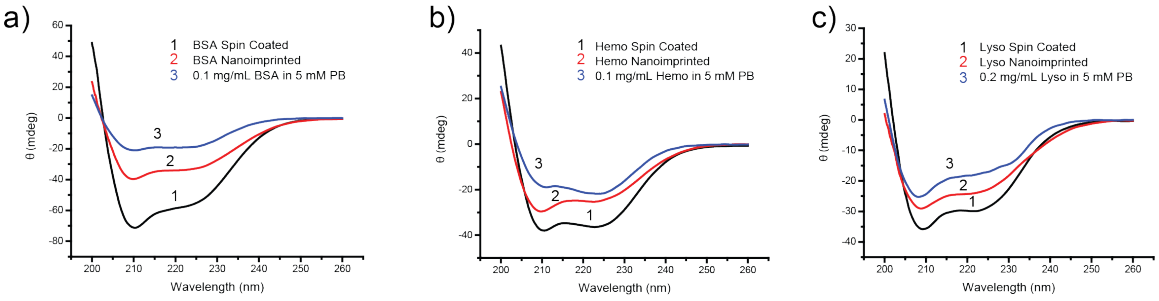

Figure 2.2: Structural characterization of protein films. a) CD spectra of BSA. b) CD spectra of Hemo. c) CD spectra of Lyso. The individual proteins in phosphate buffer are also shown for comparison.

We next focused on the potential utility of these materials as biomaterials. Film stability is an important issue for all applications, with stability required for many

applications and degradability useful for controlled release applications. We first explored the biodegradability of the protein films using trypsin as a model protease. After incubating in 0.01 % trypsin solution for 24 hours, all films imprinted at 150 °C were degraded (Figure 2.3b), making these films promising candidates for controlled release. BSA and Hemo films fabricated at 180 °C, however, showed resistance to the protease making them suitable for a wide range of applications.

Resistance to biofouling is an important characteristic for both implantable devices and for *ex vivo* applications. We evaluated biocompatibility of our films by incubating films in 10 % serum solutions for 48 hrs and then measuring the film thickness by ellipsometry. As shown in Figure. 2.3c, there were no significant changes in film thickness, indicating films are both stable to serum conditions and resist non-specific protein adsorption.

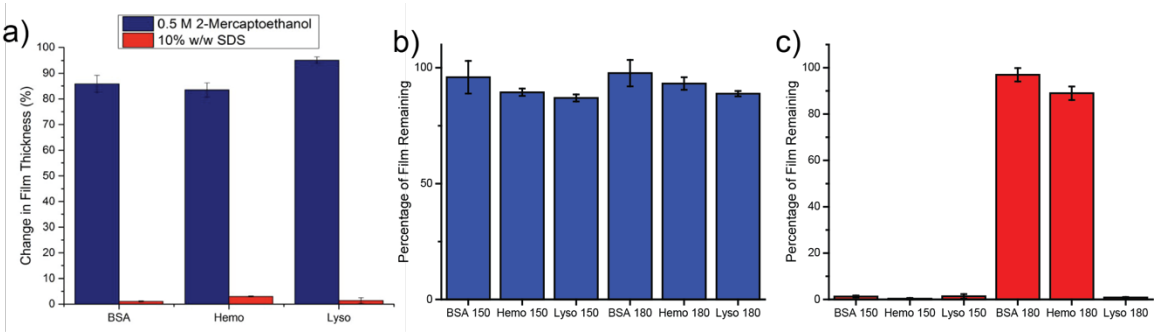

Figure 2.3: Thickness change in protein films measured by ellipsometry after a) 48 hours incubation in 0.5 M 2-mercaptoethanol and 10% sodium dodecyl sulfate (SDS), and b) in 10% serum solution. c) Thickness change in protein films after 24 hrs of incubation in 0.01 % trypsin solution.

The retention of protein structure in the imprinted films implied that the choice of protein could be used to dictate the charge of the resulting surfaces, an important tool for numerous applications. Kelvin probe force microscopy (KPFM) was used to measure the local work function difference between the metallized probe (Pt) and the protein surfaces.

Figure 2.4a shows histograms of measured surface potential contrast (SPC) relative to the evaporated gold supporting substrate. As expected based on precursor protein charge, the BSA surfaces present a negative surface potential, while the Lyso films possesses positive surface potential. Hemo showed a near neutral potential, consistent with its pI value. The retention of charge was further probed through charge-selective adhesion of positively charged quantum dots (Figure 2.4b), supporting the surface charge differences established by KPFM translation into functional control of adhesion.

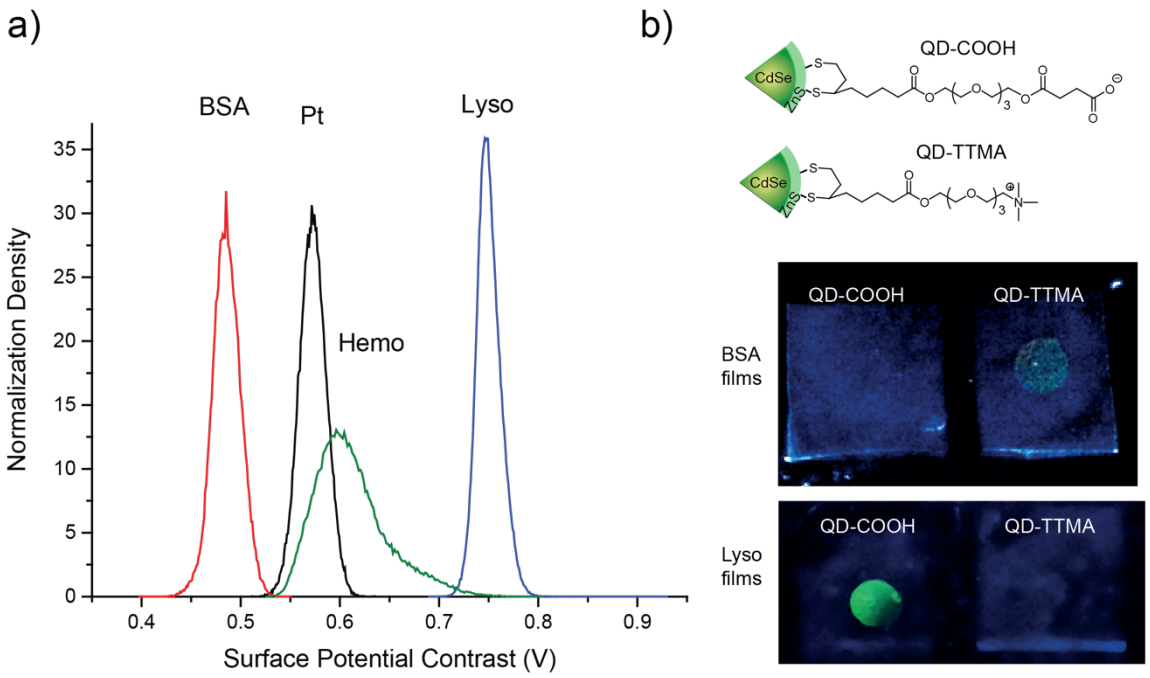

Figure 2.4: a) Surface potential of individual proteins films as determined by Kelvin probe force microscopy (KPFM) and b) charged QD adhesion. 10 µL of 1 µM QD probes were drooped and incubated for 15 mins before washing.

Previous studies have demonstrated that charged molecules on surfaces are important for directing cellular adhesion, with more efficient attachment observed with positively charged surfaces.[31] Given the differing charges of the precursor proteins, our expectation is that the interactions with cells would likewise vary. To test this hypothesis, NIH3T3 fibroblast cells were seeded onto protein films for 2 days. After being washed by

PBS, the cells were fixed and stained with Calcein-AM. Fluorescence microscopy images (Figure 2.5) show that films made from negatively charged BSA and neutral Hemo cells had limited adhesion on films fabricated at 150 ºC while the films fabricated at 180 ºC demonstrated no adhesion. In contrast, Lyso films provided excellent adhesion at both processing temperatures. These reveal that the cytophilic and cytophobic properties can be tuned by both choice of protein precursor and imprinting conditions.

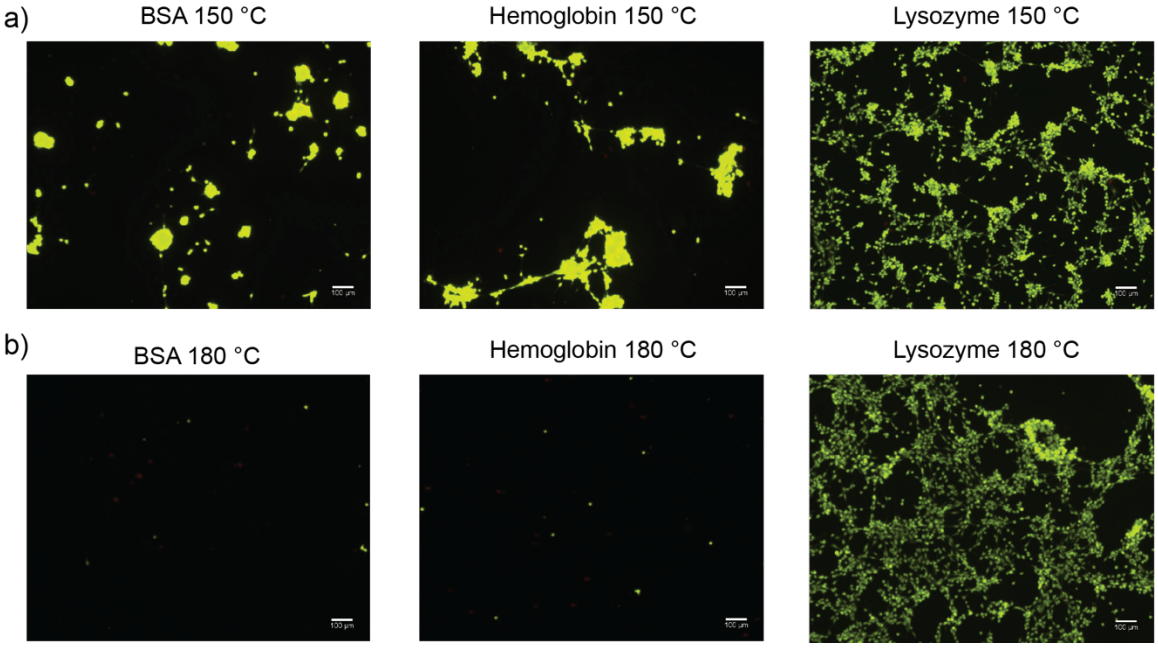

Figure 2.5: Cellular adhesion to protein films. Adhered cells on protein films generated at a) 150 °C and b) 180 °C were stained with calcein-AM after 48 hours. Scale bars were 100 μm.

The NIL process used in our method provides direct access to nanoscale pattering that can be used to dictate cellular alignment. Based on the cellular adhesion studies, Lyso was chosen to investigate prospective patterning of the films. As shown in Figure 2.6a, the Lyso film was readily patterned according to the 300 nm grooved pattern on the master mold. Next, NIH3T3 fibroblast cells were then cultured on the patterned film. Cells were fixed, stained with phalloidin to visualize actin filaments, and alignments measured using

microscopy. Figure. 2.6b shows a majority of the cells aligned with the nanoscale pattern. The high degree of alignment taken together with homogeneous spread of the cytosketeton F-actin fibers demonstrate that the patterned protein films can effectively direct cellular growth.

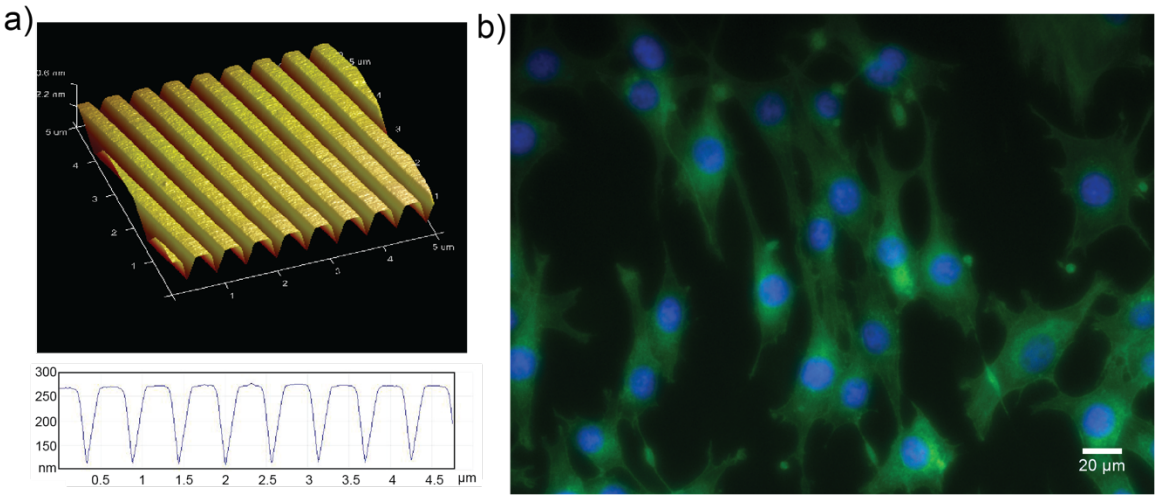

Figure 2.6: Cell culture adhesion and cellular alignment with patterned surfaces. a) 3D atomic force microscopy image of the Lyso film generated with a patterned master mold. b) Fluorescence micrography of fibroblast cells cultured on the patterned Lyso film. Cell were stained with Hoechast 33342 and phalloidin.

2.3 Conclusion

In summary, we have demonstrated that the thermal NIL process generates water-stable films from a range of precursor proteins. These films are generated without additives and retain substantial native protein structure, which renders them biocompatible and zwitterionic. The films also retain physical properties of the precursor proteins, allowing surface charge and stability to be tuned by choice of precursor protein and processing conditions. This bottom-up method provides a platform for using the enormous variety of proteins to generate films with a commensurately vast range of properties. These films

should find use in a broad range of applications ranging from biomedicine through sustainable materials for consumer and industrial applications.

2.4 Experimental methods

2.4.1 Materials

BSA, Hemo, and Lyso were purchased from Fisher Scientific and used without further purification. Silica wafers were purchased from WRS Materials. Quartz microscopy slides were purchased from Electron Microscopy Sciences.

2.4.2 Film Preparation

Protein solutions were prepared by dissolving 10 % w/w solutions of protein in MilliQ water and filtered by using a 0.22 μm filter, following by being spin-coated at 3000 rpm for 60 s onto an oxygen plasma cleaned silicon substrate, yielding a thin film of protein.

2.4.3 Nanoimprint Lithography (NIL)

Nanoimprinting of protein films was performed by using a Nanonex NX-2000 nanoimprinter with silicon molds. Imprinting was performed at various temperatures and pressures for 5 min. A silicon NIL mold (line width 303 nm, period 606 nm, and groove depth 190 nm) from Lightsmyth Technologies was used in the cell patterning. All molds were treated with heptadecafluoro-1,1,2,2-(tetrahydrodecyl)dimethyl-chlorosilane at 80 °C for 2 days in a vacuum chamber.

2.4.4 Cell Culture and cell adhesion

Mouse fibroblast cells 3T3 (ATCC CRL-1658) were cultured in Dulbecco's modified Eagle's medium (DMEM; ATCC 30-2002) supplemented with 10% bovine calf serum (ATCC 30-2030) and 1 % antibiotics in T75 flasks. Cells were maintained at 37 °C

in a humidified atmosphere of 5 % CO_2 and were sub-cultured once in 4 days. For cell adhesion studies, 3T3 cells grown in T75 flasks were washed with phosphate buffered saline (PBS), trypsinized with 1X trypsin and collected in DMEM media. Cells were centrifuged and were re-suspended in fresh DMEM media and counted by using a hemocytometer. Protein film coated surfaces were placed in a six-well plate where 3T3 cells were added to each well (100000 cells/well) and incubated for 48 h at 37 °C in a humidified atmosphere of 5 % CO_2. Following incubation, cells were washed with phosphate-buffered saline (PBS) three times and incubated with calcein AM (Biotium Inc, 80011-2) and propidium iodide (Invitrogen) in PBS (final concentration 3 μM each) for 30 min. Fluorescence microscopy images were taken by using an Olympus IX51 microscope to visualize the adhered live (Calcein AM stained, green) and dead cell (PI stained, red) population in each surface.

2.4.5 Cell Alignment on Nano-patterned Surfaces

100000 cells were incubated with the nano-patterned surface for 48 h and washed twice with pre-warmed PBS and fixed with 3.7 % methanol-free formaldehyde solution (Electron Microscopy Sciences 15714-S). Cells were then washed three times with PBS and extracted with 0.1 % Triton X-100 in PBS for 5 min. Surfaces were then washed with PBS and incubated with a solution of Oregon Green 488 phalloidin (Invitrogen O7466) to stain actin filaments and Hoechst nuclear stain (Invitrogen H1399) at final concentrations of 200 nM and 1 μg/mL respectively in PBS. After 30 minutes, the cells were washed three times and the images were captured using a confocal microscope (Olympus).

2.4.6 Characterization

The KPFM was conducted with platinum coated tips (ANSCM-PA) purchased from AppNano on a Digital Instrument atomic force microscope in room temperature under ambient atmosphere. Work functions for the samples were determined using the work function of the Pt tip (5.9 eV) minus the surface potential contrast. Bright field images and fluorescence were detected by using an Olympus IX51 microscope with excitation wavelengths of 470 nm and 535 nm. AFM imaging of the surfaces was done on a Dimensions 3000 (Veeco) in tapping mode using a RTESP7 tip (Veeco). Confocal images were obtained by using a Zeiss LSM 510 Meta microscope. The film thickness of the protein films was measured by a Rudolph Research Auto EL ellipsometer. Far-UV circular dichroism (CD) spectra were measured on a JASCO J-720 spectropolarimeter with a quartz cuvette of 1 mm path length at 25 °C. The spectra were recorded from 200 to 260 nm as an average of three scans at a rate of 20 nm/min.

2.5 References

(1) K. H. Smith, E. Tejeda-Montes, M. Poch, A. Mata, *Chem. Soc. Rev.* **2011**, *40*, 4563.

(2) X. Hu, P. Cebe, A. S. Weiss, F. Omenetto, D. L. Kaplan, *Mater. Today* **2012**, *15*, 208.

(3) S. Kim, B. Marelli, M. A. Brenckle, A. N. Mitropoulos, E.-S. Gil, K. Tsioris, H. Tao, D. L. Kaplan, F. G. Omenetto, *Nat. Nanotechnol.* **2014**, *9*, 306.

(4) J.-W. Rhim, H.-M. Park, C.-S. Ha, *Prog. Polym. Sci.* **2013**, *38*, 1629.

(5) X. Wang, X. Zhang, J. Castellot, I. Herman, M. Iafrati, D. L. Kaplan, *Biomaterials* **2008**, *29*, 894.

(6) A. Abarrategi, A. Civantos, V. Ramos, J. V. Sanz Casado, J. L. López-Lacomba, *Biomacromolecules* **2008**, *9*, 711.

(7) M. Sato, K. Kojima, C. Sakuma, M. Murakami, Y. Tamada, H. Kitani, *Sci. Rep.* **2014**, *4*, 4080.

(8) J. J. Amsden, P. Domachuk, A. Gopinath, R. D. White, L. D. Negro, D. L. Kaplan, F. G. Omenetto, *Adv. Mater.* **2010**, *22*, 1746.

(9) L. Meinel, S. Hofmann, V. Karageorgiou, L. Zichner, R. Langer, D. Kaplan, G. Vunjak-Novakovic, *Biotechnol. Bioeng.* **2004**, *88*, 379.

(10) C. J. Bettinger, J. P. Bruggeman, A. Misra, J. T. Borenstein, R. Langer, *Biomaterials* **2009**, *30*, 3050.

(11) H. Perry, A. Gopinath, D. L. Kaplan, L. Dal Negro, F. G. Omenetto, *Adv. Mater.* **2008**, *20*, 3070.

(12) F. G. Omenetto, D. L. Kaplan, *Science* **2010**, *329*, 528.

(13) Y. Zhao, Q. Jiang, H. Xu, N. Reddy, L. Xu, Y. Yang, *J. Biomed. Mater. Res. Part B Appl. Biomater.* **2013**, *102*, 729.

(14) B. Kundu, N. E. Kurland, S. Bano, C. Patra, F. B. Engel, V. K. Yadavalli, S. C. Kundu, *Prog. Polym. Sci.* **2014**, *39*, 251.

(15) M. J. Roberts, N. Bhatt, C. M. Voge, E. R. Meshot, J. P. Stegemann, A. J. Hart, *J. Mater. Chem. B* **2013**, *1*, 4711.

(16) T. P. J. Knowles, T. W. Oppenheim, A. K. Buell, D. Y. Chirgadze, M. E. Welland, *Nat. Nanotechnol.* **2010**, *5*, 204.

(17) H.-J. Jin, J. Park, V. Karageorgiou, U.-J. Kim, R. Valluzzi, P. Cebe, D. L. Kaplan, *Adv. Funct. Mater.* **2005**, *15*, 1241.

(18) E. M. Pritchard, T. Valentin, B. Panilaitis, F. Omenetto, D. L. Kaplan, *Adv. Funct. Mater.* **2012**, *23*, 854.

(19) D.-H. Kim, J. Viventi, J. J. Amsden, J. Xiao, L. Vigeland, Y.-S. Kim, J. A. Blanco, B. Panilaitis, E. S. Frechette, D. Contreras, D. L. Kaplan, F. G. Omenetto, Y. Huang, K.-C. Hwang, M. R. Zakin, B. Litt, J. A. Rogers, *Nat. Mater.* **2010**, *9*, 511.

(20) A. R. Murphy, P. St. John, D. L. Kaplan, *Biomaterials* **2008**, *29*, 2829.

(21) M. Wihodo, C. I. Moraru, *J. Food Eng.* **2013**, *114*, 292.

(22) A. Bigi, G. Cojazzi, S. Panzavolta, K. Rubini, N. Roveri, *Biomaterials* **2001**, *22*, 763.

(23) J. O. Anyango, J. Taylor, J. R. N. Taylor, *J. Agric. Food Chem.* **2011**, *59*, 12674.

(24) S. Matsuda, H. Iwata, N. Se, Y. Ikada, *J. Biomed. Mater. Res.* **1999**, *45*, 20.

(25) H. Tsuchiya, Y. Hoshino, K. Tajima, N. Takagi, *J. Prosthet. Dent.* **1994**, *71*, 618.

(26) F. Song, D.-L. Tang, X.-L. Wang, Y.-Z. Wang, *Biomacromolecules* **2011**, *12*, 3369.

(27) S. Y. Chou, P. R. Krauss, P. J. Renstrom, *Science (80-.).* **1996**, *272*, 85.

(28) C. Subramani, N. Cengiz, K. Saha, T. N. Gevrek, X. Yu, Y. Jeong, A. Bajaj, A. Sanyal, V. M. Rotello, *Adv. Mater.* **2011**, *23*, 3165.

(29) S. H. Ahn, L. J. Guo, *ACS Nano* **2009**, *3*, 2304.

(30) N. J. Greenfield, *Nat. Protoc.* **2006**, *1*, 2876.

(31) C. Subramani, K. Saha, B. Creran, A. Bajaj, D. F. Moyano, H. Wang, V. M. Rotello, *Small* **2012**, *8*, 1209

CHAPTER 3

BIOCIDAL AND ANTIFOULING CHLORINATED PROTEIN FILMS

3.1 Introduction

More than 2 million cases of bacterial infection occur every year in United States according to Center for Disease Control (CDC) statistics.[1] Infections caused by bacterial contamination of medical devices such as stainless steel IV poles, bedrails and implants are serious healthcare problems. In 2011, approximately 720,000 patients acquired infections while being treated in hospitals, out of which more than 75,000 people died.[2] In hospitals, bacteria can frequently be transmitted by contamination of the surfaces of medical instruments and patient-care devices.[3] A particularly challenge arises from biofilm formation, where the adhered bacteria proliferate and produce extracellular polymeric substance, increasing their resistance to disinfectants and antibiotics.[4,5,6] Routine sterilization of medically-used objects reduces the possibilities of their contamination, however, it is challenging to maintain and ensure their sterility.

One strategy for enhancing the safety of biomedical devices is to prevent initial bacterial colonization on the surface.[7] Tuning the chemical and morphological characteristics of a surface is crucial for controlling bacterial adhesion. Adhesion of bacteria can be broadly attributed to electrostatic and hydrophobic interactions with the surface.[8] Polyethylene glycol and zwitterionic polymers provide useful platforms for preventing bacterial adhesion.[9] For example, poly(sulfobetaine methacrylate) coated

urinary catheters inhibit the adhesion of bacteria, prolonging the utility of these implements.[10]

Biocidal coatings can be fabricated using multiple strategies. One of the most useful approach is to incorporate antibacterial agents such as silver nanoparticles,[11,12] halogens,[13,14] nitric oxide[15,16] and antibiotics,[17,18] into polymeric matrixes. For instance, *N*-halamine polyurethane films created by halogenation of methacrylamide-grafted polymeric films have been used to generate antimicrobial dental unit waterline tubing with biocidal activity.[19] Similarly, other antimicrobial small molecules can be loaded into non-fouling surfaces to generate long term antimicrobial coatings.[20,21] For instance, essential oils are utilized in protein-based edible films to incorporate antimicrobial property.[22]

Proteins have emerged as an alternative precursor for fabrication of films due to their biocompatibility and degradability.[23] Protein films reduce the adherence and colonization of microorganisms on the surface, hence they are widely used in several fields, including artificial organs,[24] drug-releasing patches,[25] food packaging, cosmetics and healthcare.[26] Antimicrobial peptides can be incorporated into silk fibroin via bioengineering to produce protein-based biocidal films.[27] These materials exhibit substantial antimicrobial activity originally and can inhibit bacterial adhesion and growth. However, their ability to inhibit bacterial adhesion is compromised by accumulation of dead bacterial cells.[28] Alternatively, antibiotics can be incorporated into crosslinked protein films.[29]

3.2 Results and discussion

Recently, we reported fabrication of stable protein films using nanoimprint lithography (NIL).[30] This process combines temperature and pressure to create water-stable films that retain significant native protein structure. These surfaces resist bacterial adhesion due to their inherently zwitterionic surface properties. We envisioned that these films could be treated with chlorinating agents to generate N- or S-chloro species that would slowly release chlorine, providing a potent biocidal effect (Figure 3.1).[31,32]

Here, we report the fabrication of protein-based thin films that prevent bacterial adhesion and feature potent antimicrobial activity against uropathogenic bacteria. These films present a new direction in the creation of antimicrobial surfcaes for biomedical and other applications.

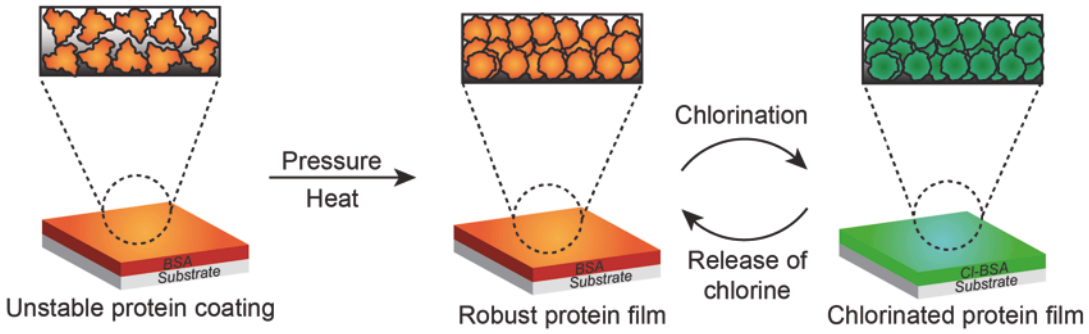

Figure 3.1: Schematic representation of film processing strategy to generate chlorinated protein films. The combination of heat and pressure provides water-stable protein films that prevent bacterial adhesion. Treatment with a chlorinating agent then provides biocidal materials that kill bacteria through controlled release of chlorine.

Protein films were made using bovine serum albumin (BSA). BSA is inexpensive and readily available and features an overall negative surface potential to prevent cellular adhesion.[30] An aqueous solution of BSA was deposited on plasma-cleaned silicon wafers by spin casting. The deposited BSA layer was then hot-embossed using NIL (2.75 MPa

and 180 ˚C for 5 minutes). After NIL processing, the BSA films were stable in water, buffer and serum solutions as confirmed by their thickness measurements.[30] The films used for the current study were 200 nm in thickness with low surface roughness, as determined using cross-sectional scanning electron microscopy (SEM) image (Figure 3.2a,b), atomic force microscopy (Figure 3.2c), and ellipsometry (Table 3.1).

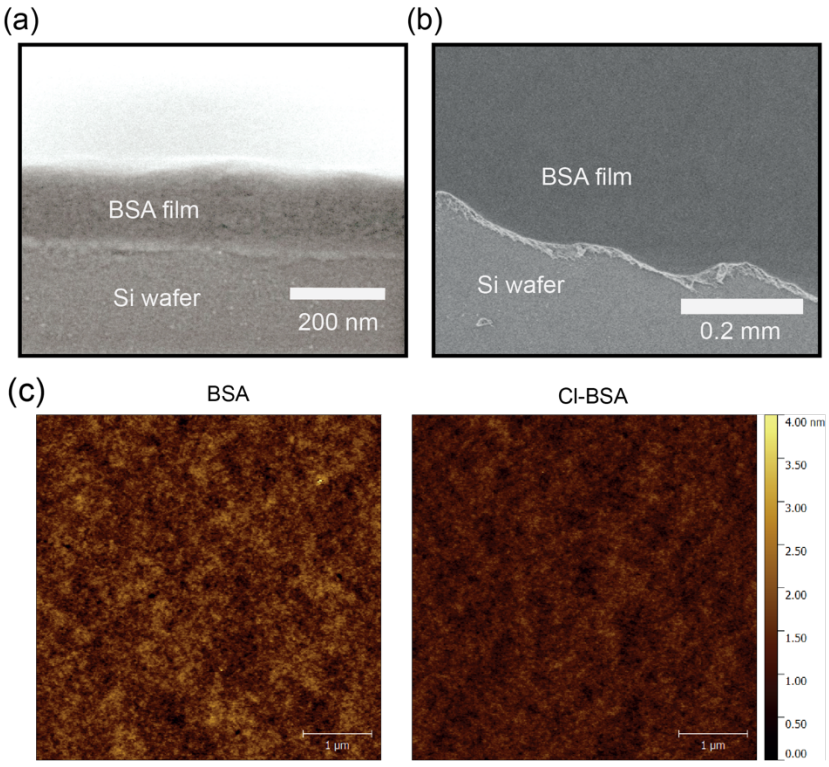

Figure 3.2: a) Cross-sectional scanning electron microscopy (SEM) image of BSA film, showing around 200 nm thickness. b) SEM image of scratched BSA film, showing a thin film with low surface roughness. c) Atomic force microscopy images of BSA and Cl-BSA films, showing low surface roughness.

Chlorine disinfectants such as bleach and chlorinated isocyanurates have been used to chlorinate surfaces, imparting biocidal properties.[33] Trichlor-O-Cide 5600 is a multi-purpose sanitizer with sodium dichloroisocyanurate as the active ingredient. Chlorinated BSA films (Cl-BSA) were fabricated by immersing BSA films in an aqueous solution of

Trichlor-O-Cide 5600 for 24 hours to ensure complete chlorination. The Cl-BSA films were then washed with water to remove the residual chemicals. We observed only a modest change in physical properties of the film after chlorination, namely a slight increase in hydrophilicity. (Table 3.1)

Table 3.1: Properties of protein films before and after chlorination.

Film properties	**BSA**	**Cl-BSA**
Thickness (nm)[a]	184.5 ± 0.8	194.6 ± 1.6
RMS Roughness (nm)[b]	0.4	0.3
Contact angle (°)[c]	69.9 ± 0.7	53.2 ± 2.2

a) Thickness was measured using ellipsometry. b) Roughness was measured by atomic force microscopy. c) Contact angle was measured by static sessile drop method.

Chlorination of protein films was characterized using X-ray photoelectron spectroscopy (XPS) (Figure 3.3, and Figure 3.4). After chlorination, a Cl_{2p} peak was observed in Cl-BSA films, whereas, no chlorine signal was detected in pristine BSA films, indicating successful loading of chlorines.[34] The binding energy of Cl_{2p} in Cl-BSA was different from the chlorinating reagent, indicating that the chlorine signal was not a result of the residual or embedded sodium dichloroisocyanurate. The nature of chlorination is apparent from comparison of the N_{1s} and S_{2p} spectra. The binding energy of N_{1s} did not change after chlorination, ruling out *N*-halogenation. Instead, the binding energy of the S_{2p} peak shifted after chlorination, indicating the formation of oxidized sulfur species.[35]

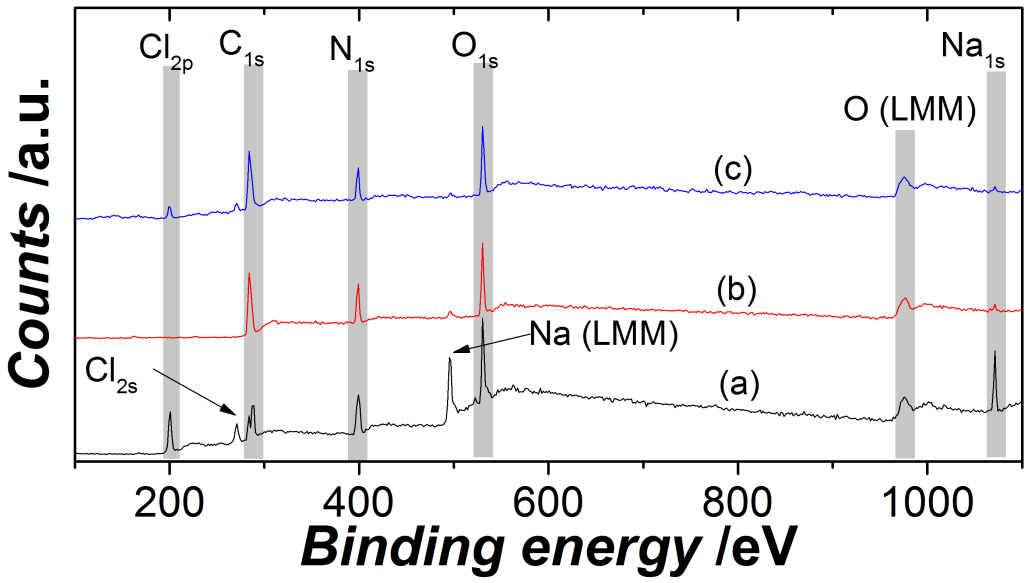

Figure 3.3: The survey spectrum obtained from (a) Trichlor-O-Cide 5600, (b) BSA film and (c) Cl-BSA film. The peaks corresponding to the respective elements have been marked.

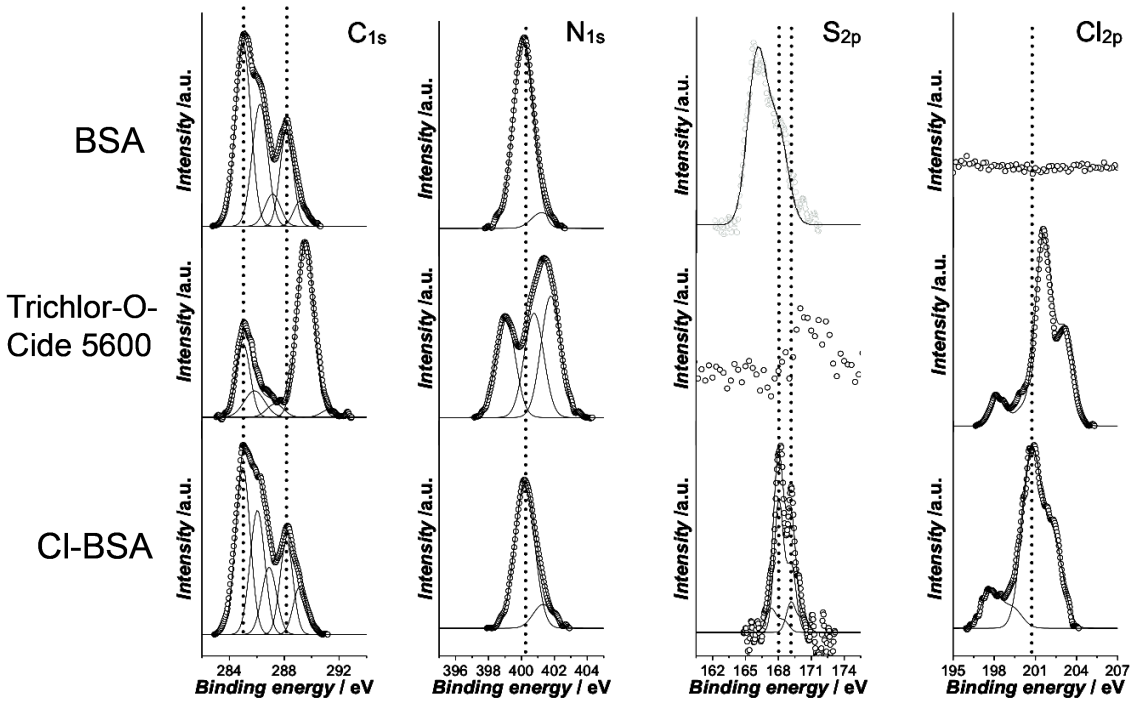

Figure 3.4: X-ray photoelectron spectra of BSA film, Trichlor-O-Cide® 5600, and Cl-BSA film. The change of binding energy of S_{2p} on Cl-BSA film was observed, while the signal of N_{1s} remained identical after chlorination, indicating that chlorination occurred at sulfur.

In Chapter two, we demonstrated that protein films prevent adhesion of mammalian cells. This property was reproduced with bacteria (Figure 3.5). We next wanted to know if chlorination affected the resistance of bacterial adhesion on BSA films, red fluorescent protein (RFP) expressing *E. coli* was incubated with the protein films for 24 hours to evaluate the antifouling property of the BSA and Cl-BSA films (Figure 3.6). The microscopy images show a significant decrease in bacterial adhesion on protein films as compared to silicon wafer. Using image analysis (ImageJ),[36] we were able to quantitatively compare bacteria adhesion by calculating the fluorescence intensities in different images (Figure 3.6d). BSA films showed 20 times less adhesion compared to bare silicon, indicating that protein coatings prevent bacteria adhesion. As expected, the Cl-BSA film had even fewer bacteria attached on the surface due to the bactericidal effect of the

chlorination. Similar results were also observed using scanning electron microscopy (Figure 3.7).

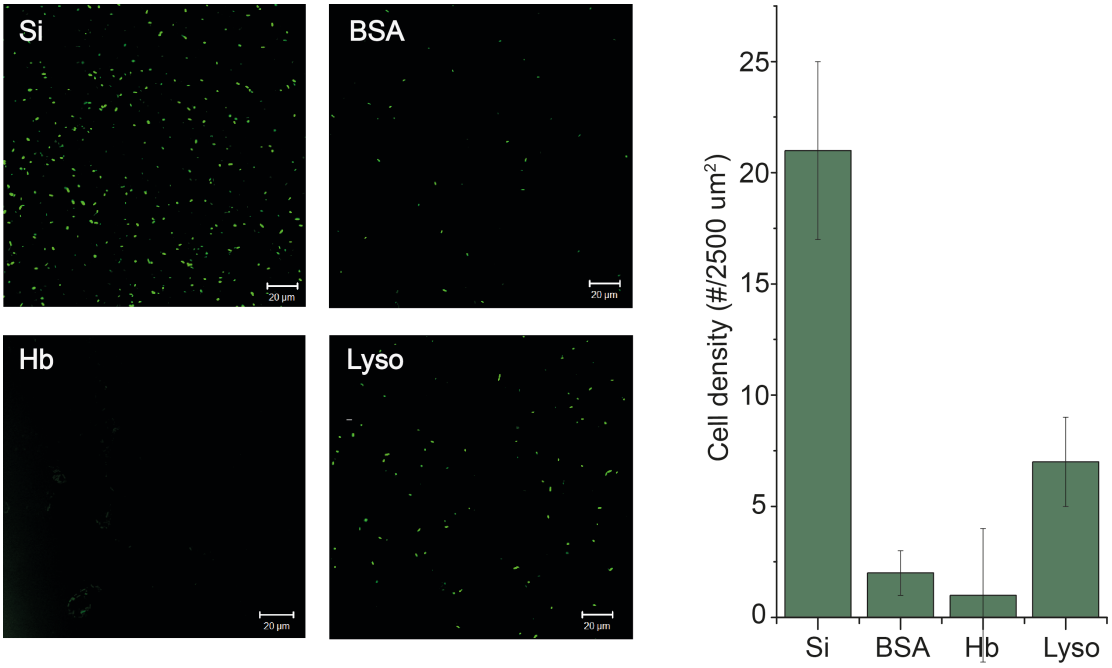

Figure 3.5: Adhesion of GFP expressed *E. coli* on silicon substrates and protein films after 24 hours incubation.

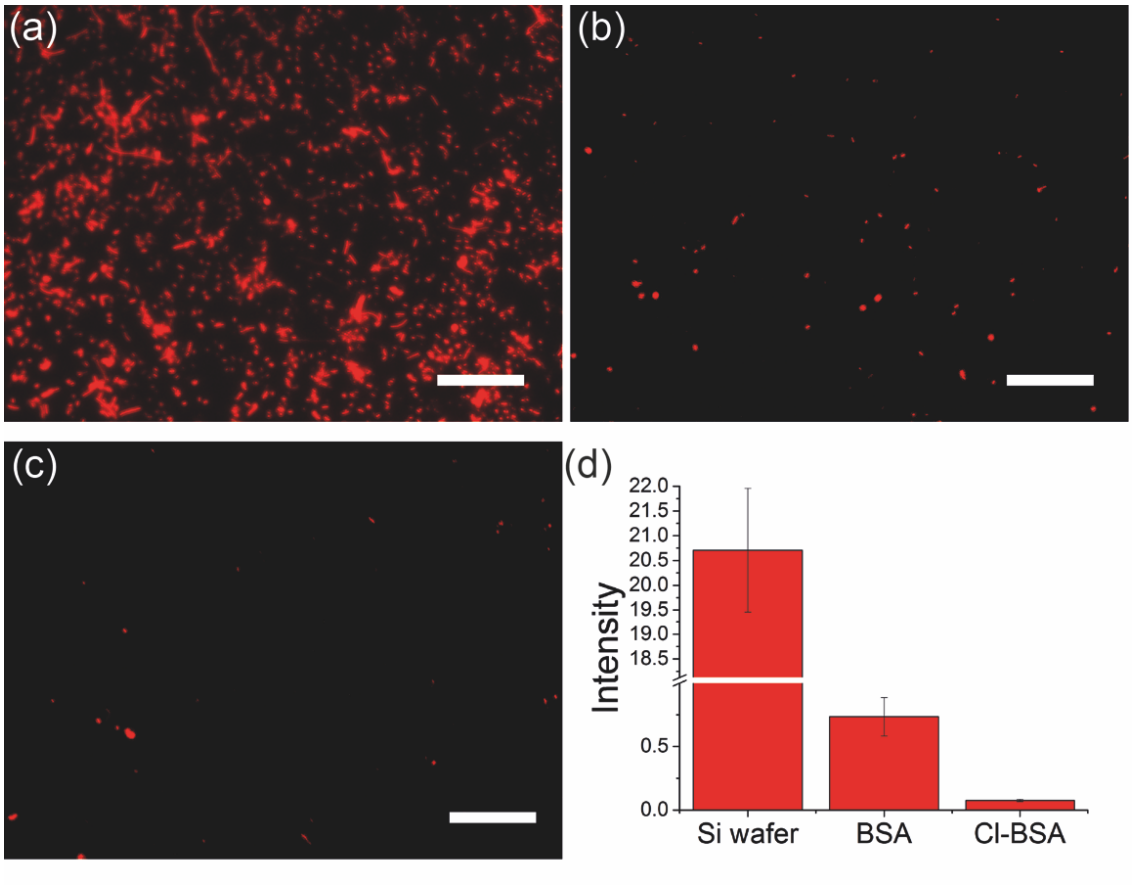

Figure 3.6: Fluorescent microscopy images of (a) Si wafer, (b) BSA, and (c) Cl-BSA surfaces incubated with Red Fluorescent Protein (RFP) expressing *E. coli* for 24 hours. (d) Quantitative analysis of bacteria observed in (a), (b) and (c). The scale bars for (a), (b) and (c) are 100 μm.

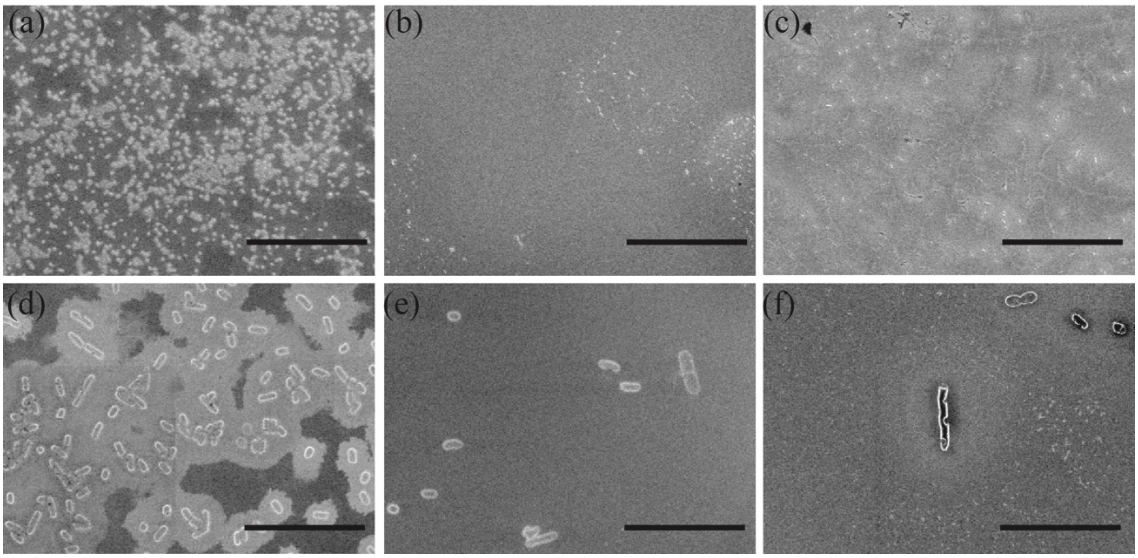

Figure 3.7: SEM images of *E. coli* adhered on (a,d) silicon substrate, (b,e) BSA film, and (c,f) Cl-BSA film. Scale bars were 120 μm for (a), (b), (c), and 12 μm for (d), (e), (f).

The release of chlorine from Cl-BSA was monitored using DPD (N,N-diethyl-p-phenylenediamine) assay.[33] Upon interacting with free chlorine, the colorless DPD is oxidized into a magenta product. As-prepared Cl-BSA films (1 cm^2) were incubated in 2 mL Milli-Q water, the supernatants were collected, and the DPD reagent was added. The Cl-BSA films gradually released chlorine over the course of 24 hours (Figure 3.8a). Presumably, this release pattern can be tuned by changing protein film structure, e.g. film thickness and protein composition.

The released chloride species can not only kill bacteria on the surface, but also inhibit their growth in the surrounding solution.[37] The bactericidal activity of chlorinated protein films was assessed against multi-drug resistant clinical isolates of *P. aeruginosa* (CD-1006), *E. coli* (CD-2), and Methicillin-Resistant *S. aureus* (MRSA). The surfaces were incubated with bacteria for 24 hours. As shown in Figure 3.8b, Cl-BSA suppressed

bacterial growth for all strains, with little or no effect was observed with either the BSA film or the bare silicon substrate. The stability of Cl-BSA films was examined by measuring the thickness change after incubating in water (Figure 3.8c).

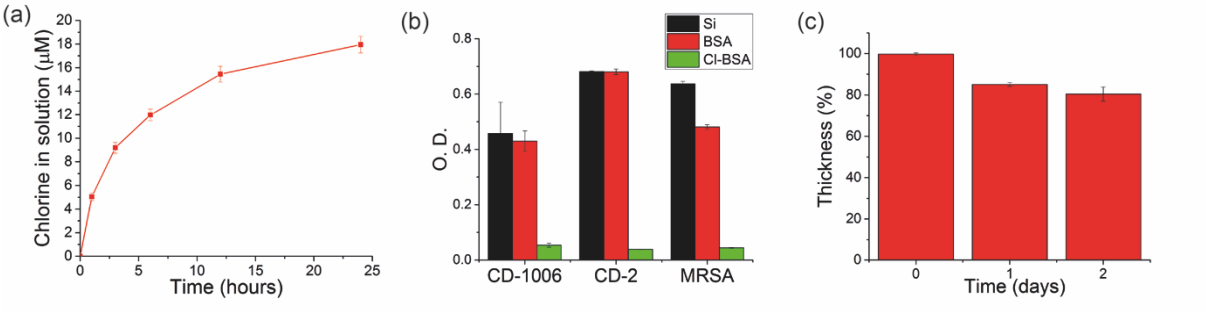

Figure 3.8: (a) Chlorine content in water after incubating with Cl-BSA film (b) Bacterial growth in solution after 24 hours incubation with Silica, BSA and Cl-BSA surfaces. (c) Film stability of Cl-BSA after incubating in water for 2 days.

3.3 Conclusion

In summary, we have demonstrated a new approach for fabricating antimicrobial surfaces employing naturally abundant proteins as precursors. Using commercially available sanitizer, proteins films can be easily functionalized with chlorine, retaining their antifouling properties while gaining microbicidal activity through slow release of chlorine. These protein films provide biodegradable, biocompatible and sustainable materials for coatings with both biocidal and antifouling properties, making them promising materials for biomaterial-based antimicrobial coatings.

3.4 Experimental methods

3.4.1 Materials

Bovine serum albumin (BSA) was purchased from Fisher Scientific and used without further purification. Silica wafers were purchased from WRS Materials. Trichlor-O-Cide 5600 was purchased from Ecolab. DPD (N,N-diethyl-p-phenylenediamine) reagent was purchased from Fisher Scientific. MilliQ water was purified by using a Millipore water purification system.

3.4.2 Characterization

Atomic force microscopy was performed on a DI Dimension-3100 AFM. The average roughness of the determined sample area was calculated by Gwyddion, a freeware with the agreement of GNU General Public License. XPS analysis was performed on a Physical Electronics Quantum 2000 spectrometer using a monochromatic Al Kα excitation at a spot size of 10 mm with pass energy of 46.95. Chemically distinct species were resolved using a Gaussian Lorentzian function with nonlinear least-squares fitting procedure. All XPS spectra were background corrected using the Shirley algorithm and aligning the elemental binding energies to the adventitious carbon (C 1s) binding energy of 284.6 eV. The thickness of protein films was measured by a Rudolph Research Auto EL ellipsometer. Static water contact angle measurements were performed using a VCA Optima surface analysis/goniometry system with water droplets size of 2 μL. Scanning electron microscopic images were obtained by using FEI Magellan 400 field emission scanning electron microscope operated at 1 kV with 13 μA of beam current. Samples were coated with Au for 1 min before measuring.

3.4.3 Fabrication of protein films (BSA)

10% w/w solutions of BSA in MilliQ water were filtered by using a 0.22 μm filter and spin-coated at 3000 rpm for 30 s onto an oxygen plasma-cleaned silicon substrate, yielding a thin film of protein. Nanoimprinting of protein films was performed by using a Nanonex NX-2000 nanoimprinter with flat silicon molds. Imprinting was performed at 180 °C and 2.8 MPa for 5 min. All molds were treated with heptadecafluoro-1,1,2,2-(tetrahydrodecyl)dimethyl-chlorosilane at 85 °C for 2 days in a vacuum chamber prior to use.

3.4.4 Fabrication of chlorinated protein film (Cl-BSA)

BSA films were cut into 1 cm^2 and immersed in 2 mL of 0.36 mg/mL of Trichlor-O-Cide 5600 solution in sample vials. After 24 hours, films were washed by Milli-Q water for 5 times and dry by nitrogen flow.

3.4.5 Release study of Cl-BSA film

Cl-BSA films were placed into 2 mL Milli-Q water in vials. After a period of time, the supernatants were collected for measuring the chlorine content, and replaced 2 mL of fresh Milli-Q water for the next period measurement. The concentration of chlorine in supernatants were determined by a *N*,*N*-diethyl-*p*-phenylenediamine (DPD) assay. 50 μL of DPD reagent (prepared by mixing a foil packet of DPD total chlorine reagent powder (Hach, Loveland, CO) with 1 mL of DI water) were added into 2 mL of supernatants. The tubes were shaken for 5 min before measuring the absorbance at 512 nm. Chlorine content of each sample was calculated by comparison to a standard curve prepared by Trichlor-O-Cide 5600 in water.

3.4.6 Biocidal evaluation

Bacteria were inoculated in lysogeny broth (LB) medium at 37 ºC until stationary phase. The cultures were then harvested by centrifugation and washed with 0.85% sodium chloride solution three times. Concentrations of resuspended bacterial solution were determined by optical density (O.D.) measured at 600 nm. M9 medium was used to make dilutions of bacterial solution to a concentration of 1×10^6 cfu/mL.[38] Samples were then incubated in 2mL of bacterial suspension for 24 h at 37 ºC at 275 rpm in 12-well culture plates. The optical densities of these solutions were then measured at 600 nm using a UV–vis Spectrometer. A growth control group without antimicrobial films and a sterile control group with only growth medium were carried out at the same time. Cultures were performed in triplicates, and at least two independent experiments were repeated on different days.

3.4.7 Antifouling evaluation

Bacteria were inoculated in 3 mL LB broth and grown to stationary phase at 37 °C. The cultures were then diluted to O.D 0.1 in an M-9 media supplemented with 1 mM IPTG (isopropyl β-D-1-thiogalactopyranoside).[39] 2 mL of the dilution was poured onto the surfaces kept in 12 well culture plates. The surfaces were kept at 25 °C and the bacteria were allowed to grow for 24 hours. In general, the surfaces with bacteria were rinsed in deionized water for three times before analysis under the microscope.

3.5 References

(1) T. Frieden, *Centres for Disease Control and Prevention* **2013**. Atlanta, Georgia U.S.A.

(2) S. S. Magill, J. R. Edwards, W. Bamberg, Z. G. Beldavs, G. Dumyati, M. A. Kainer, R. Lynfield, M. Maloney, L. McAllister-Hollod, J. Nadle, S. M. Ray, D. L. Thompson, L. E. Wilson, S. K. Fridkin, *N. Engl. J. Med.* **2014**, *370*, 1198

(3) D. J. Weber, W. A. Rutala, M. B. Miller, K. Huslage, E. Sickbert-Bennett, *Am. J. Infect. Control* **2010**, *38*, S25.

(4) J. W. Costerton, P. S. Stewart, E. P. Greenberg, *Science (80-.).* **1999**, *284*, 1318 LP.

(5) R. M. Donlan, *Emerg. Infect. Dis.* **2001**, *7*, 277

(6) L.-S. Wang, A. Gupta, V. M. Rotello, *ACS Infect. Dis.* **2016**, *2*, 3.

(7) M. L. W. Knetsch, L. H. Koole, *Polym.* **2011**, *3*, 340

(8) L. D. Renner, D. B. Weibel, *MRS Bull.* **2011**, *36*, 347.

(9) D. Campoccia, L. Montanaro, C. R. Arciola, *Biomaterials* **2013**, *34*, 8533.

(10) C. Diaz Blanco, A. Ortner, R. Dimitrov, A. Navarro, E. Mendoza, T. Tzanov, *ACS Appl. Mater. Interfaces* **2014**, *6*, 11385.

(11) H. Kong, J. Jang, *Langmuir* **2008**, *24*, 2051.

(12) A. Agarwal, T. L. Weis, M. J. Schurr, N. G. Faith, C. J. Czuprynski, J. F. McAnulty, C. J. Murphy, N. L. Abbott, *Biomaterials* **2010**, *31*, 680.

(13) L. Timofeeva, N. Kleshcheva, *Appl. Microbiol. Biotechnol.* **2011**, *89*, 475

(14) B. Demir, I. Cerkez, S. D. Worley, R. M. Broughton, T.-S. Huang, *ACS Appl. Mater. Interfaces* **2015**, *7*, 1752.

(15) E. J. Brisbois, R. P. Davis, A. M. Jones, T. C. Major, R. H. Bartlett, M. E. Meyerhoff, H. Handa, *J. Mater. Chem. B* **2015**, *3*, 1639.

(16) A. Ghaffari, C. C. Miller, B. McMullin, A. Ghahary, *Nitric Oxide* **2006**, *14*, 21.

(17) B. Wang, T. Jin, Q. Xu, H. Liu, Z. Ye, H. Chen, *Bioconjug. Chem.* **2016**, *27*, 1305.

(18) E. M. Hetrick, M. H. Schoenfisch, *Chem. Soc. Rev.* **2006**, *35*, 780.

(19) J. Luo, N. Porteous, Y. Sun, *ACS Appl. Mater. Interfaces* **2011**, *3*, 2895.

(20) A. N. Zelikin, *ACS Nano* **2010**, *4*, 2494.

(21) R. Wang, K. L. Chua, K. G. Neoh, *ACS Biomater. Sci. Eng.* **2015**, *1*, 405.

(22) M. Oussalah, S. Caillet, S. Salmiéri, L. Saucier, M. Lacroix, *J. Agric. Food Chem.* **2004**, *52*, 5598.

(23) M. G. A. Vieira, M. A. da Silva, L. O. dos Santos, M. M. Beppu, *Eur. Polym. J.* **2011**, *47*, 254.

(24) Y. S. Choi, S. R. Hong, Y. M. Lee, K. W. Song, M. H. Park, Y. S. Nam, *Biomaterials* **1999**, *20*, 409.

(25) S. Hofmann, C. T. Wong Po Foo, F. Rossetti, M. Textor, G. Vunjak-Novakovic, D. L. Kaplan, H. P. Merkle, L. Meinel, *J. Control. Release* **2006**, *111*, 219.

(26) J.-W. Rhim, H.-M. Park, C.-S. Ha, *Prog. Polym. Sci.* **2013**, *38*, 1629.

(27) S. C. Gomes, I. B. Leonor, J. F. Mano, R. L. Reis, D. L. Kaplan, *Biomaterials* **2011**, *32*, 4255.

(28) W. Hartleb, J. S. Saar, P. Zou, K. Lienkamp, *Macromol. Chem. Phys.* **2015**, *217*, 225.

(29) Z. Peles, M. Zilberman, *Acta Biomater.* **2012**, *8*, 209.

(30) E. Jeoung, B. Duncan, L. S. Wang, K. Saha, C. Subramani, P. Wang, Y. C. Yeh, T. Kushida, Y. Engel, M. D. Barnes, V. M. Rotello, *Adv. Mater.* **2015**, *27*, 6251.

(31) F. Hui, C. Debiemme-Chouvy, *Biomacromolecules* **2013**, *14*, 585.

(32) M. J. Gray, W.-Y. Wholey, U. Jakob, *Annu. Rev. Microbiol.* **2013**, *67*, 141.

(33) L. J. Bastarrachea, J. M. Goddard, *J. Agric. Food Chem.* **2015**, *63*, 4243.

(34) S. Saravanan, S. Nethala, S. Pattnaik, A. Tripathi, A. Moorthi, N. Selvamurugan, *Int. J. Biol. Macromol.* **2011**, *49*, 188.

(35) C. Debiemme-Chouvy, S. Haskouri, G. Folcher, H. Cachet, *Langmuir* **2007**, *23*, 3873.

(36) E. C. Jensen, *Anat. Rec.* **2013**, *296*, 378.

(37) I. Zhuk, F. Jariwala, A. B. Attygalle, Y. Wu, M. R. Libera, S. A. Sukhishvili, *ACS Nano* **2014**, *8*, 7733.

(38) X. Li, S. M. Robinson, A. Gupta, K. Saha, Z. Jiang, D. F. Moyano, A. Sahar, M. A. Riley, V. M. Rotello, *ACS Nano* **2014**, *8*, 10682.

(39) X. Li, Y.-C. Yeh, K. Giri, R. Mout, R. F. Landis, Y. S. Prakash, V. M. Rotello, *Chem. Commun.* **2015**, *51*, 282.

CHAPTER 4

GRADIENT AND PATTERNED PROTEIN FILMS STABILIZED VIA NANOIMPRINT LITHOGRAPHY FOR ENGINEERED INTERACTIONS WITH CELLS

4.1 Introduction

Protein based biomaterials offer versatile platforms for generating functional surfaces for biomedical applications. [1,2,3] Furthermore, the protein surface creates a molecular template for controlling interaction with biological systems.[4,5,6] These favorable properties have made these protein –based materials highly modulable to interface with cells for wound healing[7,8] and tissue engineering applications. [9,10]

In chapter 2, we developed an additive free, nanoimprint lithography (NIL) based method for the generation of water stable protein films. [11] In this study, we hypothesized that inkjet printing of proteins would provide a versatile method for the "direct-writing" of two-dimensional biomolecular patterns to complement our NIL protein film fabrication strategy. Herein, we describe a combined inkjet printing based deposition with NIL stabilization methodology generates materials surfaces with tunable biological responses. We chose to probe cellular adhesion as a model biological response as the regulation of cellular adhesion/migration has been shown to be a critical factor in a variety of biological processes. Moreover, the ability to tailor surface cytophilicity is promising for directing cell adhesion to generate patterned cell culture,[12] which is appealing for various biological applications, including tissue engineering, sensing, and developing co-culture systems.[13]

The utility of these films was demonstrated through the controlled adhesion of mammalian fibroblasts. This self-sorted cellular patterning technique is promising for the

development of cell arrays as well as co-culture platforms.[14] More specifically, side-by-side coculture facilitated the research of cell-cell interaction at the interface,[15] such as phagocytosis-based therapeutics.[16] By manipulating the cell behaviors of macrophage (RAW264.7) and human embryonic kidney cells (HEK293) using inkjet printed protein films, cell pattern composite of multiple cell types was generated. This versatile nonmanufacturing is a promising system for the rapid fabrication of macrophage co-culture platforms.

4.2 Results and discussion

Inkjet printing provides a reproducible method for controlling precise mixing and deposition of nanomaterials on the surface.[17] We hypothesized that the parametric control offered by inkjet printing would allow us to modulate the biological response to combinatorial protein films. Bovine serum albumin (BSA, MW: 66.3 kDa, pI: 4.8) and lysozyme (Lyso, MW: 14.4 kDa, pI: 11.0) were selected as our model anionic and cationic protein inks, respectively. Films were generated through the deposition of the protein inks in a parametric fashion. As shown in Figure 4.1a, inkjet deposition of protein-based inks generates patterns whose components can be modularly assembled. Following this directed deposition, the proteins are stabilized into a functional film using NIL-based method.

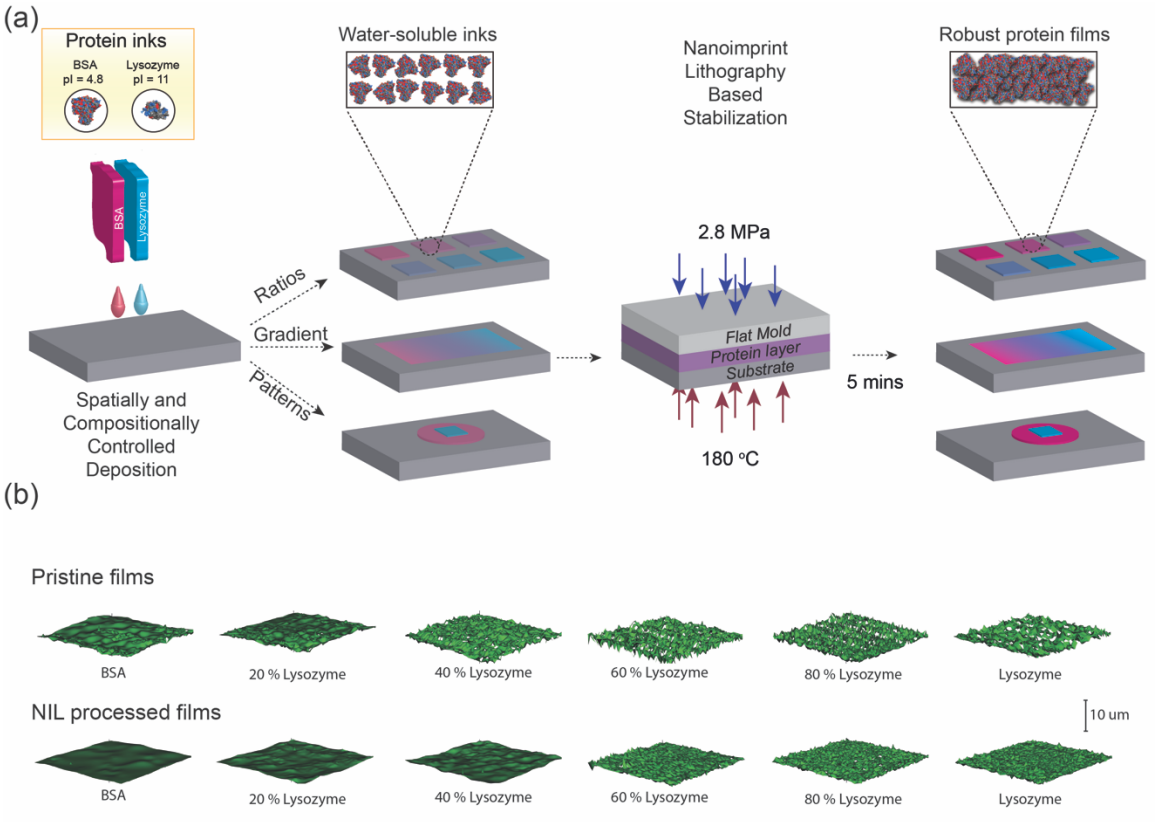

Figure 4.1: a) Inkjet directed deposition controls both the film composition and spatial presentation of the protein components. b) Topography of protein films with different ratio of BSA and Lyso before and after NIL processing. The scale bar for z-axis was 10 µm. The lateral areas measured were 0.70 mm x 0.53 mm.

Inkjet printing of water-based inks produces coffee rings that results in high roughness of printed films.[23] Addition of organic solvents or polymers has been utilized to reduce coffee ring formation,[24, 25] however, the compatibility of organic solvents and the toxicity of polymers hindered the application of inkjet printing protein films.[26] In our approach, we found that NIL process can be applied for flattening the inkjet-printed films (Figure 4.1b). The thickness and roughness of pristine films were found decreased twice after NIL (Table 4.1).

Table 4.1: Thickness and roughness of protein films with different ratio of BSA and Lyso before and after NIL processing. The data were measured using profilometer (n=3).

	Pristine films		NIL processed films	
Composition	Thickness (nm)	Roughness (nm)	Thickness (nm)	Roughness (nm)
100 % BSA	2168±184	375±14	814±13	163±19
20 % Lyso	2255±85	386±58	1010±11	192±33
40 % Lyso	2036±177	558±81	843±26	270±23
60 % Lyso	1742±57	753±45	733±4	322±15
80 % Lyso	1235±89	631±29	562±19	324±27
100 % Lyso	1626±54	789±51	665±41	265±22

Previously, we have shown that NIL can be used to generate water stable protein films while maintain their inherent surface properties. These results were reproduced on inkjet-printed protein films as well. The stability of inkjet-printed protein films was demonstrated by measuring the thickness change of films after washing by water (Figure 4.2a). No significant loss of films was observed after 3 days incubation. Kelvin probe force microscopy (KPFM) was employed to demonstrate the control of surface potentials on inkjet printed protein films. The surface potentials of mixed films were gradually increased with the increase of lysozyme component (Figure 4.2b).

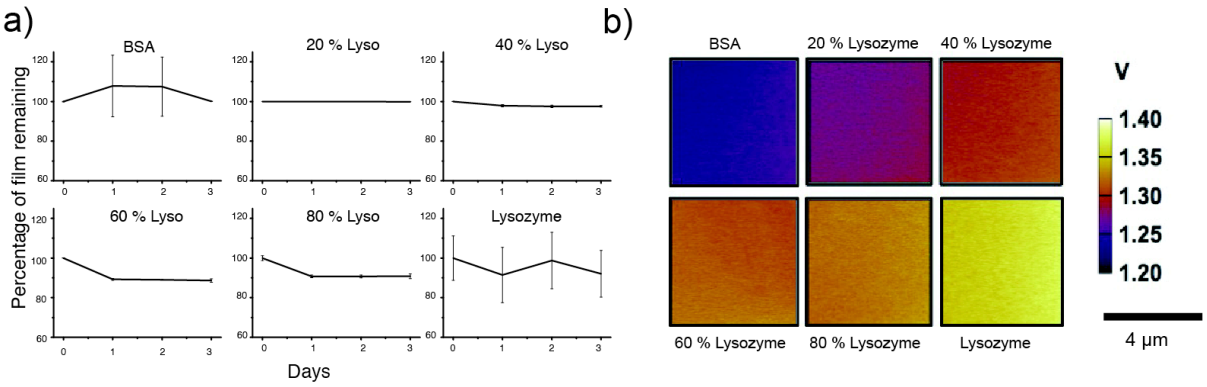

Figure 4.2: a) Thickness changes of protein films after immersing in water. b) Surface potential determined by KPFM. Protein films were generated by varying the BSA:Lyso ratio of the film in 20 % increments.

We determined whether this physiochemical property was translatable to biological systems by quantifying the adhesion of mammalian fibroblast cells using films generated from increasing ratios of BSA:Lyso. As shown in Figure 4.3, cells adhere to films generated with grater percentages of Lyso with a drastic increase observed with films comprised of 80 % or more of Lyso. Films fabricated with higher BSA amounts demonstrated minimal adhesion confirming the incorporation of protein charge into the overall materials properties of the film.

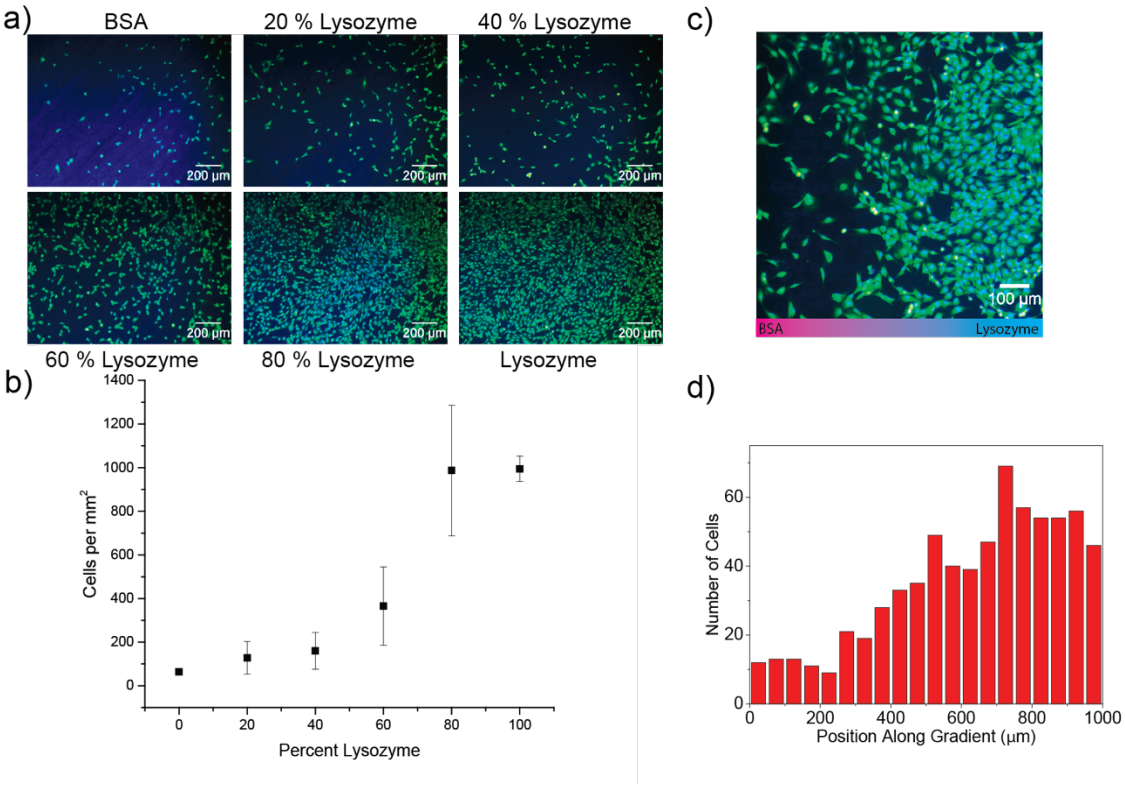

Figure 4.3: Adhesion of mammalian fibroblasts on films with a) varying ratios of protein components, and c) a gradient pattern. b,d) Number of cells with respect to different ratios of protein components and position along gradient. Cells were stained with Hoescht 33343 and Calcein AM to label the cell nuclei and cytosol, respectively. Scale bars are 200 µm.

We next generated micropatterned coatings to direct cell attachment on the printed Lyso patches, while avoiding the BSA area. (Figure 4.4) Inkjet printing advantageously affords spatial control over the deposition of film components. To probe the control over cell growth as a function of protein component, we deposited a rectangle of Lyso surrounded by a circle of BSA. As shown in Figure 4.4, the cells preferentially adhere to the Lyso pattern and can be easily washed away from the BSA coated surface.

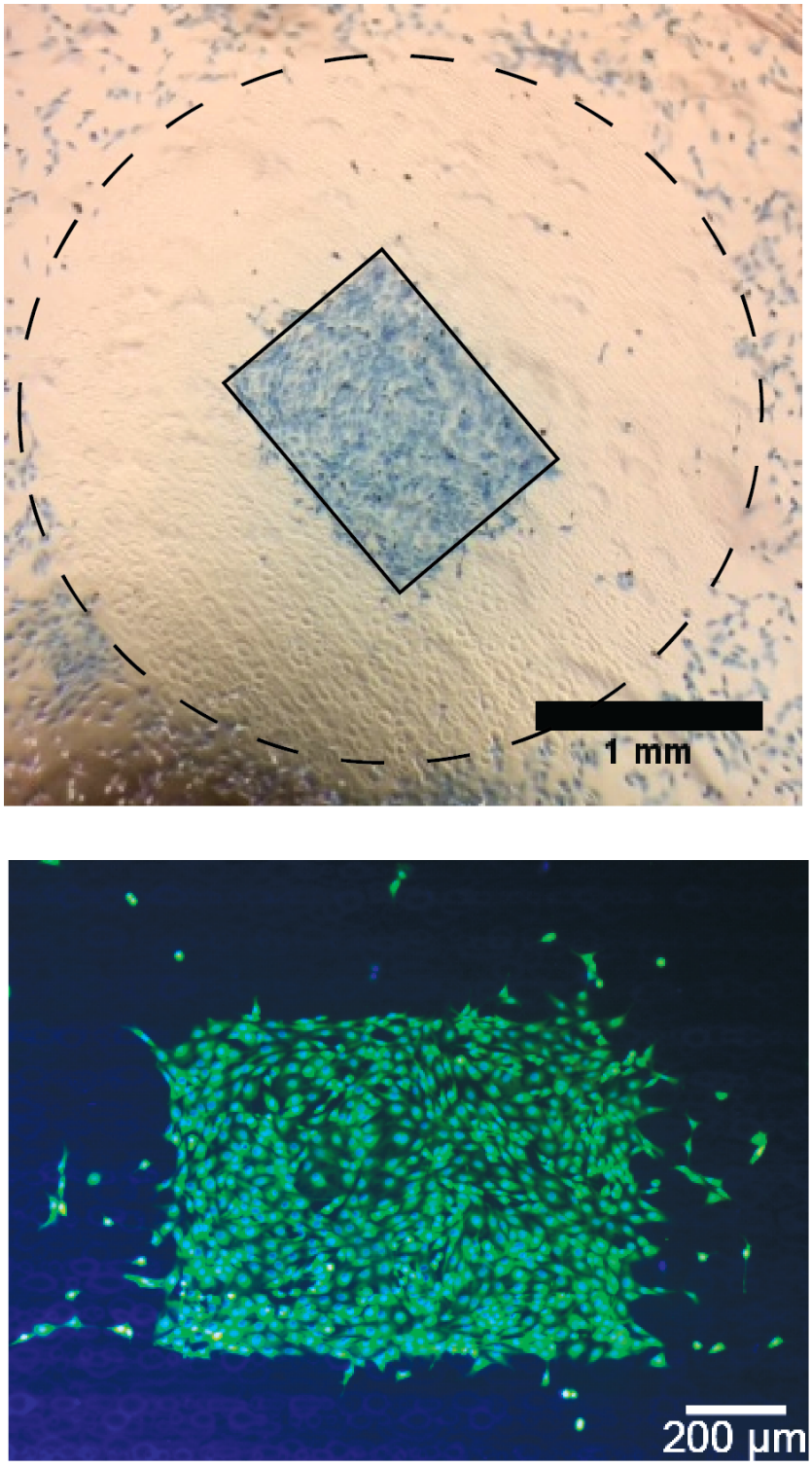

Figure 4.4: (top) Fibroblasts adhesion to patterned film with discrete Lyso and BSA domains. The solid line (Lyso) and dotted line (BSA) were drawn to aid the eye. (bottom) Fluorescence micrograph of cells adhered to Lyso pattern surrounded by BSA.

Cellular co-culture systems have been applied for inflammatory studies by mixing macrophages with other cells.[18] Side-by-side co-culture facilitated the studying of cell-cell interaction at the interface, however, attaching different cells on specific area has been challenging.[19] Taking advantage of different cellular interactions with protein films, we were able to demonstrate a patterned side-by-side co-culture of RAW 264.7 and deGFP-expressed HEK293 cells. Similar to fibroblast cells, HEK293 only adhered on Lyso area(Figure 4.5a). On the other hand, RAW 264.3 were able to adhere on both BSA and LYSO region (Figure 4.5b). After 24 hours incubation of HEK 293 cells on patterned protein film, a patch of HEK293 cells was formed and RAW 264.3 was then introduced. Since the HEK293 has preoccupied the Lyso area, RAW 264.3 was forced to adhere on only BSA region, resulting in a side-by-side cell culture (Figure 4.6).

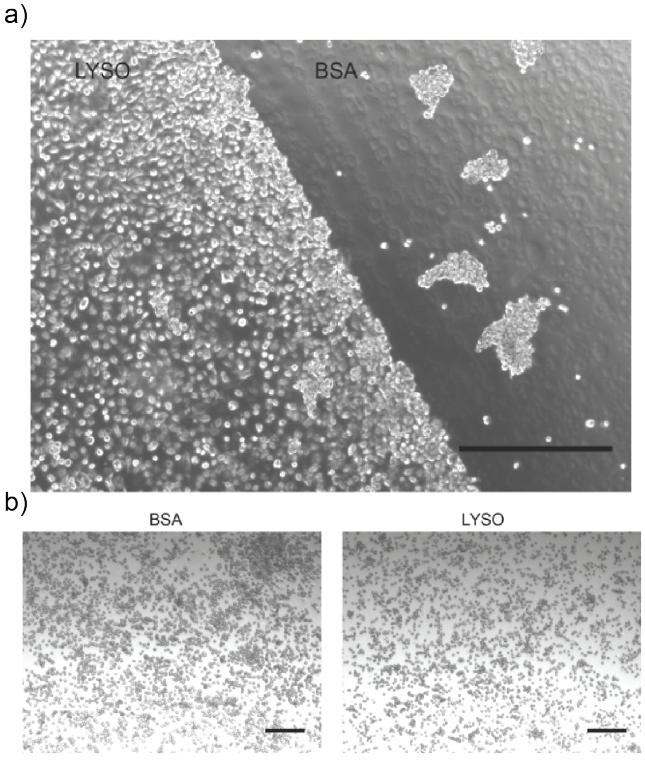

Figure 4.5: a) Cell adhesion of HEK293 on patterned BSA and LYSO films. Scale bar is 100 µm. b) Cell adhesion of RAW264.7 on spin coated BSA and LYSO films. Scale bars are 200 µm.

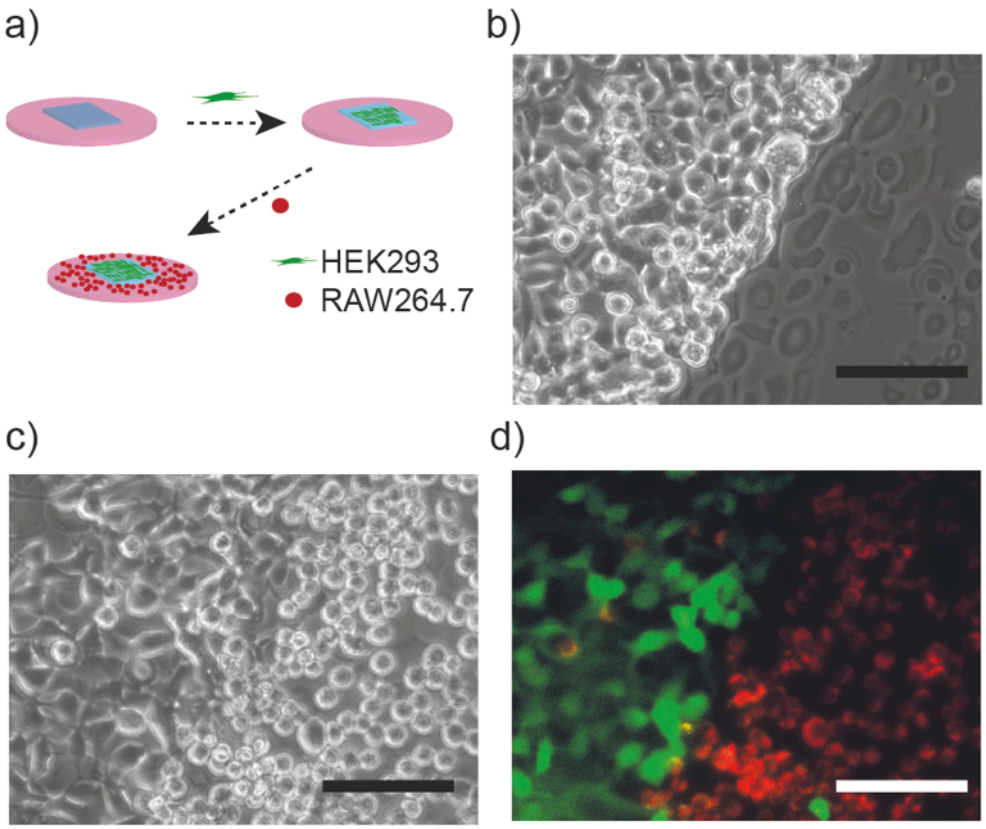

Figure 4.6: (a) Schematic of co-culture procedure (b) HEK293 Cell adhesion on protein patterns (c) optical and (d) fluorescence micrograph of the co-culture pattern (green: GFP-expressed HEK293; red: DiD lipophilic tracer labeled RAW264.7). Scale bars were 100 μm.

4.3 Conclusion

In summary, we have a high-throughput method to designing stable, functional biomaterials by combining inkjet deposition of protein inks with a nanoimprint lithography based methodology. This strategy readily incorporates the intrinsic properties of the protein and transmutes the individual protein components into stable biomolecular films. The environmentally friendly processing taken with the parametric control over the surface chemistry provides a multidimensional platform for understanding and controlling biological interactions with protein coated surfaces. In addition, NIL not only provides stabilization of protein films but also smoothen the coffee rings resulting from inkjet

deposition. Due to the spatial and compositional control of inkjet deposition, various functional films can be generated using the combination of different protein precursors to generate functional biomaterials.

4.4 Experimental methods

4.4.1 Materials

Bovine serum albumin and lysozyme were purchased from Fisher Scientific and used without further purification. Silicon wafers were purchased from WRS Materials. Lipophilic tracer, DiD, used for labelling RAW 264.7 cells was purchased from Invitrogen. Glass microscopy slides were purchased from Fisher Scientific. MilliQ water was purified by using a Millipore water purification system.

4.4.2 Inkjet deposition of protein inks

The bovine serum albumin (BSA) and lysozyme (Lyso) were diluted to a concentration of 5 wt% with 80:20 volume ratio of water/ethanol solution, filtered through a 0.2 μm polypropylene membrane (Puradisc 25AS, Whatman), and syringed into a virgin aftermarket Epson inkjet cartridge for printing (MIS Associates, Auburn Hills, MI USA). For this work, the BSA solution was loaded in magenta channel and the lysozyme solution was loaded in cyan channel. Printing was done using an Epson Artisan 50 inkjet printer (Long Beach, CA USA) which was used as packaged. The protein patterns and ratios deposited on oxygen plasma cleaned silicon wafers or glass slides by setting RGB values corresponding to the cartridge channels in the Print CD software provided with the Epson printer. To ensure fully coverage of protein films, printing procedure was repeated 5 times for each pattern. The glass or silicon wafer substrate was loaded into the printer by taping the bottom of the substrate to the included CD tray. In order to print only the channel of

interest, the color of the pattern has to match the channel printed. To print only the magenta channel, the RGB value must be set to (255,0,255); the cyan channel, (0,255,255). The ICM color management also must be turned off in the Advanced tab of the printer properties to ensure no mixing of the channels occurs. To print BSA/Lyso mixed patterns, the ratio of magenta/cyan were converted into corresponding RGB value on the website: http://web.forret.com/tools/color.asp. The gradient pattern from 100% BSA to 100% Lyso was made by color gradient tool in the Print CD software. Before printing, the printheads were cleaned two times using the "Head Cleaning" function in the Maintenance tab of the printer properties to ensure that the channels were filled.

4.4.3 Nanoimprint lithography

Nanoimprinting of protein films was performed by using a Nanonex NX-2000 nanoimprinter with flat silicon molds. Imprinting was performed at 180 °C and 2.8 MPa for 5 min. All molds were treated with heptadecafluoro-1,1,2,2-(tetrahydrodecyl)dimethyl-chlorosilane at 80 °C for 2 days in a vacuum chamber prior to use.

4.4.4 Profilometer

Topography and roughness was measured by a Zygo Newview 7300 optical profilometer. The thickness was obtained by measuring the scratched films and by using a Rudolph Research Auto EL elliposometer.

4.4.5 Kelvin probe force microscopy

KPFM measurements were performed on a commercial AFM (Asylum Research MFP-3D; Santa Barbara, CA) using a Ti/Ir coated silicon tip (f ~ 70 kHz; k ~ 2 N/m (ASYELEC-01)) to probe the surface potential. During the measurement, the silicon

substrate was kept at ground and the tip sequentially scanned along the top of each composition of BSA/LYSO sample surface to collect the surface potential. All KPFM images were acquired at a scan rate of 0.6 Hz, a 3 V_{AC} applied tip bias, and a 10 nm fixed separation between the tip and sample surface during the second pass.

4.4.6 Cell culture

NIH 3T3 cells were cultured in a humidified atmosphere (5 % CO_2) at 37 °C, and grown in Dulbecco's modified Eagle's medium (DMEM, low glucose) supplemented with 10 % fetal bovine serum (FBS) and 1 % antibiotics (100 U/mL penicillin and 100 μg/mL streptomycin). Cell adhesion experiments were performed by incubating 150,000 NIH 3T3 cells with protein films placed in a 12-well plate for 1 h. The surfaces were then washed by cold phosphate buffer saline (PBS) 3 times to remove floating cells, followed by incubation with 1 mL of fresh media for 23 h. Cells were then stained with Calcein AM and Hoescht 33342 to label cytosol and nucleus, respectively, for fluorescent microscopic imaging according to the protocol from Life Technology using an Olympus IX51 microscope with excitation wavelengths of 470 nm and 535 nm.

4.4.7 Cellular coculture

A total of 200,000 deGFP-expressing HEK293 cells were seeded in a 12-well plate and cultured in Roswell Park Memorial Institute (RPMI) 1640 Medium (DMEM; ATCC 30-2001) with 10% bovine calf serum and 1% antibiotics at 37 °C in a humidified atmosphere of 5% CO2. After 24 hours incubation, the cells were washed with phosphate buffer saline (PBS) for three times and 200,000 of DiD-labeled RAW 264.7 were inoculated and harvested for another 24 hours. After removing medium, the cells were

washed three times with cold PBS for fluorescence imaging under an Olympus IX51 microscope.

4.5 References

(1) N. H. C. S. Silva, C. Vilela, I. M. Marrucho, C. S. R. Freire, C. Pascoal Neto, A.J.D. Silvestre, *J. Mater. Chem. B* **2014**, *2*, 3715.

(2) E. Kharlampieva, V. Kozlovskaya, B. Wallet, V. V Shevchenko, R. R. Naik, R. Vaia, D. L. Kaplan, V. V Tsukruk, *ACS Nano* **2010**, *4*, 7053.

(3) F. G. Omenetto, D. L. Kaplan, *Science* **2010**, *329*, 528.

(4) T. P. J. Knowles, T. W. Oppenheim, A. K. Buell, D. Y. Chirgadze, M. E. Welland, *Nat. Nanotechnol.* **2010**, *5*, 204.

(5) A. R. Murphy, P. S. John, D. L. Kaplan, *Biomaterials* **2008**, *29*, 2829.

(6) W. Zheng, W. Zhang, X. Jiang, *Adv. Healthc. Mater.* **2013**, *2*, 95.

(7) E. S. Gil, B. Panilaitis, E. Bellas, D. L. Kaplan, *Adv. Healthc. Mater.* **2013**, *2*, 206.

(8) Y. Har-el, J. A. Gerstenhaber, R. Brodsky, R. B. Huneke, P. I. Lelkes, *Wound Med.* **2014**, *5*, 9.

(9) S. Gomes, I.B. Leonor, J. F. Mano, R. L. Reis, D. L. Kaplan, *Prog. Polym. Sci.* **2012**, *37*, 1.

(10) J. A. Werkmeister, J. A. M. Ramshaw, *Biomed. Mater.* **2012**, *7*, 012002.

(11) E. Jeoung, B. Duncan, L.-S. Wang, K. Saha, C. Subramani, P. Wang, Y.-C. Yeh, T. Kushida, Y. Engel, M. D. Barnes, V. M. Rotello, *Adv. Mater.*, **2015**, *27*, 6251.

(12) R. Craven, *Nat. Rev. Neurosci.* **2005**, *6*, 585.

(13) R. Murugan, P. Molnar, K. P. Rao, J. J. Hickman, *Int. J. Biomed. Eng. Technol.* **2009**, *2*, 104.

(14) S. Toda, L. R. Blauch, S. K. Y. Tang, L. Morsut, W. A. Lim, *Science* **2018**. (doi: 10.1126/science.aat0271)

(15) S. Javaherian, K. J. Li, A. P. McGuigan, *Biotechniques* **2013**, *55*, 21.

(16) M. Ray, Y.-W. Lee, J. Hardie, R. Mout, G. Yeşilbag Tonga, M. E. Farkas, V. M. Rotello, *Bioconjug. Chem.* **2018**, *29*, 445.

(17) B. Creran, B. Yan, D. F. Moyano, M. M. Gilbert, R. W. Vachet, V. M. Rotello, *Chem. Commun.* **2012**, *48*, 4543.

(18) D. J. Holt, L. M. Chamberlain, D. W. Grainger, *Biomaterials*, **2010**, *31*, 9382.

(19) J. Fukuda, A. Khademhosseini, J. Yeh, G. Eng, J. Cheng, O.C. Farokhzad, R. Langer, *Biomaterials*, **2006**, *27*, 1479.

CHAPTER 5

TRANSLATION OF PROTEIN CHARGE AND HYDROPHILICITY TO MATERIALS SURFACE PROPERTIES USING THERMAL TREATMENT IN FLUOROUS MEDIA

5.1 Introduction

Protein-based materials provide a uniquely sustainable and biocompatible platform for biological applications.[1,2,3] The inherent structural and surface diversity of proteins makes them versatile building blocks for functional materials for use in medical implants,[4] tissue engineering,[5,6,7] drug delivery,[8,9,10] and bioelectronics.[11, 12, 13] Furthermore, the aqueous processability and biodegradability of proteins produces minimal environmental impact, making them ideal building blocks for eco-friendly materials.[14]

The vast majority of applications of protein films require stability in aqueous environments[15,16] Current strategies to produce aqueous-stable protein films include: (i) Using a relatively limited range of naturally self-assembling proteins, such as silk fibroin, to produce stable protein films.[17] However, post-functionalization techniques[18] or protein engineering[19] are required to generate films with diverse surface properties while using this strategy. (ii) Employing cross-linkers to create polymeric structures by covalent bonding of proteins.[20] However, the unreacted additives retained by the resulting cross-linked protein film can adversely alter film properties.[21, 22] Moreover, many commercially available cross-linkers are toxic and therefore hinder the applicability of such materials in biological systems.[23] (iii) Heat-curing provides a universal and readily employed platform for fabricating films from any protein precursor.[24] Traditional heat curing, however, results in denaturation of the protein precursors. This loss of structure leads to hydrophobic films

that do not retain the surface properties of the native protein, in particular their overall charge and inherent zwitterionic nature. As a result, these hydrophobic surfaces can induce severe protein/bacterial fouling,[25] and trigger immune responses.[26]

Beyond their eco- and biocompatible composition, the use of proteins as building blocks for materials applications has the potential to leverage structural components of proteins, such as charge and hydrophobicity, to provide control over film surface properties.[27] We previously developed an additive-free, thermal nanoimprint lithography (NIL)-based methodology for developing protein-based functional biomaterials on two-dimensional substrates.[28] These NIL-stabilized films retained substantial native protein structure, concomitantly providing inherently hydrophilic, zwitterionic and biodegradable films. Through choice of protein, the surface charge of these films could be readily controlled. Due to the nature of NIL, however, this method could only be used for flat (2D) surfaces.

5.2 Results and Discussion

The NIL-based strategy for generating stable protein films employed a combination of heat and pressure applied using a fluorosilane-modified stamp. We hypothesized that the retention of surface properties of protein films upon heating in the NIL process was potentially due to the fluorous environment provided by the fluorinated stamp,[29] as opposed to the effect of the compression pressure. Fluorous media, also known as perfluorocarbon fluids are inert, stable and immiscible with water. These unusual immiscibility and stability properties have led to the use of fluorous media as an alternative to water for performing polymerization.[30] We hypothesized that these immiscible and non-reactive properties prevent the dissolution of protein films in the heating media, as well as

protein rearrangement on the surface upon heating. This results in the formation of water stable and hydrophilic protein films. This hypothesis was tested by the comparison of surface properties of protein films heat cured in a fluorous solvent versus those heated in air (Figure 5.1). The protein films cured in the fluorous environment retained a much higher degree of native protein structure and were substantially more hydrophilic than those heated in air. We report here the creation and characterization of stable protein films through heat treatment in fluorous media, and demonstrate the versatility of this strategy through fabrication of antifouling coatings on complex three-dimensional surfaces.

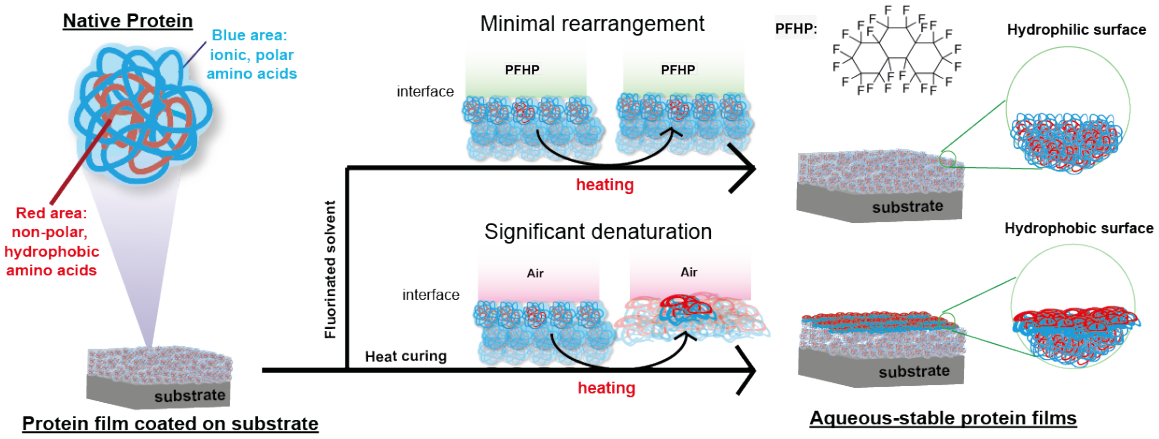

Figure 5.1: Methods for protein film fabrication. Proteins were spin-cast and then heated in either fluorous solvent (perfluoroperhydrophenanthrene, PFHP) or air to generate stable thin films. Fluorous solvent provides an environment that prevents protein denaturation at the interface, resulting in hydrophilic films that retain intrinsic properties of the precursor proteins. In contrast, heat curing in air results in protein denaturation to minimize surface energy, resulting in the generation of hydrophobic films.

Our initial protein stabilization and denaturation studies focused on bovine serum albumin (BSA, an anionic protein). Protein films of thickness ~200 nm were generated by spin-casting 10% w/w BSA solution onto plasma-cleaned substrates.These water-soluble films were next stabilized by heating at 180°C in perfluoroperhydrophenanthrene (PFHP), air, or using NIL. The secondary structure of protein building blocks in each film was

characterized using circular dichroism spectroscopy. Consistent with our prior studies, a substantial amount of the secondary structure was retained in films stabilized by PFHP and NIL. In contrast, protein films stabilized by traditional heat-curing (HC) resulted in essentially complete loss of native structure (Figure 5.2a). Protein denaturation induces surface hydrophobicity due to the migration of hydrophobic residues to the film surface to minimize interfacial energy. The correlation between structure retention and surface hydrophobicity of protein films was quantified through contact angle measurement. NIL and PFHP stabilization methods both provide hydrophilic surface (Figure 5.2b). In contrast, heat-curing in air generates hydrophobic surface (Figure 5.2b). Taken together, these results indicate that fluorous environment prevents proteins from significant denaturation while heating, thus enabling the fabrication of hydrophilic protein films.

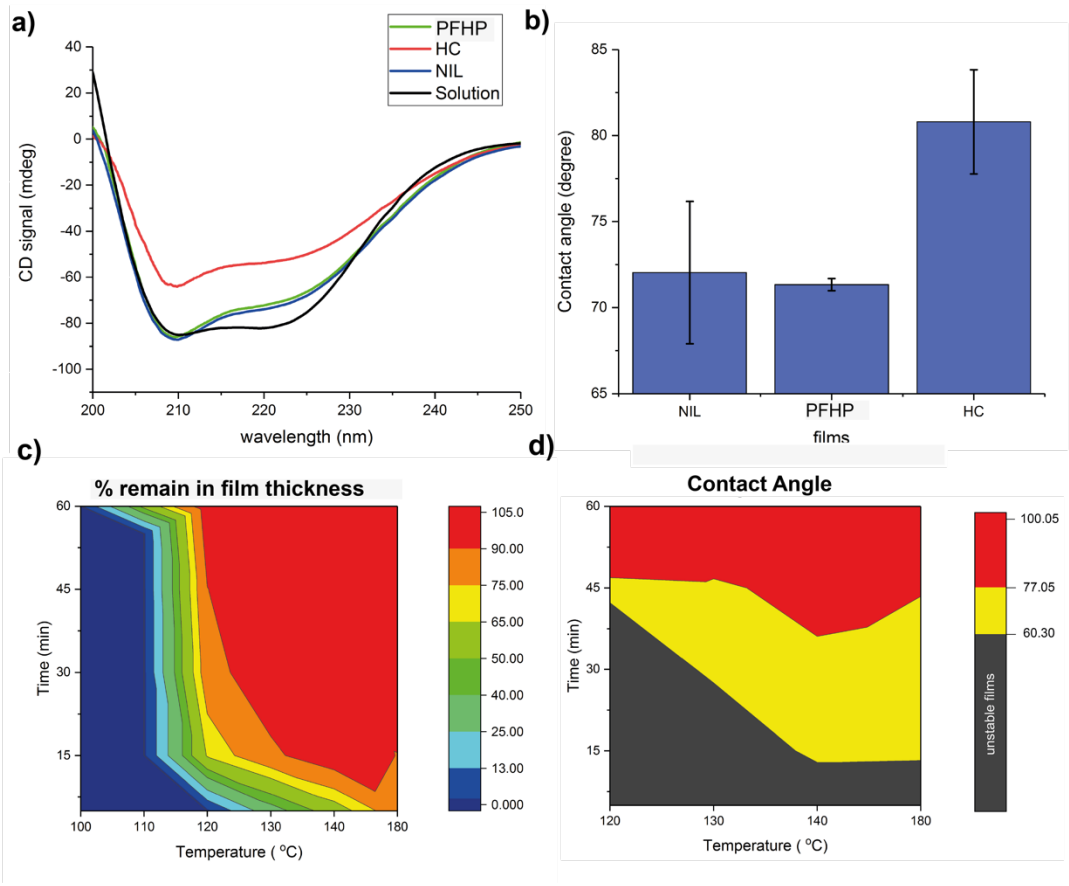

Figure 5.2: Structural and surface characterization of protein films. a) Circular dichroism spectra of BSA in phosphate buffer (solution), and BSA films prepared by nanoimprinting (NIL), heat-curing (HC) and stabilizing in PFHP (PFHP). b) Water contact angle on BSA films stabilized by NIL, PFHP and heat-curing methods. c) Heat map showing the effect of time and temperature on film stability in water. Films were washed for 1 min with water and the thickness measured by ellipsometry after drying. d) Heat map showing the effect of time and temperature on film hydrophilicity. Water contact angle was measured by static sessile drop method using 2 µL of water.

The processing temperature and time in PFHP method were varied to determine the conditions at which aqueous stability was achieved and hydrophilicity of protein films was maintained (Figure 5.2c-d). The results demonstrate that stable films were generated at temperatures > 140°C in 15 min when heating in PFHP. These films were stable in PBS without degradation or dissolution for more than 10 days (Figure 5.3). In addition, no residue of fluorine in protein films was observed even at the highest operation temperature

(Figure 5.4), indicating that no chemical reaction occurred between fluorous solvent and protein films, nor was any solvent entrained in the film. Stability can also be achieved at lower temperatures by prolonging the heating time. However, such films tend to be slightly more hydrophobic owing to longer exposure to elevated temperatures (Figure 5.2d). Although the protein films stabilized in the fluorous environment were stable in aqueous solution, they are digested by proteases, e.g. trypsin (Figure 5.5), demonstrating their biodegradability.

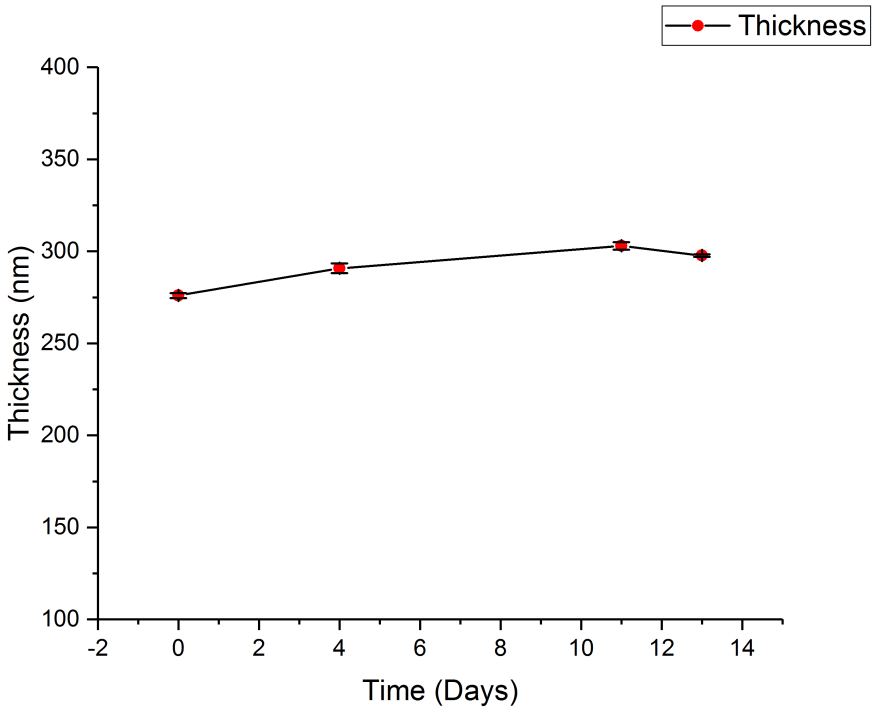

Figure 5.3: Thickness changes of BSA films in PBS. The films were first stabilized using PFHP method at 180 °C for 15 mins, then incubated in PBS solution for 13 days. The slightly increase of thickness was presumably due to the swelling effect.

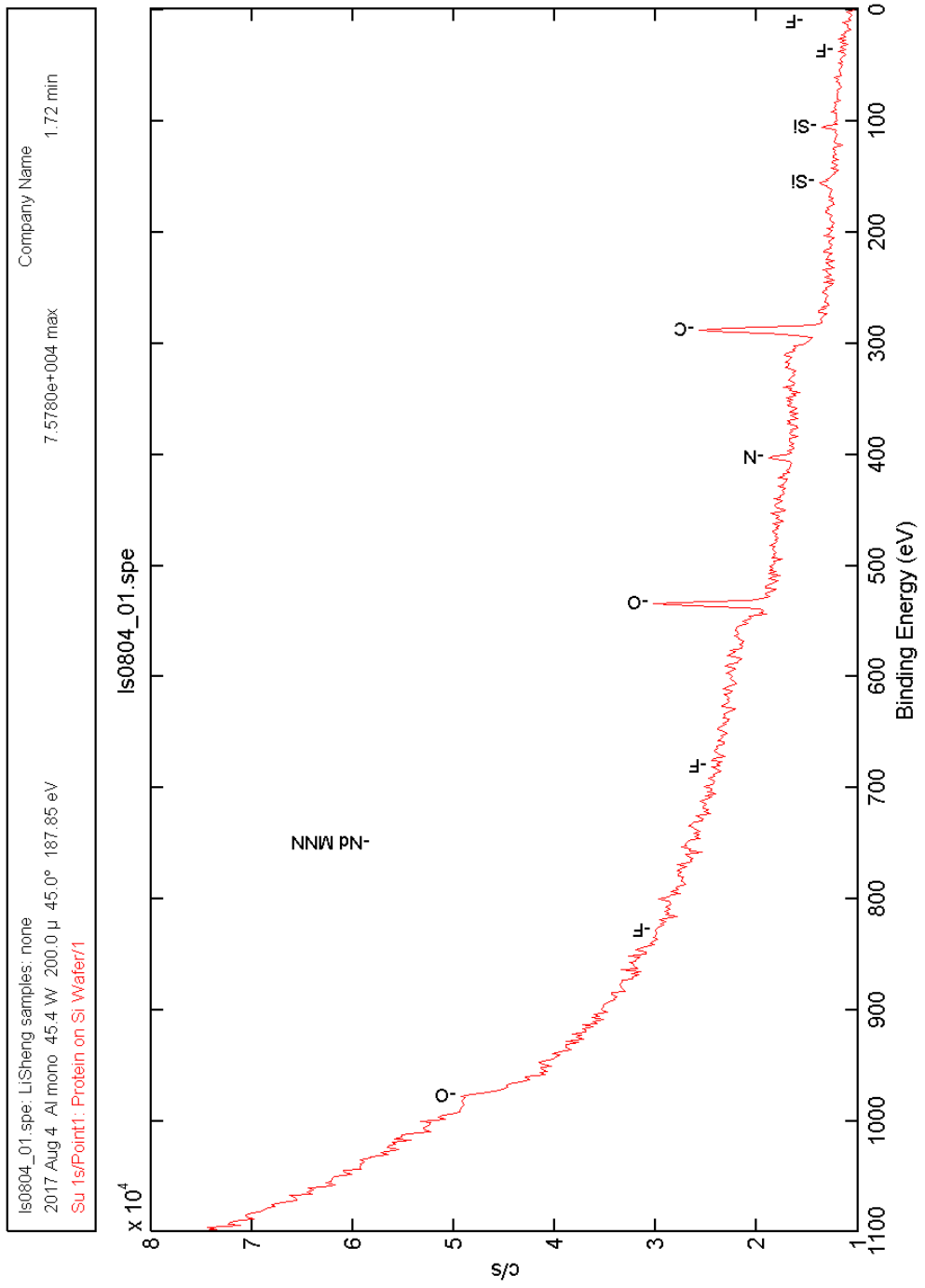

Figure 5.4: X-ray photoelectron spectroscopy of PFHP stabilized BSA film.

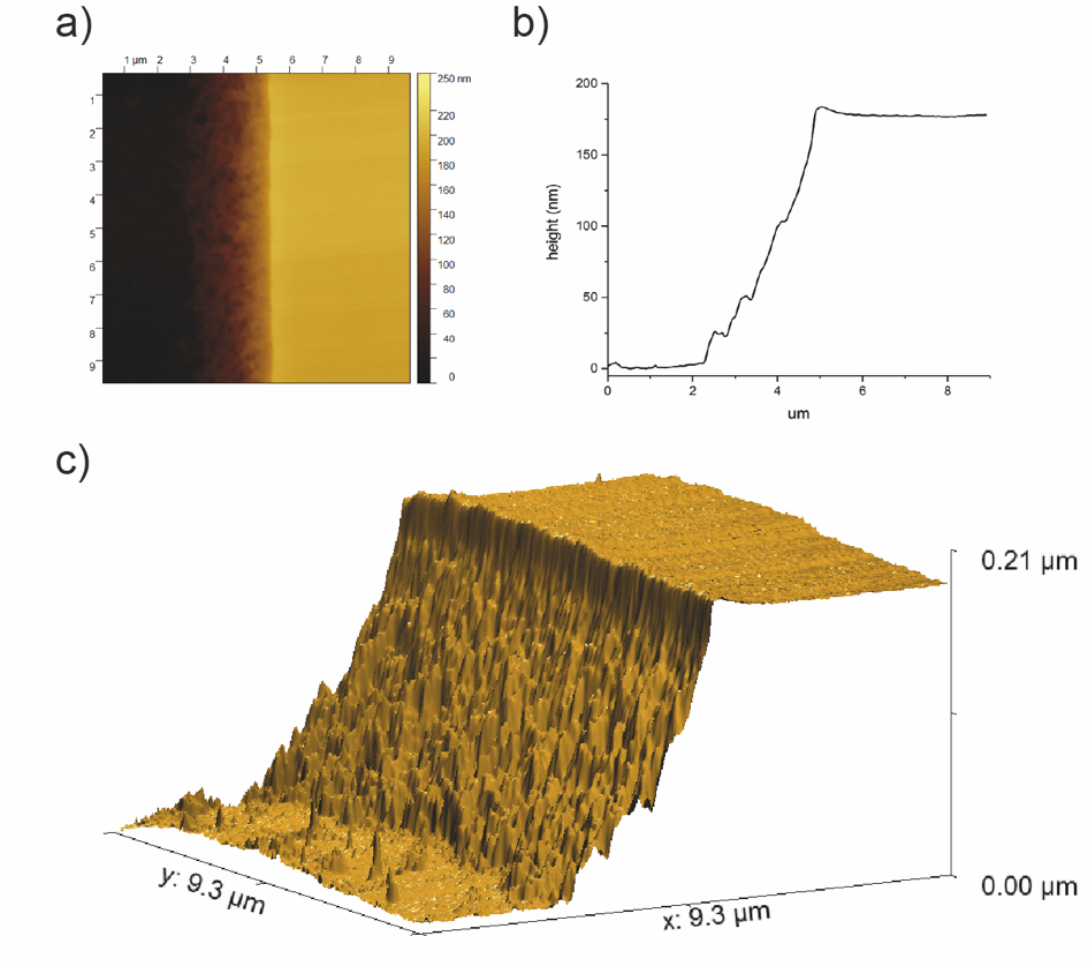

Figure 5.5: AFM images of PFHP film treated with protease. a) Topographic image b) cross-section and c) 3D reconstruction of PFHP film, in which the left-half of the film was incubated in 0.05% trypsin solution for 24 hours.

The retention of protein structure and surface hydrophilicity of films heated in fluorous solvent implies that proteins' molecular properties, such as degradability and surface charge, can be translated into macroscopic films for different biomaterial applications. The translation of surface charge into protein films was demonstrated using cationic lysozyme (LYSO, pI 11) and anionic BSA (pI 4.8) as protein precursors. The surface potential of resulting films was quantified using Kelvin Probe Force Microscopy (KPFM). As expected, the PFHP-LYSO surface exhibits a more positive surface potential

as compared to PFHP-BSA (Figure 5.6a). The potential difference between PFHP-LYSO and PFHP-BSA is 0.28V, which remains consistent with our previous research with NIL films. In contrast, hydrophobic heat-cured films present a lower surface potential for both BSA and LYSO surfaces, and the difference between the surface potential is significantly lesser. The loss of surface property of protein precursors in traditional heat cured films was presumably due to the oxidation reactions that occur upon heating.[31]

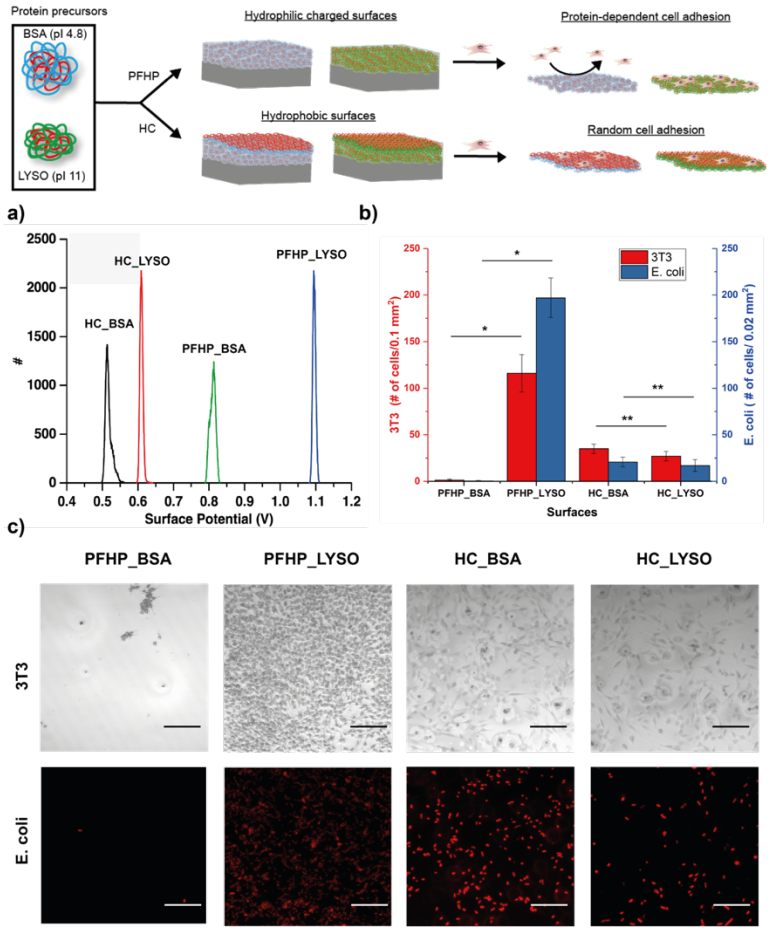

Figure 5.6: Cellular adhesion to protein films. a) Surface potential of BSA and LYSO films fabricated by HC or PFHP method as determined by Kelvin probe force microscopy (KPFM). b) Number of mammalian cells (3T3) and bacterial cells (*E. coli*) adhered on protein films. c) Optical and fluorescent microscopy images for mammalian and bacterial cells adhered on protein films. Scale bars are 200 µm and 60 µm for 3T3 and *E. coli* respectively. *p<0.0005, **p>0.05 (n=5).

The surface properties of protein films can be tailored to the biomaterial application. For example, positively charged surfaces promote cellular attachment, which can be employed for tissue engineering. Conversely, zwitterionic or negatively charged surfaces are suitable for bio-inert coatings, especially for medical implants.[32] Based on our capability of controlling the surface potential of protein films, a functional demonstration of charged protein films was performed by cellular adhesion studies. 3T3 fibroblast cells were seeded onto the protein films for 24 hours and examined by microscopy after washing with PBS (Figure 5.6b). PFHP-LYSO provided excellent adhesion for 3T3 cells, while PFHP-BSA showed essentially complete anti-fouling. These results are in agreement with our previous observations with the NIL films. In contrast, heat-cured films show no control of cellular adhesion, indicating the surface properties of protein precursors were lost during the stabilization process. Similar behavior of protein films was observed with bacterial adhesion. PFHP-BSA showed complete resistance to bacterial fouling, while PFHP-LYSO triggered a strong interaction with bacteria. These results, along with the contact angle studies, indicate the importance of the use of the fluorous environment in the retention the surface hydrophilicity and consequently the ability to control protein films properties.

The stabilization of protein films using heating in fluorous media provides a technology for generating seamless protein coatings on three-dimensional (3D) substrates. Medical devices with complex geometry, e.g. dental and orthopedic implants, are often susceptible to bacterial contamination.[33] Protein films, being biocompatible, are potentially advantageous candidates for antifouling coatings on such implants. Based on the cellular adhesion studies, BSA was chosen to generate antifouling coating on dental implant screws

as a functional demonstration. The BSA coatings showed comparable antifouling properties with conventional polyethylene glycol coated surfaces. Moreover, the BSA coatings continued to prevent bacterial fouling over prolonged exposure for 3 days. In addition, similar antifouling property was observed regardless of the deposition methods (Figure 5.7, Figure 5.8). An oxygen plasma-cleaned screw was dip-coated with 20% w/w BSA solution, and the coating was stabilized using heating in PFHP. To verify that the coating was uniform and seamless, coated and uncoated screws were stained by incubating in a Brilliant Blue staining solution for 10 min. The protein film is prone to strong electrostatic interaction with Brilliant Blue resulting in a blue-colored screw after washing. In contrast, the bare screw showed no retention of Brilliant Blue after washing (Figure 5.9a). Another evidence of uniform coating was observed by scanning electron microscopy. The topography of the coated is smooth as compared to that of the bare screw, which is explained by the attachment of a uniformly-coated thin protein film. The retention of functionality of the BSA film was demonstrated by incubating both bare and coated screws in DsRed-expressing *E. coli* for 24 hours. Fluorescence microscopy images show that the BSA-coated screw prevents bacteria adhesion uniformly throughout the screw while substantial amounts of *E.* coli were observed on the bare screw, especially between the threads. To test the mechanical stability of BSA coatings, the BSA-coated screws were screwed into a synthetic bone mimic PU block (10 PCF polyurethane foam, Sawbones) then extracted via unscrewing.[34] Although there were some small cracks observed in SEM image (Figure 5.9b), the overall coating remained attached after extraction (Figure 5.9a). These results demonstrate that the PFHP-stabilized protein films can be employed to generate anti-fouling BSA coatings on medical implants such as dental screws.

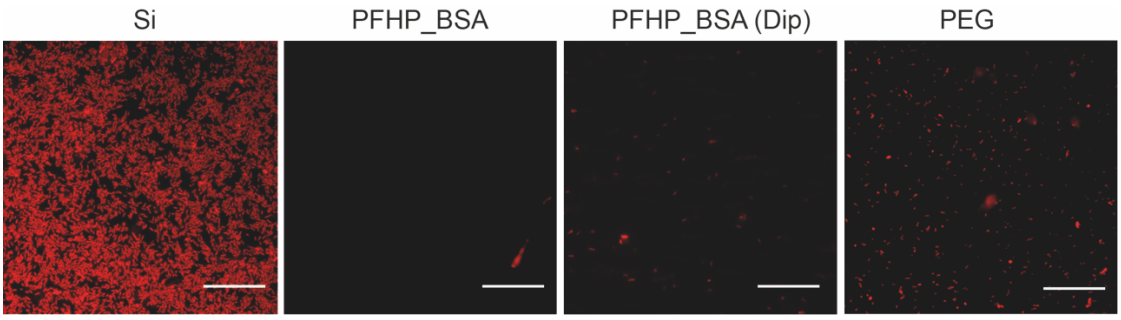

Figure 5.7: Fluorescent microscopy images for *E. coli* cells adhered on Si wafer, PFHP_BSA, PFHP_BSA prepared by dip coating, and polyethylene glycol (PEG) coated surfaces after one day of incubation. Scale bars are 60 um. The PEG coated surface was prepared following Liying's procedure.[35] Plasma cleaned silicon wafers were immersed in a 95% ethanol solution containing 3% 2-[methoxy(polyethyleneoxy)$_{6-9}$propyl]trimethoxysilane (Gelest) at 37 ^{o}C for 3 hours, following by washing with deionized water and dried with N_2 gas.

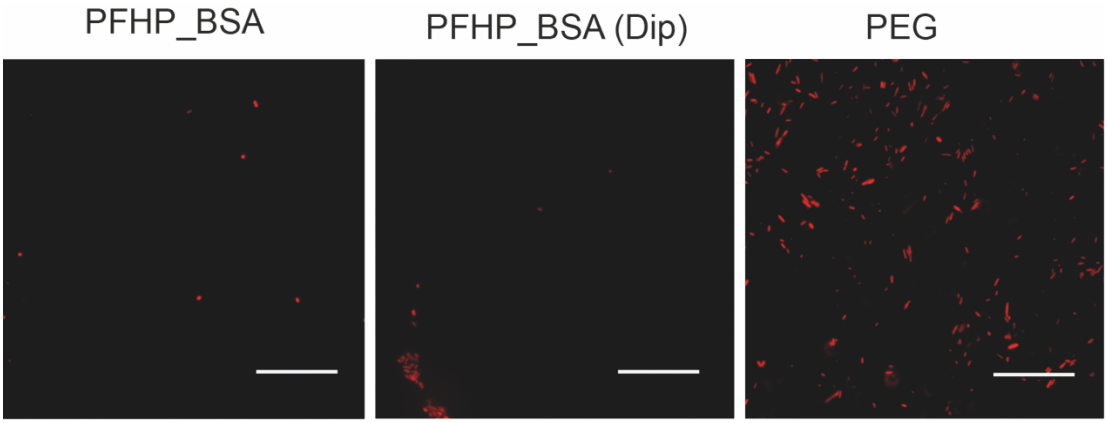

Figure 5.8: Fluorescent microscopy images for *E. coli* cells incubated with PFHP_BSA, PFHP_BSA prepared by dip coating, and PEG coated surfaces for 3 days. Scale bars are 60 μm.

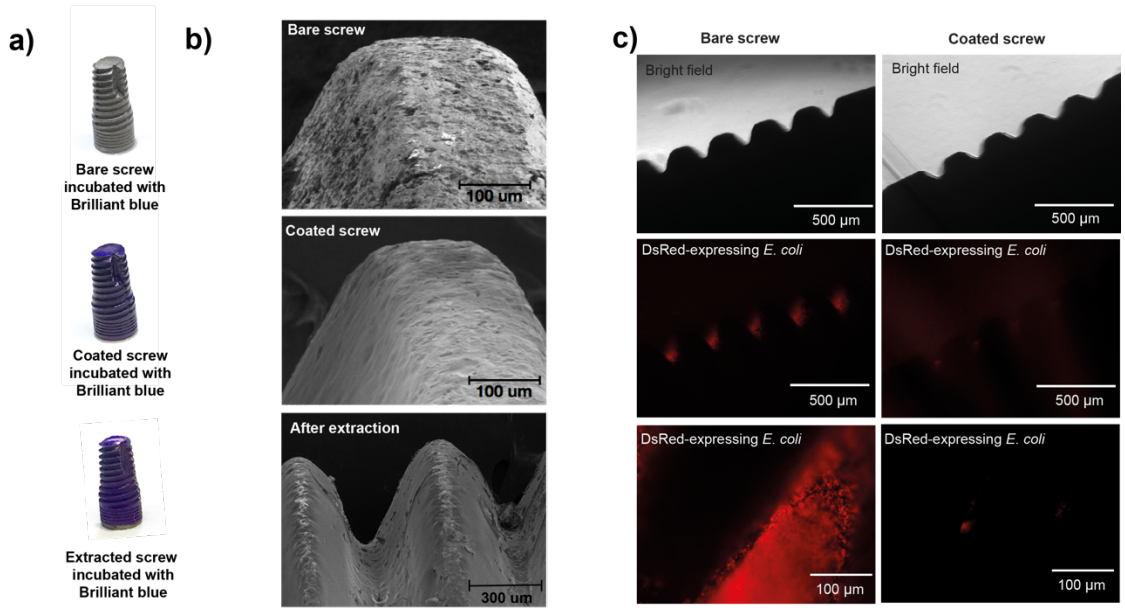

Figure 5.9: Three-dimensional protein film coating on dental implant screw. a) Images of brilliant blue stained screws that are bare, BSA coated, and extracted from a bone mimic PU block. b) Scanning electron microscopic images for bare, coated, and extracted screws. c) Optical and fluorescent microscopy images of DsRed-expressing *E. coli* on bare and coated screws after 24 hours incubation.

5.3 Conclusion

In summary, we have demonstrated that the fluorous environment provided by PFHP preserves protein structure upon heating, preventing protein denaturation and hydrophobic rearrangement at the interface, while generating stable films. Thus, aqueous-stable protein films were fabricated without the use of additives. The protein film retained intrinsic physical properties from the precursor proteins that allowed for the fabrication of biocompatible and versatile functional protein films by altering the choice of protein precursors. The versatility of this coating procedure was demonstrated through generation of antifouling coatings on medically relevant 3D substrates. Taken together, our study provides a scalable and generalizable route for the creation of surface derived from the vast variety of naturally-occurring as well as engineered proteins. Moreover, it widens the scope

of functional protein coatings to medically relevant 3D devices such as antifouling implants and drug eluting stents.

5.4 Experimental methods

5.4.1 Materials

BSA and Lyso were purchased from Fisher Scientific and used without further purification. Perfluoperhydrophenanthrene and tetradecafluorohexane were purchased from Sigma-Aldrich. Silica wafers were purchased from WRS Materials. Quartz microscopy slides were purchased from Electron Microscopy Sciences. MilliQ water was purified by using a Millipore water purification system. Titanium dental implant screw was purchased from Alpha Bio Tec.

5.4.2 Film preparation

10% w/w solutions of protein in MilliQ water were spin-coated at 300 rpm for 25 seconds onto an oxygen plasma cleaned silicon substrate or quartz slides, yielding a thin film of protein.

5.4.3 Protein film stabilized by fluorous solvent

As-prepared protein films were incubated in preheated perfluoperhydrophenanthrene solvent at 180 °C for 15 mins, following by washing with tetradecafluorohexane.

5.4.4 Protein film stabilized by Nanoimprint Lithography (NIL)

Nanoimprinting of protein films was performed by using a Nanonex NX-2000 nanoimprinter with silicon molds. Imprinting was performed at various temperatures and pressures for 5 min. All molds were treated with heptadecafluoro-1,1,2,2-(tetrahydrodecyl) dimethylchlorosilane at 90 °C for 2 days in a vacuum chamber.

5.4.5 Kelvin probe force microscopy (KPFM)

KPFM measurements were performed on a commercial AFM (Asylum Research MFP-3D; Santa Barbara, CA) using a Ti/Ir coated silicon tip (f ~ 70 kHz; k ~ 2 N/m (ASYELEC-01)) to probe the surface potential. During the measurement, the silicon substrate was kept at ground and the tip sequentially scanned along the top of each sample surface to collect the surface potential. All KPFM images were acquired at a scan rate of 0.6 Hz, a 3 V_{AC} applied tip bias, and a 10 nm fixed separation between the tip and sample surface during the second pass.

5.4.6 3D coating

Dental implant screw was cleaned by oxygen plasma before dip coating with 20% w/w BSA solution. The screw was dried in a flame hood for 3 hours before heating in fluorous solvent. After washing with tetradecafluorohexane, the screw was dried by nitrogen gas.

5.4.7 Cell Culture

Mouse fibroblast cells 3T3 (ATCC CRL-1658) were cultured in Dulbecco's modified Eagle's medium (DMEM; ATCC 30-2002) supplemented with 10% bovine calf serum (ATCC 30-2030) and 1 % antibiotics in T75 flasks. Cells were maintained at 37 °C in a humidified atmosphere of 5 % CO_2 and were sub-cultured once in 4 days.

5.4.8 Cellular Adhesion

3T3 cells grown in T75 flasks were washed with phosphate buffered saline (PBS), trypsinized with 1X trypsin and collected in DMEM media. Cells were centrifuged and were re-suspended in fresh DMEM media and counted by using a hemocytometer. Protein film coated surfaces were placed in a six-well plate where 3T3 cells were added to each

well (100000 cells/well) and incubated for 48 h at 37 °C in a humidified atmosphere of 5 % CO_2.

5.4.9 Bacterial adhesion

DsRed-expressing *E. coli* bacteria were inoculated in 3 mL LB broth and grown to stationary phase at 37 °C. The cultures were then diluted to O.D 0.1 in an M-9 media supplemented with 1 mM IPTG (isopropyl β-D-1-thiogalactopyranoside).[36] 2 mL of the dilution was poured onto the surfaces kept in 12 well culture plates. The surfaces were kept at 25 °C and the bacteria were allowed to grow for 24 hours. In general, the surfaces with bacteria were rinsed with PBS three times before analysis under the microscope.

To test the extent of anti-fouling over prolonged exposure, the surfaces were challenged with DsRed-expressing *E. coli* bacteria for 3 days. The cultures were as described above on Day 1. The bacteria solution was replaced with fresh OD 0.1 bacteria solution each day for two additional days. The surfaces were washed and characterized as described above on Day 4, after a total exposure of 3 days.

5.4.10 Characterization

Bright field images and fluorescence were detected by using an Olympus IX51 microscope with excitation wavelengths of 470 nm and 535 nm. AFM imaging of the surfaces was done on a Dimensions 3000 (Veeco) in tapping mode using a RTESP7 tip (Veeco). The film thickness of the protein films was measured by a Rudolph Research Auto EL ellipsometer. Far-UV circular dichroism (CD) spectra were measured on a JASCO J-720 spectropolarimeter with a quartz cuvette of 1 mm path length at 25 °C. The spectra were recorded from 200 to 260 nm as an average of three scans at a rate of 20 nm/min. X-ray photoelectron spectroscopic (XPS) analysis was performed on a Physical Electronics

Quantum 2000 spectrometer using a monochromatic Al Kα excitation at a spot size of 10 mm with pass energy of 46.95. Chemically distinct species were resolved using a Gaussian Lorentzian function with nonlinear least-squares fitting procedure.

5.5 References

(1) F. G. Omenetto, D. L. Kaplan, *Science* **2010**, *329*, 528.

(2) L.-S. Wang, A. Gupta, B. Duncan, R. Ramanathan, M. Yazdani, V. M. Rotello, *ACS Biomater. Sci. Eng.* **2016**, *2*, 1862.

(3) Y.-C. Chen, H.-C. Yu, C.-Y. Huang, W.-L. Chung, S.-L. Wu, Y.-K. Su, *Sci. Rep.* **2015**, *5*, 10022.

(4) L. Uebersax, T. Apfel, K. M. R. Nuss, R. Vogt, H. Y. Kim, L. Meinel, D. L. Kaplan, J. A. Auer, H. P. Merkle, B. von Rechenberg, *Eur. J. Pharm. Biopharm.* **2013**, *85*, 107.

(5) R. Zhu, Y.-X. Chen, Q.-F. Ke, Y.-S. Gao, Y.-P. Guo, *J. Mater. Chem. B* **2017**, *5*, 5009.

(6) C. Dhand, S. T. Ong, N. Dwivedi, S. M. Diaz, J. R. Venugopal, B. Navaneethan, M. H. Fazil, S. Liu, V. Seitz, E. Wintermantel, R. W. Beuerman, *Biomaterials* **2016**, *104*, 323.

(7) H. Knopf-Marques, M. Pravda, L. Wolfova, V. Velebny, P. Schaaf, N. E. Vrana, P. Lavalle, *Adv. Healthc. Mater.* **2016**, *5*, 2841.

(8) M. Rezvanian, N. Ahmad, M. C. I. Mohd Amin, S.-F. Ng, *Int. J. Biol. Macromol.* **2017**, *97*, 131.

(9) M. A. Brenckle, B. Partlow, H. Tao, M. B. Applegate, A. Reeves, M. Paquette, B. Marelli, D. L. Kaplan, F. G. Omenetto, *Adv. Funct. Mater.* **2016**, *26*, 44.

(10) C. S. B. Gil, V. S. B. Gil, S. M. Carvalho, G. R. Silva, J. T. Magalhaes, R. L. Orefice, A. Mansur, H. S. Mansur, P. S. O. Patricio, L. C. A. Oliveira, *New J. Chem.* **2016**, *40*, 8502.

(11) Q. Wang, M. Jian, C. Wang, Y. Zhang, *Adv. Funct. Mater.* **2017**, *27,* 1605657.

(12) Y. Shon, H. Kim, H. S. Hwang, E. S. Bae, T. Eom, E. J. Park, W.-S. Ahn, J. J. Wie, B. S. Shim, *Sensors Actuators B Chem.* **2017**, *244*, 1.

(13) M. Oliviero, R. Rizvi, L. Verdolotti, S. Iannace, H. E. Naguib, E. Di Maio, H. C. Neitzert, G. Landi, *Adv. Funct. Mater.* **2017**, *27*, 1605142.

(14) J. Gu, Y. Su, P. Liu, P. Li, P. Yang, *ACS Appl. Mater. Interfaces* **2017**, *9*, 198.

(15) D. Wang, Y. Ha, J. Gu, Q. Li, L. Zhang, P. Yang, *Adv. Mater.* **2016**, *28*, 7414.

(16) Y. Zhao, Q. Jiang, H. Xu, N. Reddy, L. Xu, Y. Yang, *J. Biomed. Mater. Res. Part B Appl. Biomater.* **2014**, *102*, 729.

(17) G. H. Altman, F. Diaz, C. Jakuba, T. Calabro, R. L. Horan, J. Chen, H. Lu, J. Richmond, D. L. Kaplan, *Biomaterials* **2003**, *24*, 401.

(18) D. K. Kim, J. I. Kim, T. I. Hwang, B. R. Sim, G. Khang, *ACS Appl. Mater. Interfaces* **2017**, *9*, 1384.

(19) Y. Kambe, K. Kojima, Y. Tamada, N. Tomita, T. Kameda, *J. Biomed. Mater. Res. Part A* **2016**, *104*, 82.

(20) P. J. Nowatzki, D. A. Tirrell, *Biomaterials* **2004**, *25*, 1261.

(21) J. Sun, L. Yang, M. Jiang, Y. shi, B. Xu, H. Ma, *J. Chromatogr. B* **2017**, *1054*, 57.

(22) R. Güzel, A. Ersöz, İ. Dolak, R. Say, *Mater. Sci. Eng. C* **2017**, *79*, 336.

(23) D. R. Smith, R.-S. Wang, *Environ. Health Prev. Med.* **2006**, *11*, 3.

(24) N. Rangavajhyala, V. Ghorpade, M. Hanna, *J. Agric. Food Chem.* **1997**, *45*, 4204.

(25) S. Chen, L. Li, C. Zhao, J. Zheng, *Polymer.* **2010**, *51*, 5283.

(26) D. F. Moyano, Y. Liu, D. Peer, V. M. Rotello, *Small* **2016**, *12*, 76.

(27) L.-S. Wang, B. Duncan, R. Tang, Y.-W. Lee, B. Creran, S. G. Elci, J. Zhu, G. Yesilbag Tonga, J. Doble, M. Fessenden, M. Bayat, S. Nonnenmann, R. W. Vachet, V. M. Rotello, *ACS Appl. Mater. Interfaces* **2017**, *9*, 42.

(28) E. Jeoung, B. Duncan, L.-S. Wang, K. Saha, C. Subramani, P. Wang, Y.-C. Yeh, T. Kushida, Y. Engel, M. D. Barnes, V. M. Rotello, *Adv. Mater.* **2015**, *27*, 6251.

(29) M. Sarkari, I. Darrat, B. L. Knutson, *Biotechnol. Prog.*, **2003**, *19*, 448.

(30) D.-W. Zhu, *Macromolecules* **1996**, *29*, 2813.

(31) K. R. Millington, H. Ishii, G. Maurdev, *Amino Acids* **2010**, *38*, 1395.

(32) C. Subramani, K. Saha, B. Creran, A. Bajaj, D. F. Moyano, H. Wang, V. M. Rotello, *Small* **2012**, *8*, 1209.

(33) E. H. Abdulkareem, K. Memarzadeh, R. P. Allaker, J. Huang, J. Pratten, D. Spratt, *J. Dent.* **2015**, *43*, 1462.

(34) J. Raphel, J. Karlsson, S. Galli, A. Wennerberg, C. Lindsay, M. G. Haugh, J. Pajarinen, S. B. Goodman, R. Jimbo, M. Andersson, *Biomaterials* **2016**, *83*, 269.

(35) L. Peng, L. Chang, X. Liu, J. Lin, H. Liu, B. Han, S. Wang, *ACS Appl. Mater. Interfaces* **2017**, *9*, 17688.

(36) X. Li, Y.-C. Yeh, K. Giri, R. Mout, R. F. Landis, Y. S. Prakash, V. M. Rotello, *Chem. Commun.* **2015**, *51*, 282.

CHAPTER 6

FABRICATION OF DRUG-ELUTING COATINGS BY HARNESSING ELECTROSTATIC INTERACTIONS WITH NATIVE PROTEIN FILMS

6.1 Introduction

Antimicrobial coatings prevent bacterial contamination of surfaces and materials, [1] with applications in food packaging materials,[2,3] water treatment membranes,[4,5] medical devices,[6,7] and medical implants.[8,9,10] Infections caused by bacterial contamination of medical devices such as stainless-steel IV poles and implants are a serious healthcare problem.[11,12] Nosocomial infections are caused by bacterial colonization on biomedical surfaces in healthcare settings.[13,14] In 2011, more than 700,000 nosocomial infections occurred in the United States, resulting in nearly 75,000 deaths.[15]

Antimicrobial surfaces have shown promise in the prevention of nosocomial infections.[16] The general design of antimicrobial coatings are based on two main strategies - bacteria repulsion[17] and antimicrobial release.[18] Tuning the chemical and morphological characteristics of a surface coating can prevent bacterial adhesion or eliminate bacteria upon contact.[19] On the other hand, biocidal activity can be imparted to polymeric coatings by loading antibacterial agents, such as nanoparticles,[20] halogens,[21] and antibiotics.[22] The release of antimicrobials can efficiently reduce bacteria colonization on biomaterial surfaces as well as in the surrounding environment.

The biocompatibility of coating materials is crucial, especially for medical devices such as implants and catheters that directly contact tissue and biofluids.[23] Therefore, many efforts have been made on increasing the biocompatibility of these coating scaffolds.[24] Proteins in particular, are considered as useful candidates for fabricating functional biomaterials, due to their inherent biocompatibility, biodegradability and functional diversity.[25, 26,27] However, most of the protein-based thin film coatings require the use of cross-linkers to provide aqueous stability, thereby adversely affecting their biocompatibility, degradability, and their overall behavior. [28 29]

In Chapter 5, we developed an additive-free methodology for fabricating protein films using fluorous media,[30] demonstrating that heating films in a fluorous environment provided water-stable films with minimal protein denaturation. This retention of protein structure concomitantly translated the properties of the proteins to the film surface, generating coatings that are hydrophilic and zwitterionic. These surface properties prevent bacterial adhesion, providing promising materials for biomedical applications. [31]

6.2 Results and discussion

Imparting bactericidal properties to protein films provides a strategy for generating biomaterial-based coatings that prevent infections from indwelling devices. We report here the fabrication of protein coatings that serve as a reservoir for the controlled release of antibiotics, with release profiles dictated by the charges of the film and payload. (Figure 6.1). The role of electrostatic interactions on cargo incorporation was quantified using charged fluorescent dyes, demonstrating that loading is enhanced in protein films with complementary charge. The release behaviors were also dominated by these electrostatic

interactions, with rate controlled by degree of electrostatic complementarity. The bactericidal properties of these protein films were demonstrated through generation of antibiotic-loaded protein films featuring efficient drug release and high biocidal activity.

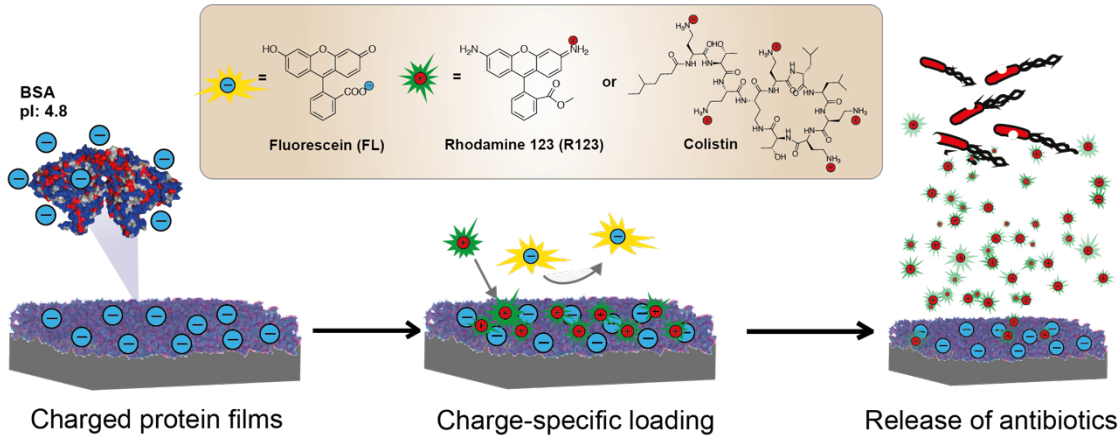

Figure 6.1: Protein films retain their surface properties and can be loaded with charged cargos via electrostatic interaction. Antimicrobial coatings are fabricated by loading negatively charged BSA nanofilms with cationic antibiotics.

Our initial studies focused on bovine serum albumin (BSA) nanofilms. BSA (MW: 66.4 kDa, pI: 4.8) is inexpensive and readily available and is considered a non-reactive protein that has often been used as a blocker in immunohistochemistry.[32,33] The surface charge and inherent zwitterionic property of BSA prevents biomolecular and cellular adhesion, making films from this protein useful as antifouling coatings.[34] BSA films were fabricated by spin-casting a 20% w/w BSA aqueous solution onto plasma-cleaned silicon wafers. These protein films were next stabilized by immersing protein coated substrates into a preheated fluorous media - perfluoroperhydrophenanthrene (PFHP). After curing at 170 °C for 15 min in PFHP, a stable BSA film was generated with thickness ~450 nm.

Films with different thickness were obtained by changing the concentration of precursor protein solution (Figure 6.2a).

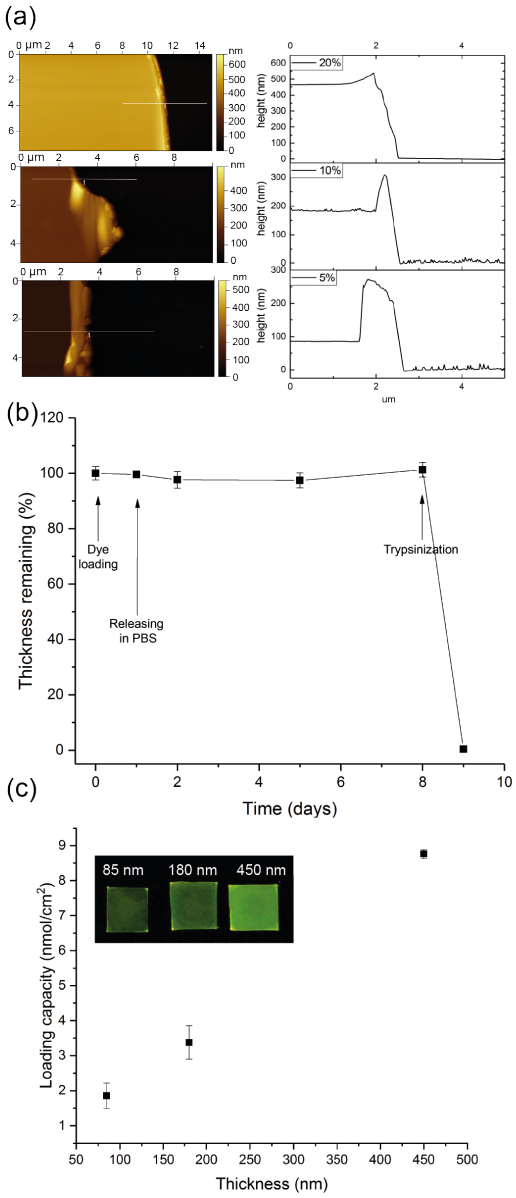

Figure 6.2: (a) Atomic force microscopic images and cross sections for scratched protein films prepared by 5%, 10% and 20% w/w BSA solution. (b) Films stability measured by the change of thickness after loading with dye, incubating in PBS, and treating with protease. (c) Loading capacity of protein films with different thickness (inset is the pictures of films taken under UV irradiation).

The stability of BSA films in aqueous media was tested in phosphate-buffered saline (PBS), before and after loading with R123. The thickness of R123-BSA films was measured after loading with dyes, incubating in PBS and treatment with protease (Figure 6.2b). The thickness of BSA films did not change after loading with R123 for 24 hours. The films remained stable in PBS for 7 days after the release of dyes, but completely degraded in 1 day upon treatment with 0.01M trypsin solution.

The loading capacity of BSA films was quantified by measuring the released dyes from the completely degraded films (Figure 6.2c). The R123-loaded BSA films were placed in 1 mL of 0.01% trypsin for 24 hours, and amount of R123 was determined by a standard curve generated using known concentration of dyes in trypsin solution. The loading capacity increased proportionally to the film thickness, indicating that R123 was successfully incorporated within the BSA films and not simply adhered to the film surface.

The role of electrostatics on the loading properties of protein films was quantified using oppositely charged dyes with similar size and hydrophobicity.[35] Anionic fluorescein (FL) and cationic R123 (0.05 mM) were incubated with BSA films for 1, 3, 6 and 24 hours. Despite the structural similarity of these two dyes, the charge of the molecule significantly affects their loading into the film (Figure 6.3). There is almost no loading observed when the dye is negatively charged (FL), indicating that the electrostatic interaction between payload and film is the dominant factor for cargo loading. To further demonstrate that the charge of the protein film can modulate the loading process, we prepared R123 in a pH 4 solution, in which BSA (pI: 4.8) is positively charged. As expected, the loading of R123 in BSA films at pH 4 decreased substantially when both the cargo and film have the same

charge (Figure 6.3). The inverse was observed when cationic lysozyme films were used (Figure 6.4).

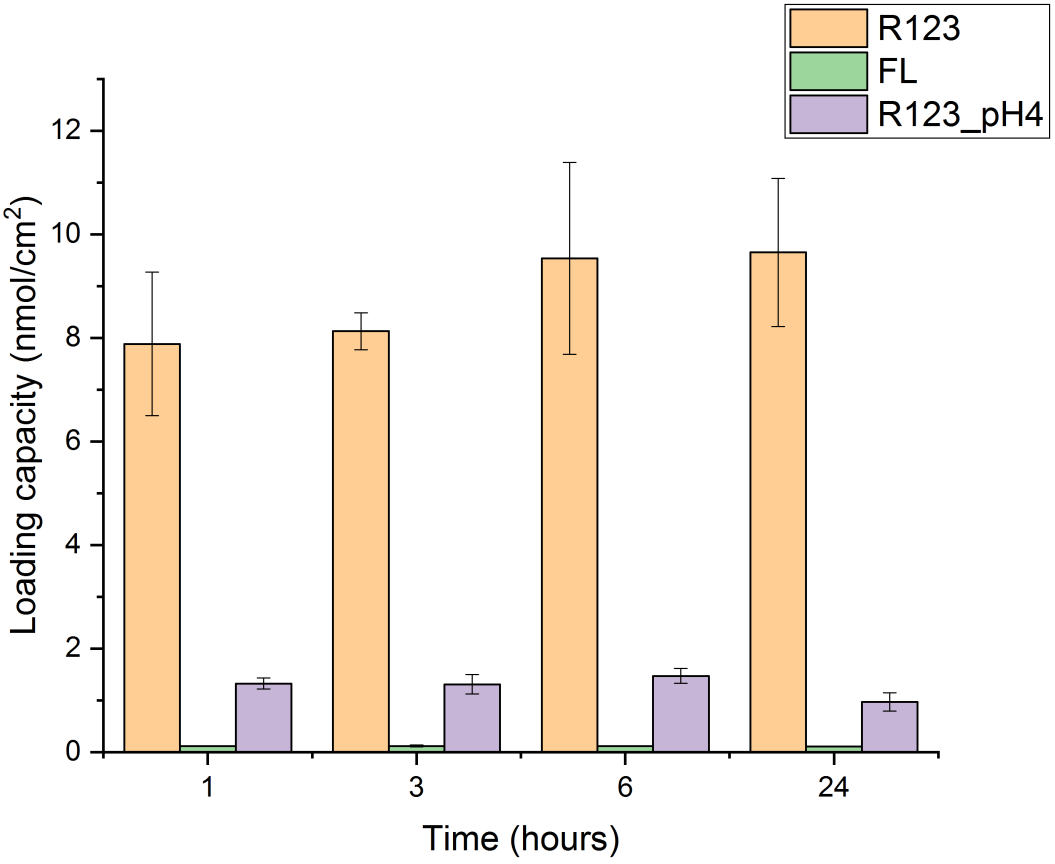

Figure 6.3: Loading capacity of BSA films prepared by incubating with Rhodamine 123 (R123), fluorescein (FL) and R123 in pH 4 for 1, 3, 6 and 24 hours.

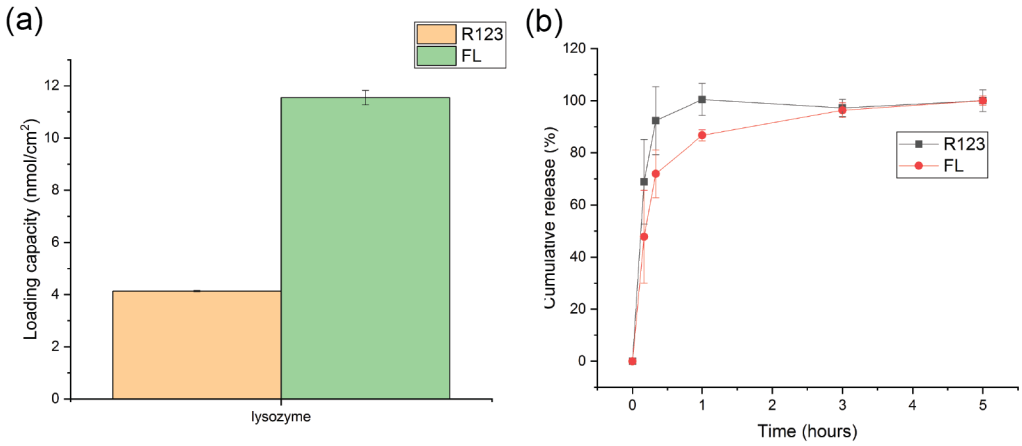

Figure 6.4: Loading and release behavior of dyes in Lysozyme films.

The release behaviour of the films was monitored by measuring the fluorescence intensity of the supernatant at different time intervals. In Figure 6.5a, a burst-release occurred within one hour regardless the charge of cargos. These results confirmed that protein precursors retained their electrostatic properties even after transforming into nanofilms, which is consistent with our previous studies. The effects of ionic strength on the interaction between R123 and BSA films were investigated by varying the salt concentration in solution. We hypothesized that the release behavior of R123 from BSA films would be affected by the salt concentration of the environment due to the change of electrostatic interactions between films and cargos. In low salt conditions (5 mM NaCl), stronger binding between R123 and BSA films was observed, leading to slow release (Figure 6.5b). On the other hand, in high salt solution (150 mM NaCl), the interaction became weaker.

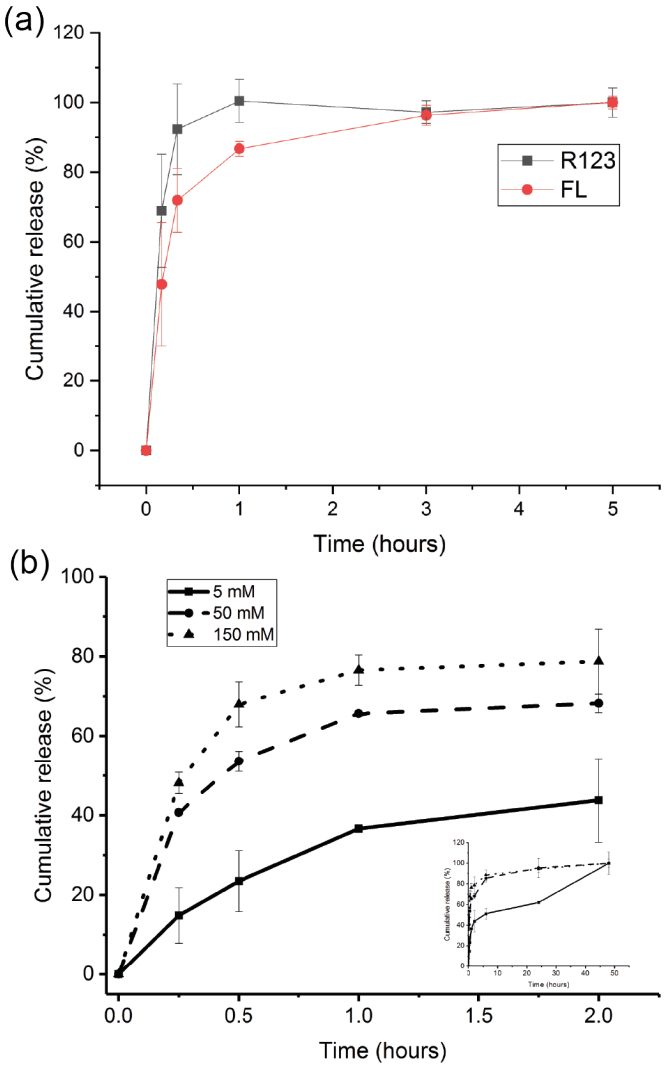

Figure 6.5: (a) Release patterns of dye-loaded BSA films prepared by incubating with 0.05 mM of R123 and FL. (b) Cumulative release of R123 from BSA films in buffers prepared using different sodium chloride concentrations.

The zwitterionic nature and overall negative charge makes BSA ideal for developing antifouling coatings. In fact, BSA has been employed as a non-reactive agent in many immunoassays to prevent non-specific binding on surfaces, e.g. ELISA. This non-fouling behaviour was demonstrated by studying the bacterial adhesion onto BSA-coated dental screws. Red fluorescent protein (RFP) expressing *E. coli* was incubated with protein-coated screws for 24 hours to evaluate the antifouling property of BSA coatings.

The microscopy images show a significant decrease in bacterial adhesion on protein films as compared to a bare dental screw (Figure 6.6). We also prepared antibiotic-loaded BSA films to evaluate the change of antifouling property after loading. We chose colistin as a model system due to its polycationic moiety and efficacy against multidrug resistant strains.[36] BSA-coated screws were loaded with colistin to generate coatings with biocidal properties through controlled antibiotic release (Figure 6.6).

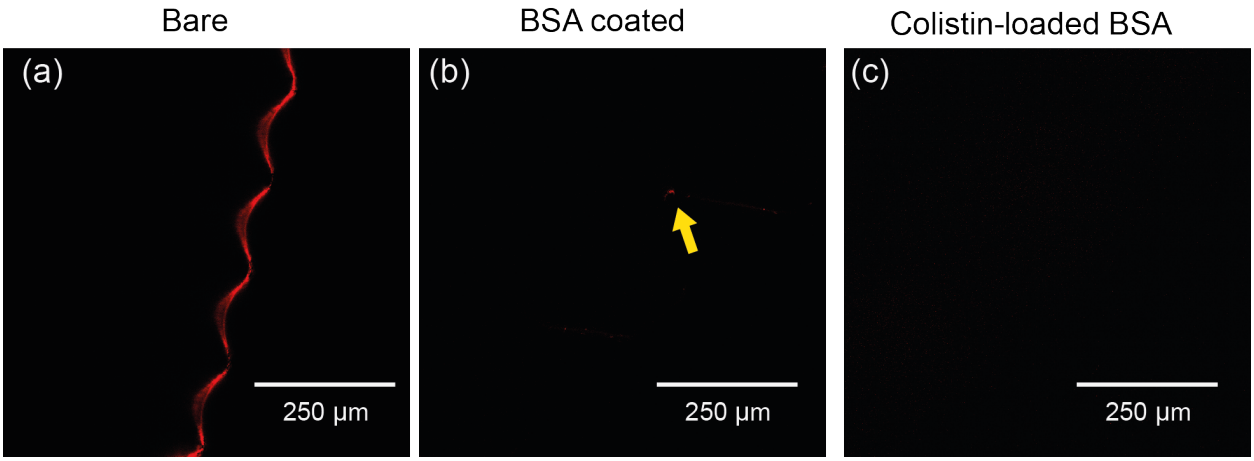

Figure 6.6: Fluorescent microscopy images of (a) bare, (b) BSA-coated and (c) colistin-loaded dental screws incubated with red fluorescent protein (RFP) expressing *E. coli* for 24 hours.

The biocidal efficacy of antibiotic-loaded BSA coatings was further quantified by Kirby-Bauer disk diffusion test. A clear inhibition zone was observed with the colistin-loaded BSA films on 2D substrates (Figure 6.7a). Furthermore, the inhibition zone was greater for thicker films due to their higher loading capacity, indicating that the BSA coatings act as effective drug reservoirs. Conversely, pure BSA coatings showed no antimicrobial activity (Figure 6.7b). We also tested this biocidal behaviour of BSA coatings on 3D substrates. BSA coated screws with and without colistin were inserted into an agar plate with seeded bacteria culture. The results are concordant with the disk diffusion tests

of the 2D coating. It was demonstrated that local release colistin through the drug-loaded screw successfully inhibits bacteria grow in the vicinity of the screw while BSA coatings alone do not possesses any biocidal activity (Figure 6.7c). These results demonstrate that antibiotic-loaded protein coatings are viable candidates for designing superior antibacterial coatings for medical implants due to their antifouling property and localized antibiotic release.

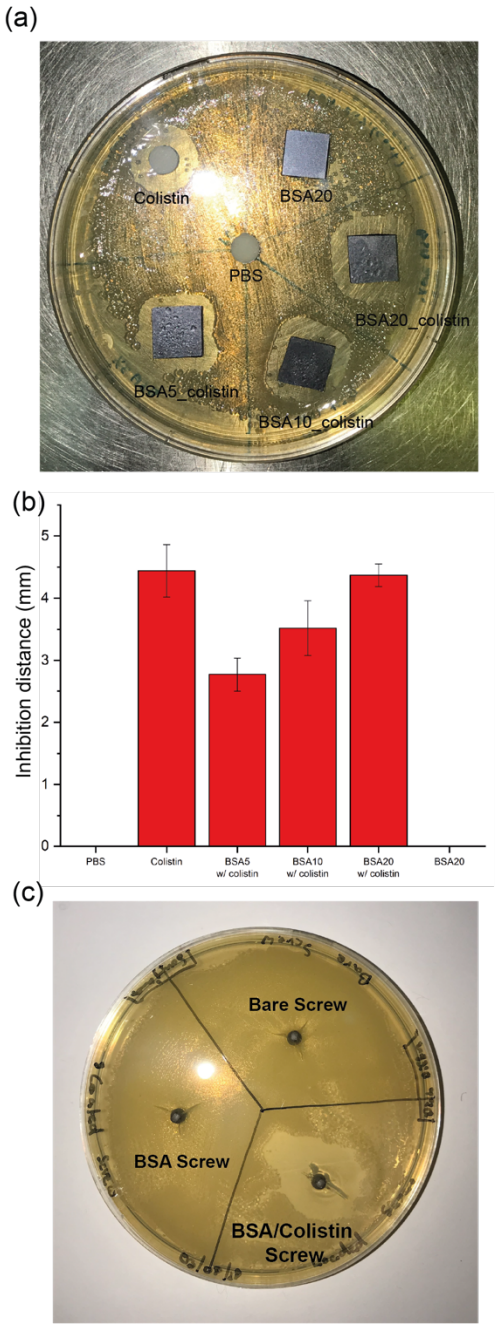

Figure 6.7: (a) Kirby-Bauer disc diffusion antibacterial activity assay for colistin loaded BSA films. (b) Bar graph shows the inhibition distance of colistin, colistin-loaded BSA films with different thickness, and blank BSA film. (c) Kirby-Bauer disc diffusion antibacterial activity assay for BSA-coated screws.

6.3 Conclusion

In summary, we have demonstrated an accessible strategy for fabricating drug-loaded coatings using naturally abundant proteins on 2D and 3D substrates. The protein film fabrication preserves the electrostatic properties of protein precursors thereby facilitating highly selective loading of oppositely-charged cargos. This coating system provides highly biocompatible and degradable platform for drug eluting devices. Moreover, through harnessing the electrostatic interaction of films and cargos, effective antimicrobial coating was obtained by loading antibiotics into antifouling BSA films.

6.4 Experimental methods

6.4.1 Materials

Bovine serum albumin and lysozyme were purchased from Fisher Scientific and used without further purification. Silica wafers were purchased from WRS Materials. Fluorescein, rhodamine 123, and colistin were purchased from Sigma. MilliQ water was purified by using a Millipore water purification system. Titanium dental implant screw was purchased from Alpha Bio Tec.

6.4.2 Film preparation

MilliQ water containing 5-20% of protein by weight were spin-coated at 3000 rpm for 25 seconds onto an oxygen plasma cleaned silicon substrate or quartz slides, yielding a thin film of protein. As prepared protein films were incubated in preheated perfluoperhydrophenanthrene solvent at 180 °C for 15 mins, following by washing with tetradecafluorohexane. Dental implant screw was cleaned by oxygen plasma before dip coating with 20% w/w BSA solution. The screw was dried in a flame hood for 3 hours

before heating in fluorous solvent. After washing with tetradecafluorohexane, the screw was dried by nitrogen gas.

6.4.3 Dye and antibiotic loaded films

Protein coatings were incubated in 0.05 mM fluorescein or rhodamine 123 solutions in PBS, separately. After 24 hours incubation, protein films were washed with MilliQ water exclusively. The procedure for antibiotic loading is the same except 20 mg/mL of colistin solution was used. For pH experiments, R123 was loaded in a pH 4 PBS buffer adjusted by HCl.

6.4.4 Control release experiment

The dye-loaded protein films were incubated in 3 mL PBS or NaCl solutions and the release was monitored by measuring fluorescence signal of the supernatant at ex: 490nm, em: 515nm for FL and ex: 500 nm, em: 525 nm for R123 using a plate reader.

6.4.5 Bacterial adhesion experiment

DsRed expressing *E. coli* were inoculated in 3 mL LB broth and grown to stationary phase at 37^{o}C. The cultures were then harvested by centrifugation and washed three times with 0.85% sodium chloride solution. The concentration of the resuspended bacteria solution was determined by measuring the optical density at 600 nm. Seeding solution were made by diluting to 0.1 OD_{600} (10^{8} colony forming units) in M9 minimal media supplemented with 1mM IPTG (isopropyl β-D-1-thiogalactopyranoside). 2 ml of this dilution was poured onto the bare, BSA-coated and Colistin-loaded screws and incubated for 24 hours in ambient conditions. The screws were then washed 3 times with PBS before analyzing under the microscope.

6.4.6 Kirby-Bauer disc diffusion

P. aeruginosa were inoculated in 3 mL LB broth and grown to stationary phase at 37 °C. The cultures were then harvested by centrifugation and washed three times with 0.85% sodium chloride solution. The concentration of the resuspended bacteria solution was determined by measuring the optical density at 600 nm. Seeding solution were made by diluting to 0.1 OD_{600} (10^8 colony forming units) in M9 minimal media. Agar gel plates were prepared by pouring a sterile solution of 6g Agar and 10g LB in 400 mL of water onto polystyrene petri dishes. 10 μL of the seeding solution was spread onto the agar plates using a sterile metal spreader. 2D surfaces were placed onto the agar plates while 3D screws were screwed in and incubated overnight at 37 °C. The inhibition zone was calculated by measuring the area around antibiotic-loaded substrates where no bacteria colonies were observed.

6.4.7 Microscopy

Bacterial film coatings were analyzed by confocal scanning light microscopy (CLSM). All analysis was performed using the A1SP: Nikon A1 Spectral Detector Confocal.

6.5 References

(1) M. Cloutier, D. Mantovani, F. Rosei, *Trends Biotechnol.* **2015**, *33*, 637.

(2) L. Mei, Z. Teng, G. Zhu, Y. Liu, F. Zhang, J. Zhang, Y. Li, Y. Guan, Y. Luo, X. Chen, Q. Wang, *ACS Appl. Mater. Interfaces* **2017**, *9*, 35297.

(3) G. Yuan, X. Chen, D. Li, *Food Res. Int.* **2016**, *89*, 117.

(4) R. Zhang, Y. Liu, M. He, Y. Su, X. Zhao, M. Elimelech, Z. Jiang, *Chem. Soc. Rev.* **2016**, *45*, 5888.

(5) M. Cloutier, D. Mantovani, F. Rosei *Angew. Chemie Int. Ed.* **2017**, *56*, 4662.
(6) H. Keum, J. Y. Kim, B. Yu, S. J. Yu, J. Kim, H. Jeon, D. Y. Lee, S. G. Im, S. Jon, *ACS Appl. Mater. Interfaces* **2017**, *9*, 19736.

(7) S. L. Percival, L. Suleman, G. Donelli, *J. Med. Microbiol.* **2015**, *64*, 323.

(8) H. Cheng, K. Yue, M. Kazemzadeh-Narbat, Y. Liu, A. Khalilpour, B. Li, Y. S. Zhang, N. Annabi, A. Khademhosseini, *ACS Appl. Mater. Interfaces* **2017**, *9*, 11428.

(9) J. Raphel, M. Holodniy, S. B. Goodman, S. C. Heilshorn, *Biomaterials* **2016**, *84*, 301.

(10) H. Yazici, M. B. O'Neill, T. Kacar, B. R. Wilson, E. E. Oren, M. Sarikaya, C. Tamerler, *ACS Appl. Mater. Interfaces* **2016**, *8*, 5070.

(11) H. Khalili, M. Sheikhbabayi, N. Samadi, H. Jamalifar, D. Dalili, N. Samadi, *Iran. J. Pharm. Res. IJPR* **2013**, *12*, 205.

(12) A. Kramer, I. Schwebke, G. Kampf, *BMC Infect. Dis.* **2006**, *6*, 130.

(13) H. A. Khan, A. Ahmad, R. Mehboob, *Asian Pac. J. Trop. Biomed.* **2015**, *5*, 509.

(14) R. M. Klevens, J. R. Edwards, J. Chesley L. Richards, T. C. Horan, R. P. Gaynes, D. A. Pollock, D. M. Cardo, *Public Health Rep.* **2007**, *122*, 160.

(15) S. S. Magill, J. R. Edwards, W. Bamberg, Z. G. Beldavs, G. Dumyati, M. A. Kainer, R. Lynfield, M. Maloney, L. McAllister-Hollod, J. Nadle, S. M. Ray, D. L. Thompson, L. E. Wilson, S. K. Fridkin, *N. Engl. J. Med.* **2014**, *370*, 1198.

(16) F. R. L. Crijns, M. M. Keinänen-Toivola, C. P. Dunne, *J. Hosp. Infect.* **2017**, *95*, 243.

(17) M. Lejars, A. Margaillan, C. Bressy, *Chem. Rev.* **2012**, *112*, 4347.

(18) E. J. Tobin, *Adv. Drug Deliv. Rev.* **2017**, *112*, 88.

(19) I. Masahiro, de M. B. K. L., M. B. J., B. B. Sonny, S. E. M., X. Chao, *J. Biomed. Mater. Res. Part A* **2017**, *105*, 3413.

(20) B. R. Knowles, P. Wagner, S. Maclaughlin, M. J. Higgins, P. J. Molino, *ACS Appl. Mater. Interfaces* **2017**, *9*, 18584.

(21) L. J. Bastarrachea, J. M. Goddard, *J. Agric. Food Chem.* **2015**, *63*, 4243.

(22) M. Yu, D. You, J. Zhuang, S. Lin, L. Dong, S. Weng, B. Zhang, K. Cheng, W. Weng, H. Wang, *ACS Appl. Mater. Interfaces* **2017**, *9*, 19698.

(23) M. Joseph, W. T. J., B. Garima, *Med. Coatings Depos. Technol.* **2016**, DOI doi:10.1002/9781119308713.ch5.

(24) W. Zheng, Y. Jia, W. Chen, G. Wang, X. Guo, X. Jiang, *ACS Appl. Mater. Interfaces* **2017**, *9*, 21181.

(25) L. S. Wang, B. Duncan, R. Tang, Y. W. Lee, B. Creran, S. G. Elci, J. Zhu, G. Y. Tonga, J. Doble, M. Fessenden, M. Bayat, S. Nonnenmann, R. W. Vachet, V. M. Rotello, *ACS Appl. Mater. Interfaces* **2017**, *9*, 42.

(26) T. B. Aigner, E. Desimone, T. Scheibel, *Adv. Mater.* **2018**, *1704636*, 1.

(27) J. Gu, Y. Su, P. Liu, P. Li, P. Yang, *ACS Appl. Mater. Interfaces* **2017**, *9*, 198.

(28) L. Chen, M.-L. Zhou, Z.-G. Qian, D. L. Kaplan, X.-X. Xia, *ACS Biomater. Sci. Eng.* **2017**, *3*, 335.

(29) A. R. Murphy, P. St. John, D. L. Kaplan, *Biomaterials* **2008**, *29*, 2829.

(30) L.-S. Wang, S. Gopalakrishnan, Y.-W. Lee, J. Zhu, S. S. Nonnenmann, V. M. Rotello, *Mater. Horizons* **2018**, *5*, 268.

(31) E. Jeoung, B. Duncan, L. S. Wang, K. Saha, C. Subramani, P. Wang, Y. C. Yeh, T. Kushida, Y. Engel, M. D. Barnes, V. M. Rotello, *Adv. Mater.* **2015**, *27*, 6251.

(32) Y. Lin, K. Liu, C. Wang, L. Li, Y. Liu, *Anal. Chem.* **2015**, *87*, 8047.

(33) B. Cai, K. Hu, C. Li, J. Jin, Y. Hu, *Appl. Surf. Sci.* **2015**, *356*, 844.

(34) L.-S. Wang, A. Gupta, B. Duncan, R. Ramanathan, M. Yazdani, V. M. Rotello, *ACS Biomater. Sci. Eng.* **2016**, *2*, 1862.

(35) G. J. A. ter Boo, R. G. Richards, T. F. Moriarty, D. W. Grijpma, D. Eglin, *Polym. Adv. Technol.* **2017**, *28*, 1325.

(36) J. Garnacho-Montero, C. Ortiz-Leyba, F. J. Jiménez-Jiménez, A. E. Barrero-Almodóvar, J. L. García-Garmendia, M. Bernabeu-Wittell, S. L. Gallego-Lara, J. Madrazo-Osuna, *Clin. Infect. Dis.* **2003**, *36*, 1111.

CHAPTER 7

PROTEIN-BASED BIODEGRADABLE POROUS GELS PREPARED USING POLYMERIZED HIGH INTERNAL PHASE EMULSIONS

7.1 Introduction

High internal phase emulsions (HIPEs) are extremely concentrated emulsions with more than 75% internal phase in volume.[1] Their ability to stabilize immiscible components provides an ideal platform for drug delivery systems as well as macroporous materials preparation via templating polymerization.[2,3] Porous structures are obtained through selectively polymerizing the external phase and extracting the internal phase of HIPEs, resulting in polyHIPEs.[4, 5, 6] The hierarchical structure of polyHIPEs has shown great potentials in diverse applications ranging from wound dressing, 3D cell culture, energy storage, to decontamination of chemical warfare agents. Moreover, the ability to encapsulate hydrophobic molecules makes polyHIPEs ideal materials for constructing drug eluting devices.[7]

The stabilization of HIPEs traditionally requires using high quantities of surfactants, which adversely affects the biocompatibility of the final product.[8,9] Recently, researchers have focused on developing biocompatible and biodegradable components for polyHIPE fabrication,[10,11] to fulfill the needs of different biological applications.[12,13,14] Several studies are dedicated to developing alternative emulsifiers, such as nanoparticles[15, 16] and polymers[17, 17], to reduce the use of surfactants. Biomacromolecules, such as

polysaccharides and proteins, are promising candidates for developing biocompatible and biodegradable scaffolds. [18,19] Nevertheless, polymerization and stabilization of HIPEs using solely biomacromolecules is challenging,[20,21] which limits the available materials for polyHIPEs biomedical applications.

We demonstrate here a versatile methodology to prepare protein-based porous antimicrobial hydrogels by fabricating polyHIPEs using bovine serum albumin (BSA) as both emulsifier and building blocks (Figure 7.1). BSA is an inexpensive and readily available protein. In this report, BSA-PolyHIPEs were obtained by introducing a reducing agent, dithiothreitol (DTT) to induce BSA gelation. The integrity and degradability of these BSA-polyHIPEs were investigated by varying the amount of DTT and the concentration of BSA. Finally, we demonstrated the versatility of this strategy by fabricating BSA-polyHIPEs using different essential oils and harnessed their antimicrobial activities through controlled release from the BSA scaffold.

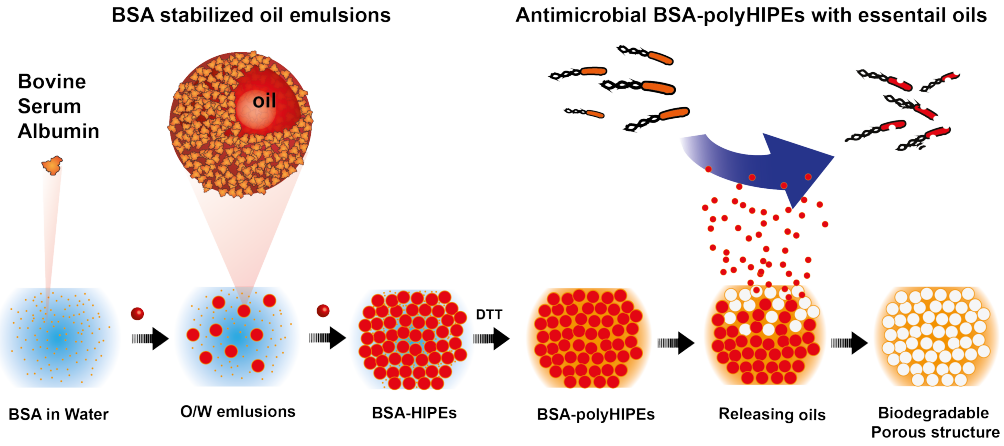

Figure 7.1: Schematic illustration of BSA-polyHIPEs fabrication.

7.2 Results and discussion

We first used toluene as the internal phase for optimizing the BSA-HIPEs fabrication conditions. An ideal emulsifier for HIPEs preparation should stabilize internal phase up to 75% of the total volume without inducing a phase reversion.[22] We prepared 20 wt% BSA aqueous solution in the water (external phase) and varied the volume fraction of toluene (internal phase) from 0.2 to 0.8. Nile red was dissolved in toluene, and fluorescence images of resulting emulsions confirmed that no phase reversion occurred during the emulsification process. Both the emulsion diameter and the size distribution decreased with the increase of oil fraction, and finally a homogeneous BSA-HIPE were obtained with emulsion size of ~40 μm for 80 v/v% toluene emulsions (Figure 7.2).

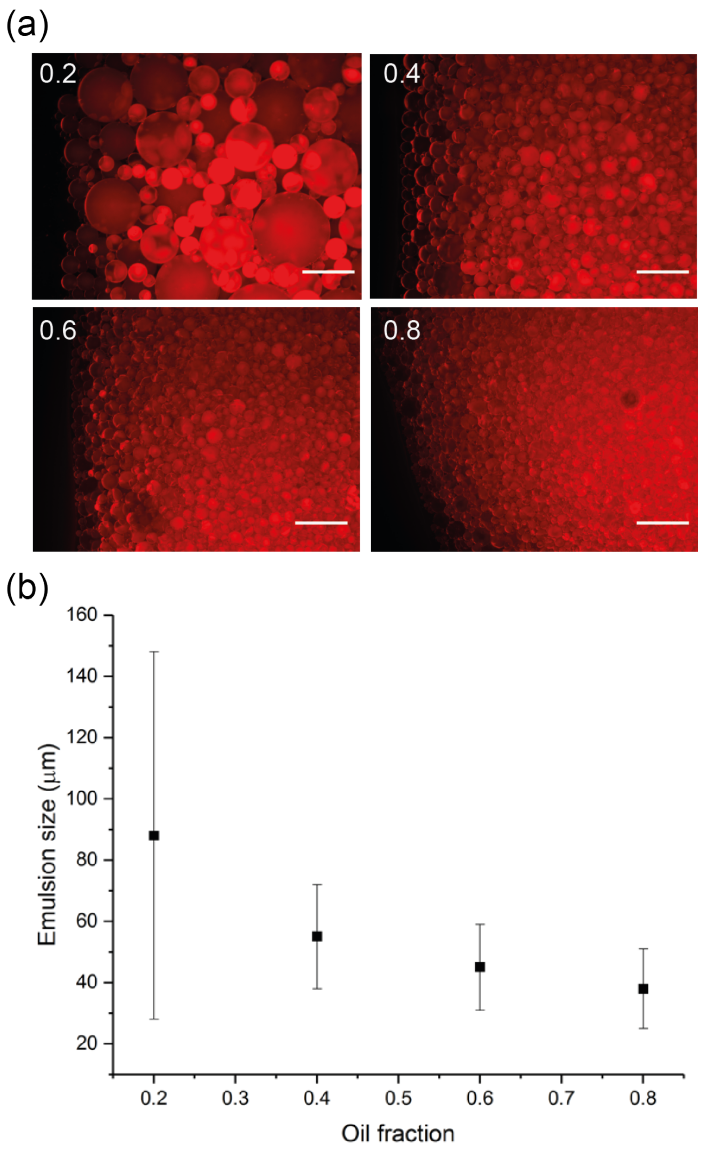

Figure 7.2: Toluene emulsions stabilized by 20 wt% BSA in water. a) Fluorescent micrograph of toluene emulsions stabilized by BSA. Nile red was dissolved in toluene for visualization. The oil to water volume ratio was adjusted from 0.2 to 0.8. b) Quantification study of emulsion size when different oil/water fraction was used. Scale bars for a) was 100 μm.

A three-dimensional hierarchical material can be obtained by polymerizing the external phase of HIPEs, resulting in stable polyHIPEs. We tested the structural integrity of BSA-polyHIPEs prepared by introducing a reducing agent DTT. DTT has been used to prepare protein-based hydrogels by disrupting the disulfide bridge in protein to induce

protein unfolding and cause subsequent gelation.[23] BSA-HIPEs were first prepared using 200 μL of 20 wt% BSA and 800 μL of toluene. After emulsification, 50 μL of DTT solution in different concentration was introduced into BSA-HIPEs, resulting in DTT final concentration of 100, 200, and 400 mM. The emulsion-DTT mixture were then transferred into a cylinder mold and incubated for 24 hours at room temperature. After removing from the mold, the BSA-polyHIPEs were characterized by measuring the stiffness of these cylinder-shaped gels using Rheometer (AR-2000, TA Instruments). The results indicate that structurally stable BSA-polyHIPEs were obtained when there is enough DTT added into the system (Figure 7.3a) and the elastic modulus of BSA-polyHIPEs increased with the increase of DTT concentration (Figure 7.3b).

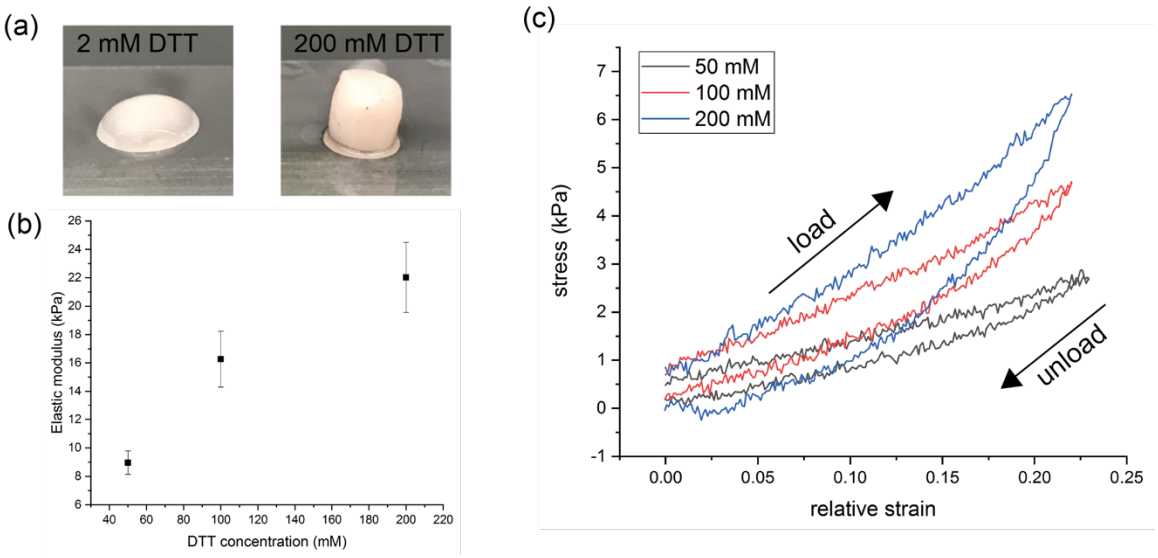

Figure 7.3: Structural integrity of BSA polyHIPEs prepared by different amount of DTT. a) Pictures of BSA polyHIPEs fabricated with 10 mM and 200 mM DTT b) The elastic modulus of BSA polyHIPEs after polymerized by different amount of DTT. c) Cyclic stress-strain curves of BSA polyHIPEs.

A salient feature of polyHIPEs is their hierarchical porous structures as the internal phase of HIPEs turns into spherical cavities separated by the polymerized external phase. Interconnecting pores between individual cavities are formed during the external phase polymerization.[24] To visualize the porous structure of BSA-polyHIPE framework, 0.1% FITC-labelled BSA was first spiked into BSA solution before emulsification, and the resulting BSA-polyHIPEs were examined using confocal microscopy. We observed that BSA was not only adsorbed at oil-water interface, but also dispersed uniformly in the external phase (Figure 7.4). The interconnecting pores was also observed using scanning electron microscopy after extracting the oils, indicating that BSA-polyHIPEs are structurally similar to most synthetic polyHIPEs (Figure 7.4). Since BSA serves as both the emulsifier and the building block for constructing the polyHIPEs, we modulated the structural property of polyHIPEs by simply varying the concentration of BSA. When lower concentration of BSA was used, the elastic modulus of BSA-polyHIPEs decreased with a slight increase in pore size (Figure 7.4).

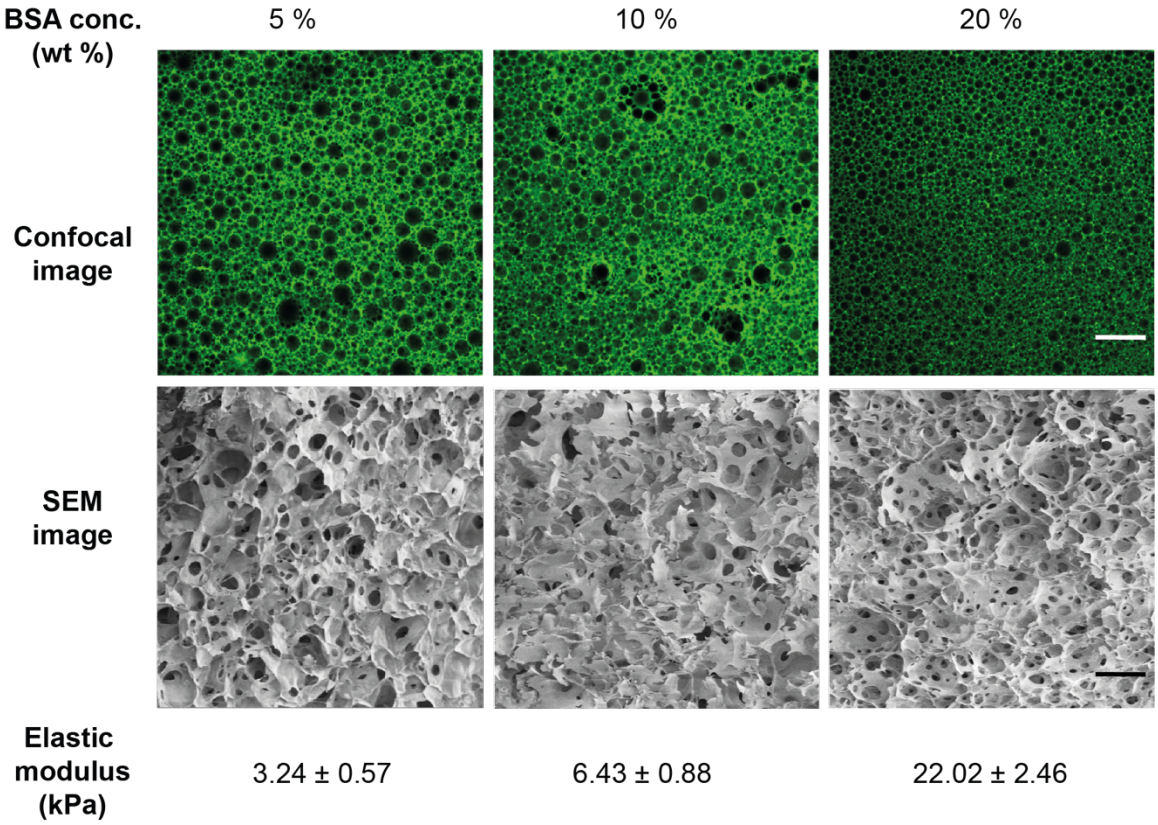

Figure 7.4: Porous structures of BSA polyHIPEs after the extraction of toluene. Confocal (top) and SEM (bottom) images of BSA polyHIPEs prepared by 5-20% w/w BSA. Scale bars were 100 μm for confocal images, and 50 μm for SEM images.

As one of the main advantages of pure protein-based HIPEs is its biodegradability, we were interested in understanding how structural properties such as elastic modulus correlated with the biodegradability. We tested the degradability using FITC-labeled BSA-polyHIPEs generated from different concentration of BSA. After treating with trypsin for 25 hours, complete digestion of BSA-polyHIPEs was observed. In contrast, BSA-polyHIPEs remained stable in PBS (Figure 7.5a). This biodegradation behavior was quantified by measuring the fluorescent intensity in the supernatant (Figure 7.5b). The results indicate BSA-polyHIPEs are digested faster by protease when less BSA used.

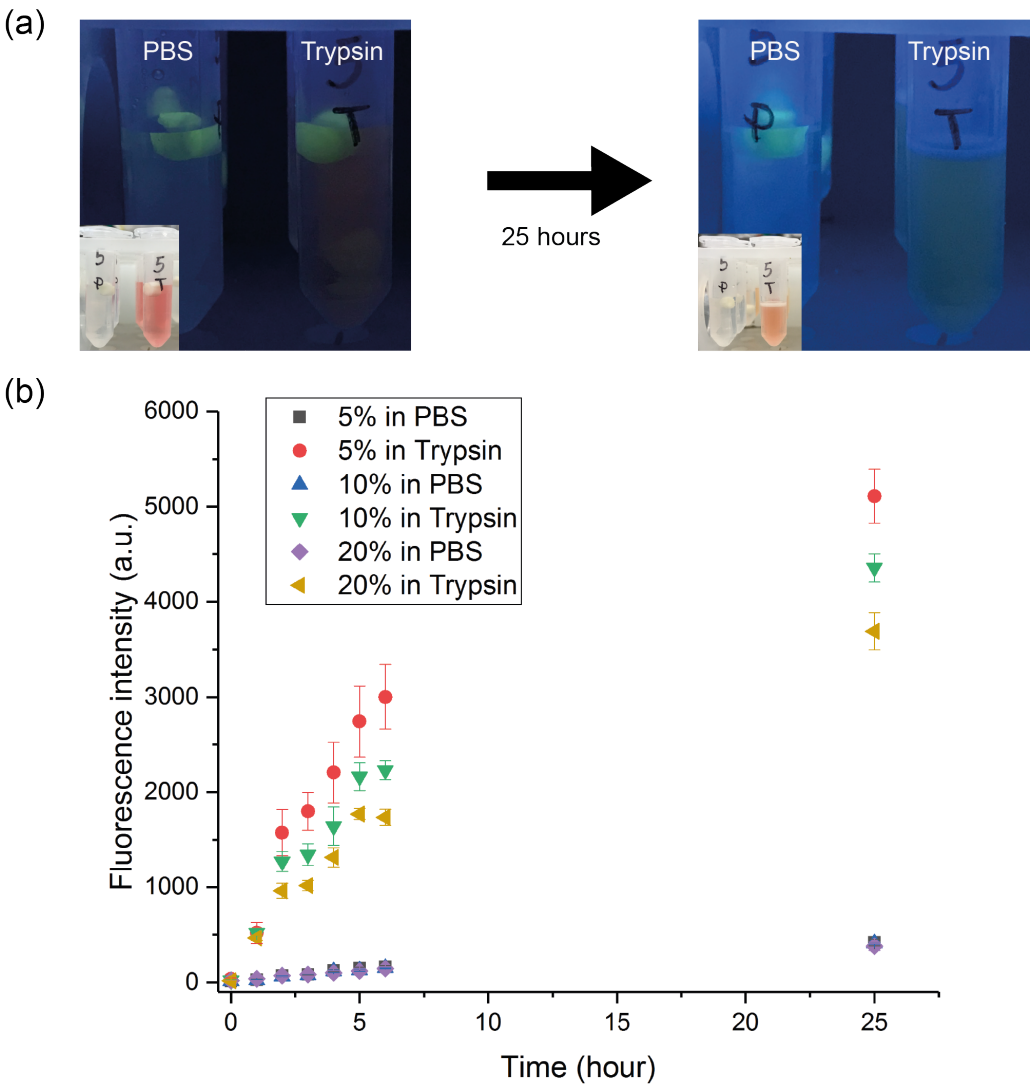

Figure 7.5: Biodegradability of BSA polyHIPEs a) Pictures of polyHIPEs prepared by 5% BSA in PBS and trypsin. FITC-label BSA was used for visualization b) Fluorescence intensity obtained by incubating BSA-polyHIPEs in PBS or Trypsin.

The versatility of our strategy was demonstrated by using different oils for fabricating BSA-polyHIPEs. Essential oils are hydrophobic liquids that have a variety of pharmacology and medical uses,[25, 26, 27] however, the poor aqueous solubility limits their practical applications. We envisioned that BSA-polyHIPEs can enable stabilizing of essential oils in aqueous solution and expand their biomedical applications. Eugenol, cymene and sunflower oils were chosen for this study. Following the same fabrication

procedure, stable BSA-polyHIPEs prepared by essential oils were formed, and their porous framework was observed through confocal microscopy, where eugenol-containing BSA-polyHIPEs showed smaller pore size to BSA-polyHIPEs prepared from toluene (Figure 7.6). We focused further studies on eugenol-containing BSA-polyHIPEs due to its effective antimicrobial activity.

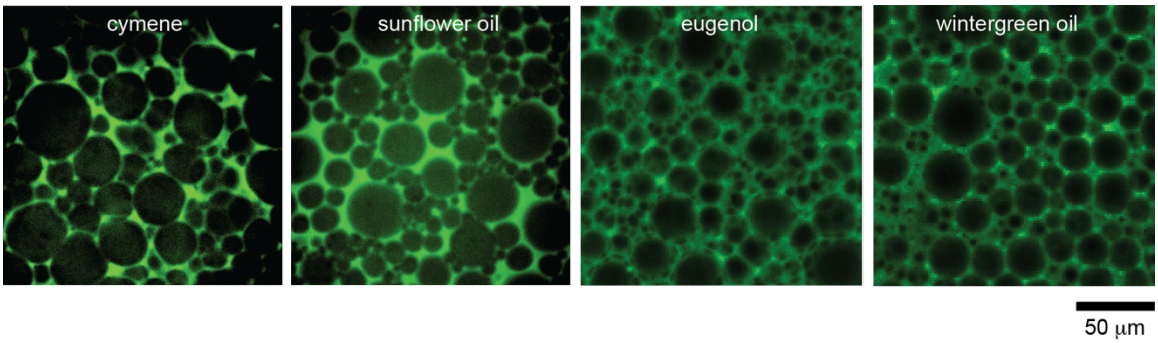

Figure 7.6: Confocal microscopic images of BSA-polyHIPEs prepared from cymene, sunflower oils, eugenol and wintergreen oils.

A functional demonstration of the antimicrobial activity of eugenol-containing BSA-polyHIPE was achieved due to the controlled release of eugenol which is known for its superior antimicrobial properties (Figure 7.7a). The content of eugenol released was monitored by measuring UV absorbance at 280 nm after placing eugenol-containing BSA-polyHIPEs in PBS. The degradation or dissolution of BSA framework could also contribute to the UV signal at 280 nm, therefore, BSA-polyHIPEs prepared by toluene were also used as control to determine the leakage of BSA molecules. In Figure 7.7a, a slow release of eugenol in PBS was observed in 24 hours, while the toluene-polyHIPEs showed no detectable release of BSA molecules.

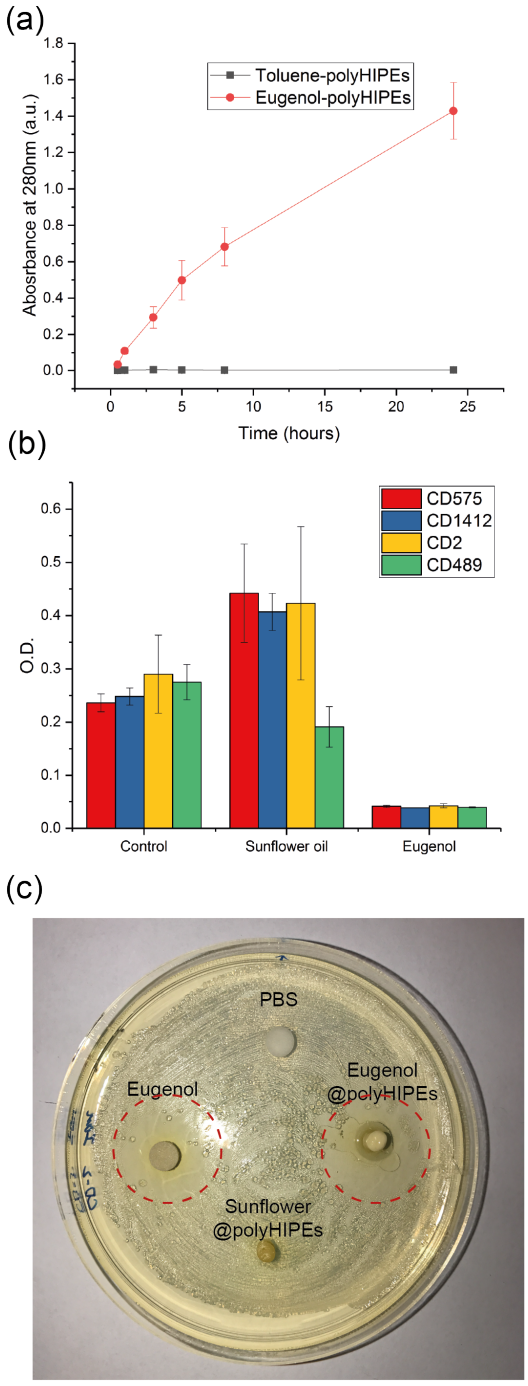

Figure 7.7: Antimicrobial activity of BSA-polyHIPEs prepared by different essential oils. a) Absorbance at 280 nm in PBS measured after incubating with polyHIPEs prepared by eugenol or toluene. b) Bacterial growth in solution containing BSA-polyHIPEs prepared by sunflower oils and eugenol after 24 hours incubation. c) Kirby-Bauer disc diffusion antibacterial activity assay for BSA-polyHIPEs prepared by essential oils

Different strains of bacteria were incubated in media containing BSA-polyHIPEs for 24 hours. BSA-PolyHIPEs prepared by eugenol showed complete inhibition of bacterial growth regardless of the strain of bacteria used (Figure 7.7b). As expected, polyHIPEs containing sunflower oil showed no antibacterial efficacy, demonstrating the imparted biocidal activity was resulted solely from the encapsulated oils. We next performed a Kirby-Bauer disc diffusion assay to confirm that the bactericidal property of BSA-polyHIPEs was due to the diffusion of eugenol oils. A clear inhibition zone was observed around the BSA-polyHIPEs containing eugenol, while no antibacterial effects were observed around the sunflower oil samples (Figure 7.7c). These results demonstrated that the antimicrobial property of BSA-polyHIPEs was gained by the release of essential oils as opposed to the DTT used during preparation of the BSA polyHIPEs.

7.3 Conclusion

In conclusion, we have developed a versatile strategy to fabricated protein-based polyHIPEs from a variety of oils. This technique of generating polyHIPEs using proteins provides a platform to generate biodegradable porous scaffolds that have numerous applications in biomaterial systems. We demonstrated this by generating a delivery system for essential oils using this porous material. Antimicrobial studies demonstrate the ability to impart biocidal properties to BSA-polyHIPEs by the choice of the loaded oil. We envision that this protein-based fabrication strategy will extend the utilities of polyHIPEs to a variety of biological applications.

7.4 Experimental methods

7.4.1 Materials

Bovine serum albumin (BSA), Nile red, Dulbecco's phosphate-buffered saline, fluorescein isothiocyanate (FITC), dithiothreitol (DTT), eugenol, sunflower oils, wintergreen oils, cymene oils were purchased from Fisher Scientific and used without further purification. MilliQ water was purified by using a Millipore water purification system.

7.4.2 Fabrication of BSA-HIPEs

BSA solutions were first prepared by dissolving 20 wt% BSA in MilliQ water. Toluene was slowly added into BSA solution while mixing with a vortex to prepare O/W emulsions with different oil fraction. 0.1 mg Nile red was dissolved in toluene for fluorescent microscopic studies. To obtain BSA-HIPEs, 800 μL toluene and 200 μL BSA solution were used.

7.4.3 Fabrication of BSA-polyHIPEs

After forming BSA-HIPEs using 800 μL toluene and 200 μL BSA, 50 μL of DTT in different concentrations (10 mM- 1000 mM) was added to the HIPEs and mixed with a vortex. The resulting solution was transferred into a cylinder-shaped PTFE mold (5 mm diameter and 5 mm height) and covered by a glass slide. After incubating for 24 hours, the cylinder-shaped BSA-polyHIPEs were washed with water to remove excess DTT. Mechanical compression tests were performed with a TA Instruments (New Castle, DE) AR-2000 rheometer at a 2 μm/s strain rate. The Young's modulus (E) for each BSA-polyHIPEs was calculated by plotting the measured normal force between 0 and 4% strain and dividing the slope of the best-fit linear regression by the hydrogel cross-sectional area.

The stiffness was obtained for 3 samples for each DTT concentration. For most of experiments, 1000 mM of DTT was used for the preparation of BSA-polyHIPEs.

7.4.4 Characterization of BSA-polyHIPEs

For microscopic studies, BSA-polyHIPEs were prepared using 5-20 wt% BSA solutions mixed with 0.1wt of FITC-labeled BSA, and analyzed by confocal scanning light microscopy (CLSM). All analysis was performed using the A1SP: Nikon A1 Spectral Detector Confocal. Scanning electron microscopic images were obtained by using FEI Magellan 400 field emission scanning electron microscope operated at 1 kV with 13 μA of beam current. Samples were coated with Au for 1 min before measuring. The stiffness tests were performed with a TA Instruments (New Castle, DE) AR-2000 rheometer at a 5 μm/s strain rate. The Young's modulus (E) for each BSA-polyHIPEs was calculated by plotting the measured stress between 0 and 10% relative strain ($I-I_0/I_0$, I_0 was defined when the measured normal force is equal to 0.01 N) and calculate the slope of the best-fit linear regression.

7.4.5 Synthesis of FITC-labelled BSA

To prepared FITC-labelled BSA, 0.50 g BSA proteins and 0.01 g FITC were dissolved in 50 ml PBS buffer. The reaction was carried out at room temperature in dark and lasted for 24 h. Then, the free FITC was removed by dialysis for 2 days.

7.4.6 Biodegradability test of BSA-polyHIPEs

BSA-polyHIPEs were incubated in 1 mL of PBS or 0.05% Trypsin (CORNING) under 37 °C for 25 hours. The quantification study was performed by measuring the fluorescence intensity in the supernatant after a period of time.

7.4.7 Preparation of essential oil loaded BSA-polyHIPEs

After emulsification of 800 μL eugenol, p-cymene or sunflower oil and 200 μL 20wt% BSA, 50 μL of 1000 mM DTT was added to the HIPEs and mixed with vortex. The resulting solution was transferred into a cylinder-shaped PTFE mold and incubated for 24 hours. After removing from the mold, BSA-polyHIPEs were washed with water to remove non-reacted DTT.

7.4.8 Release of eugenol

Eugenol-containing BSA-polyHIPEs were placed in 3 mL PBS for 48 hours. The content of eugenol in PBS was monitored by measuring the absorbance of eugenol at 280 nm.

7.4.9 Antimicrobial activity of BSA-polyHIPEs

Four strains of bacteria – *P. aeruginosa* (CD 575), *E. coli* (CD 2), *E. cloacae* (CD 1412) *and Methicillin-resistant S. aureus* (CD 489) – were inoculated in 3mL LB broth and grown to the stationary phase at 37 ^{o}C. The cultures were then harvested by centrifugation and washed thrice with 0.85% sodium chloride solution. The concentration of the resuspended bacteria solutions was estimated by measuring the optical density at 600 nm. Seeding solutions for each strain were prepared by diluting to 0.001 OD_{600} (~10^6

colony forming units) in M9 minimal media. Oil-Loaded (Sunflower and eugenol) polyHIPEs were prepared as described above and placed into 96 well plates. Seeding solutions of each bacterial strain were then seeded onto the polyHIPE wells and incubated overnight at 37 ^{o}C. Antibacterial efficacy was determined by measuring the OD_{600} of the supernatant.

7.4.10 Kirby-Bauer disc diffusion test

E. coli (CD 2) were inoculated in 3 mL LB broth and grown to the stationary phase at 37 ^{o}C. The cultures were then harvested by centrifugation and washed thrice with 0.85% sodium chloride solution. The concentration of the resuspended bacteria was determined by measuring the optical density at 600 nm. Seeding solution was prepared by diluting to 0.1 OD_{600} in M9 minimal media. Agar plates were prepared by pouring 15 mL of a sterile solution containing 6g of agar, 10 g of LB and 400 mL of MilliQ water onto sterile polystyrene petri dishes. 10μL of seeding solution was dropped onto the agar plates and spread using a sterile metal spreader. Eugenol-containing polyHIPE, sunflower oil-containing polyHIPE were placed in well-separated regions of an agar plate. As controls, 20 μL of Eugenol and 20 μL of PBS were loaded onto 6mm diameter BBL blank paper disks, procured from Fisher Scientific, and placed onto the same agar plate.

7.5 References

(1) M. S. Silverstein, *Prog. Polym. Sci.* **2014**, *39*, 199.

(2) B. C. Streifel, J. F. Parker, S. L. Giles, S. J. Williams, J. H. Duncan, J. H. Wynne, *J. Polym. Sci. Part A Polym. Chem.* **2016**, *54*, 2486.

(3) T. Yang, Y. Hu, C. Wang, B. P. Binks, *ACS Appl. Mater. Interfaces* **2017**, *9*, 22950.

(4) J. Park, K. Kim, M. Seo, *Chem. Commun.* **2018**, *54*, 7908.
(5) R. S. Moglia, J. L. Holm, N. A. Sears, C. J. Wilson, D. M. Harrison, E. Cosgriff-Hernandez, *Biomacromolecules* **2011**, *12*, 3621.

(6) N. R. Cameron, *Polymer* **2005**, *46*, 1439.

(7) R. Moglia, M. Whitely, M. Brooks, J. Robinson, M. Pishko, E. Cosgriff-Hernandez, *Macromol. Rapid Commun.* **2014**, *35*, 1301.

(8) M. N. Yukuyama, P. L. F. Oseliero, E. T. M. Kato, R. Lobënberg, C. L. P. de Oliveira, G. L. B. de Araujo, N. A. Bou-Chacra, *Colloids Surfaces A Physicochem. Eng. Asp.* **2018**, *554*, 296.

(9) F. Ríos, A. Fernández-Arteaga, M. Fernández-Serrano, E. Jurado, M. Lechuga, *J. Hazard. Mater.* **2018**, *353*, 436.

(10) B. Jiao, A. Shi, Q. Wang, B. P. Binks, *Angew. Chemie Int. Ed.* **2018**, *57*, 9274.

(11) F. Liu, J. Zheng, C.-H. Huang, C.-H. Tang, S.-Y. Ou, *Food Hydrocoll.* **2018**, *82*, 96.

(12) A. Lee, C. R. Langford, L. M. Rodriguez-Lorenzo, H. Thissen, N. R. Cameron, *Biomater. Sci.* **2017**, *5*, 2035.

(13) E. M. Christenson, W. Soofi, J. L. Holm, N. R. Cameron, A. G. Mikos, *Biomacromolecules* **2007**, *8*, 3806.

(14) S. Liu, M. Jin, Y. Chen, H. Gao, X. Shi, W. Cheng, L. Ren, Y. Wang, *J. Mater. Chem. B* **2017**, *5*, 2671.

(15) A. Carranza, D. Romero-Perez, H. Almanza-Reyes, N. Bogdanchikova, K. Juarez-Moreno, J. A. Pojman, C. Velasquillo, J. D. Mota-Morales, *Adv. Mater. Interfaces* **2017**, *4*, 1700094.

(16) Q. Wang, H. Ma, J. Chen, Z. Du, J. Mi, *J. Environ. Chem. Eng.* **2017**, *5*, 2807.

(17) S. Wang, J. Li, M. Qi, X. Gao, W.-J. Wang, *Langmuir* **2017**, *33*, 14295.

(18) Q. Zhou, H. Kang, M. Bielec, X. Wu, Q. Cheng, W. Wei, H. Dai, *Carbohydr. Polym.* **2018**, *197*, 292.

(19) H. Tan, Z. Tu, H. Jia, X. Gou, T. Ngai, *Langmuir* **2018**, *34*, 4820.

(20) S. D. Kimmins, P. Wyman, N. R. Cameron, *Polymer* **2014**, *55*, 416.

(21) A. I. Rezk, A. Rajan Unnithan, C. Hee Park, C. Sang Kim, *Chem. Eng. J.* **2018**, *350*, 812.

(22) M. S. Silverstein, *Polymer (Guildf).* **2014**, *55*, 304.

(23) Y. Sun, Y. Huang, *J. Mater. Chem. B* **2016**, *4*, 2768.

(24) A. Menner, A. Bismarck, *Macromol. Symp.* **2006**, *242*, 19.

(25) J. Su, Q. Guo, L. Mao, Y. Gao, F. Yuan, *Food Hydrocoll.* **2018**, *84*, 75.

(26) M. H. Lee, S. Y. Kim, H. J. Park, *Food Hydrocoll.* **2018**, *84*, 58.

(27) T. Xu, C. Gao, Y. Yang, X. Shen, M. Huang, S. Liu, X. Tang, *Food Hydrocoll.* **2018**, *84*, 84.

BIBLIOGRAPHY

(1) A. Abarrategi, A. Civantos, V. Ramos, J. V. Sanz Casado, J. L. López-Lacomba, *Biomacromolecules* **2008**, *9*, 711.

(2) A. Agarwal, T. L. Weis, M. J. Schurr, N. G. Faith, C. J. Czuprynski, J. F. McAnulty, C. J. Murphy, N. L. Abbott, *Biomaterials* **2010**, *31*, 680.

(3) A. Barbetta, N. R. Cameron, *Macromolecules* **2004**, *37*, 3188.

(4) A. Bigi, G. Cojazzi, S. Panzavolta, K. Rubini, N. Roveri, *Biomaterials* **2001**, *22*, 763.

(5) A. Carranza, D. Romero-Perez, H. Almanza-Reyes, N. Bogdanchikova, K. Juarez-Moreno, J. A. Pojman, C. Velasquillo, J. D. Mota-Morales, *Adv. Mater. Interfaces* **2017**, *4*, 1700094.

(6) A. González, M. C. Strumia, C. I. Alvarez Igarzabal, *J. Food Eng.* **2011**, *106*, 331.

(7) A. H. Clark, D. H. P. Sanuderson, A. Suggett, *Int. J. Pept. Protein Res.* **2018**, *17*, 353.

(8) A. I. Rezk, A. Rajan Unnithan, C. Hee Park, C. Sang Kim, *Chem. Eng. J.* **2018**, *350*, 812.

(9) A. K. Mohanty, M. Misra, L. T. Drzal, *J. Polym. Environ.* **2002**, *10*, 19.

(10) A. Kramer, I. Schwebke, G. Kampf, *BMC Infect. Dis.* **2006**, *6*, 130.

(11) A. Lee, C. R. Langford, L. M. Rodriguez-Lorenzo, H. Thissen, N. R. Cameron, *Biomater. Sci.* **2017**, *5*, 2035.

(12) A. N. Zelikin, *ACS Nano* **2010**, *4*, 2494.

(13) A. Menner, A. Bismarck, *Macromol. Symp.* **2006**, *242*, 19.

(14) A. Ghaffari, C. C. Miller, B. McMullin, A. Ghahary, *Nitric Oxide* **2006**, *14*, 21.

(15) A. R. Murphy, P. St. John, D. L. Kaplan, *Biomaterials* **2008**, *29*, 2829.

(16) A. Schneider, X. Y. Wang, D. L. Kaplan, J. A. Garlick, C. Egles, *Acta Biomater.* **2009**, *5*, 2570.

(17) B. C. Streifel, J. F. Parker, S. L. Giles, S. J. Williams, J. H. Duncan, J. H. Wynne, *J. Polym. Sci. Part A Polym. Chem.* **2016**, *54*, 2486.

(18) B. Cai, K. Hu, C. Li, J. Jin, Y. Hu, *Appl. Surf. Sci.* **2015**, *356*, 844.

(19) B. Creran, B. Yan, D. F. Moyano, M. M. Gilbert, R. W. Vachet, V. M. Rotello, *Chem. Commun.* **2012**, *48*, 4543.

(20) B. Demir, I. Cerkez, S. D. Worley, R. M. Broughton, T.-S. Huang, *ACS Appl. Mater. Interfaces* **2015**, *7*, 1752.

(21) B. Jiao, A. Shi, Q. Wang, B. P. Binks, *Angew. Chemie Int. Ed.* **2018**, *57*, 9274.

(22) B. Kundu, N. E. Kurland, S. Bano, C. Patra, F. B. Engel, V. K. Yadavalli, S. C. Kundu, *Prog. Polym. Sci.* **2014**, *39*, 251.

(23) B. Kundu, N. E. Kurland, V. K. Yadavalli, S. C. Kundu, *Int. J. Biol. Macromol.* **2014**, *70*, 70.

(24) B. R. Knowles, P. Wagner, S. Maclaughlin, M. J. Higgins, P. J. Molino, *ACS Appl. Mater. Interfaces* **2017**, *9*, 18584.

(25) B. Rost, C. Sander, *J. Mol. Biol.* **1993**, *232*, 584.

(26) B. Wang, T. Jin, Q. Xu, H. Liu, Z. Ye, H. Chen, *Bioconjug. Chem.* **2016**, *27*, 1305.

(27) C. Debiemme-Chouvy, S. Haskouri, G. Folcher, H. Cachet, *Langmuir* **2007**, *23*, 3873.

(28) C. Dhand, S. T. Ong, N. Dwivedi, S. M. Diaz, J. R. Venugopal, B. Navaneethan, M. H. Fazil, S. Liu, V. Seitz, E. Wintermantel, R. W. Beuerman, S. Ramakrishna, N. K. Verma, R. Lakshminarayanan *Biomaterials* **2016**, *104*, 323.

(29) C. Diaz Blanco, A. Ortner, R. Dimitrov, A. Navarro, E. Mendoza, T. Tzanov, *ACS Appl. Mater. Interfaces* **2014**, *6*, 11385.

(30) C. F. Welch, G. D. Rose, D. Malotky, S. T. Eckersley, *Langmuir* **2006**, *22*, 1544.

(31) C. J. Bettinger, J. P. Bruggeman, A. Misra, J. T. Borenstein, R. Langer, *Biomaterials* **2009**, *30*, 3050.

(32) C. K. Hong, R. P. Wool, *J. Appl. Polym. Sci.* **2005**, *95*, 1524.

(33) C. Le Bon, T. Nicolai, D. Durand, *Macromolecules* **1999**, *32*, 6120.

(34) C. Marquié, *J. Agric. Food Chem.* **2001**, *49*, 4676.

(35) C. S. B. Gil, V. S. B. Gil, S. M. Carvalho, G. R. Silva, J. T. Magalhaes, R. L. Orefice, A. Mansur, H. S. Mansur, P. S. O. Patricio, L. C. A. Oliveira, *New J. Chem.* **2016**, *40*, 8502.

(36) C. Subramani, N. Cengiz, K. Saha, T. N. Gevrek, X. Yu, Y. Jeong, A. Bajaj, A. Sanyal, V. M. Rotello, *Adv. Mater.* **2011**, *23*, 3165.

(37) C. Subramani, K. Saha, B. Creran, A. Bajaj, D. F. Moyano, H. Wang, V. M. Rotello, *Small* **2012**, *8*, 1209

(38) C. Vepari, D. L. Kaplan, *Prog. Polym. Sci.* **2007**, *32*, 991.

(39) D. Campoccia, L. Montanaro, C. R. Arciola, *Biomaterials* **2013**, *34*, 8533.

(40) D. F. Moyano, Y. Liu, D. Peer, V. M. Rotello, *Small* **2016**, *12*, 76.

(41) D.-H. Kim, J. Viventi, J. J. Amsden, J. Xiao, L. Vigeland, Y.-S. Kim, J. A. Blanco, B. Panilaitis, E. S. Frechette, D. Contreras, D. L. Kaplan, F. G. Omenetto, Y. Huang, K.-C. Hwang, M. R. Zakin, B. Litt, J. A. Rogers, *Nat. Mater.* **2010**, *9*, 511.

(42) D. J. Holt, L. M. Chamberlain, D. W. Grainger, *Biomaterials*, **2010**, *31*, 9382.

(43) D. J. Weber, W. A. Rutala, M. B. Miller, K. Huslage, E. Sickbert-Bennett, *Am. J. Infect. Control* **2010**, *38*, S25.

(44) D. K. Kim, J. I. Kim, T. I. Hwang, B. R. Sim, G. Khang, *ACS Appl. Mater. Interfaces* **2017**, *9*, 1384.

(45) D. R. Smith, R.-S. Wang, *Environ. Health Prev. Med.* **2006**, *11*, 3.

(46) D. Wang, Y. Ha, J. Gu, Q. Li, L. Zhang, P. Yang, *Adv. Mater.* **2016**, *28*, 7414.

(47) D.-W. Zhu, *Macromolecules* **1996**, *29*, 2813.

(48) E. C. Jensen, *Anat. Rec.* **2013**, *296*, 378.

(49) E. H. Abdulkareem, K. Memarzadeh, R. P. Allaker, J. Huang, J. Pratten, D. Spratt, *J. Dent.* **2015**, *43*, 1462.

(50) E. J. Brisbois, R. P. Davis, A. M. Jones, T. C. Major, R. H. Bartlett, M. E. Meyerhoff, H. Handa, *J. Mater. Chem. B* **2015**, *3*, 1639.

(51) E. Jeoung, B. Duncan, L. S. Wang, K. Saha, C. Subramani, P. Wang, Y. C. Yeh, T. Kushida, Y. Engel, M. D. Barnes, V. M. Rotello, *Adv. Mater.* **2015**, *27*, 6251.

(52) E. J. Tobin, *Adv. Drug Deliv. Rev.* **2017**, *112*, 88.

(53) E. Kharlampieva, V. Kozlovskaya, B. Wallet, V. V Shevchenko, R. R. Naik, R. Vaia, D. L. Kaplan, V. V Tsukruk, *ACS Nano* **2010**, *4*, 7053.

(54) E. M. Christenson, W. Soofi, J. L. Holm, N. R. Cameron, A. G. Mikos, *Biomacromolecules* **2007**, *8*, 3806.

(55) E. M. Hetrick, M. H. Schoenfisch, *Chem. Soc. Rev.* **2006**, *35*, 780.

(56) E. M. Pritchard, T. Valentin, B. Panilaitis, F. Omenetto, D. L. Kaplan, *Adv. Funct. Mater.* **2012**, *23*, 854.

(57) E. S. Gil, B. Panilaitis, E. Bellas, D. L. Kaplan, *Adv. Healthc. Mater.* **2013**, *2*, 206.

(58) F. G. Omenetto, D. L. Kaplan, *Science* **2010**, *329*, 528.

(59) F. Hui, C. Debiemme-Chouvy, *Biomacromolecules* **2013**, *14*, 585.

(60) F. Liu, J. Zheng, C.-H. Huang, C.-H. Tang, S.-Y. Ou, *Food Hydrocoll.* **2018**, *82*, 96.

(61) F. Ríos, A. Fernández-Arteaga, M. Fernández-Serrano, E. Jurado, M. Lechuga, *J. Hazard. Mater.* **2018**, *353*, 436.

(62) F. R. L. Crijns, M. M. Keinänen-Toivola, C. P. Dunne, *J. Hosp. Infect.* **2017**, *95*, 243.

(63) F. Song, D.-L. Tang, X.-L. Wang, Y.-Z. Wang, *Biomacromolecules* **2011**, *12*, 3369.

(64) G. H. Altman, F. Diaz, C. Jakuba, T. Calabro, R. L. Horan, J. Chen, H. Lu, J. Richmond, D. L. Kaplan, *Biomaterials* **2003**, *24*, 401.

(65) G. J. A. ter Boo, R. G. Richards, T. F. Moriarty, D. W. Grijpma, D. Eglin, *Polym. Adv. Technol.* **2017**, *28*, 1325.

(66) G. Yuan, X. Chen, D. Li, *Food Res. Int.* **2016**, *89*, 117.

(67) H. A. Khan, A. Ahmad, R. Mehboob, *Asian Pac. J. Trop. Biomed.* **2015**, *5*, 509.

(68) H. Cheng, K. Yue, M. Kazemzadeh-Narbat, Y. Liu, A. Khalilpour, B. Li, Y. S. Zhang, N. Annabi, A. Khademhosseini, *ACS Appl. Mater. Interfaces* **2017**, *9*, 11428.

(69) H. Keum, J. Y. Kim, B. Yu, S. J. Yu, J. Kim, H. Jeon, D. Y. Lee, S. G. Im, S. Jon, *ACS Appl. Mater. Interfaces* **2017**, *9*, 19736.

(70) H. Khalili, M. Sheikhbabayi, N. Samadi, H. Jamalifar, D. Dalili, N. Samadi, *Iran. J. Pharm. Res. IJPR* **2013**, *12*, 205.

(71) H. Knopf-Marques, M. Pravda, L. Wolfova, V. Velebny, P. Schaaf, N. E. Vrana, P. Lavalle, *Adv. Healthc. Mater.* **2016**, *5*, 2841.

(72) H. Kong, J. Jang, *Langmuir* **2008**, *24*, 2051.

(73) H. Perry, A. Gopinath, D. L. Kaplan, L. Dal Negro, F. G. Omenetto, *Adv. Mater.* **2008**, *20*, 3070.

(74) H. Sardon, A. P. Dove, *Science* **2018**, *360*, 380 LP.
(75) H. Tan, Z. Tu, H. Jia, X. Gou, T. Ngai, *Langmuir* **2018**, *34*, 4820.

(76) H. Tao, M. A. Brenckle, M. Yang, J. Zhang, M. Liu, S. M. Siebert, R. D. Averitt, M. S. Mannoor, M. C. McAlpine, J. A. Rogers, D. L. Kaplan, F. G. Omenetto, *Adv. Mater.* **2012**, *24*, 1067

(77) H. Tsuchiya, Y. Hoshino, K. Tajima, N. Takagi, *J. Prosthet. Dent.* **1994**, *71*, 618.

(78) H. Wendt, A. Hillmer, K. Reimers, J. W. Kuhbier, F. Schäfer-Nolte, C. Allmeling, C. Kasper, P. M. Vogt, *PLoS One* **2011**, *6*, e21833.

(79) H. Yazici, M. B. O'Neill, T. Kacar, B. R. Wilson, E. E. Oren, M. Sarikaya, C. Tamerler, *ACS Appl. Mater. Interfaces* **2016**, *8*, 5070.

(80) H.-J. Jin, D. L. Kaplan, *Nature* **2003**, *424*, 1057.

(81) H.-J. Jin, J. Park, V. Karageorgiou, U.-J. Kim, R. Valluzzi, P. Cebe, D. L. Kaplan, *Adv. Funct. Mater.* **2005**, *15*, 1241.

(82) I. Masahiro, de M. B. K. L., M. B. J., B. B. Sonny, S. E. M., X. Chao, *J. Biomed. Mater. Res. Part A* **2017**, *105*, 3413.

(83) I. Zhuk, F. Jariwala, A. B. Attygalle, Y. Wu, M. R. Libera, S. A. Sukhishvili, *ACS Nano* **2014**, *8*, 7733.

(84) J. A. Werkmeister, J. A. M. Ramshaw, *Biomed. Mater.* **2012**, *7*, 012002.

(85) J. Fukuda, A. Khademhosseini, J. Yeh, G. Eng, J. Cheng, O.C. Farokhzad, R. Langer, *Biomaterials*, **2006**, *27*, 1479.

(86) J. F. Almine, D. V Bax, S. M. Mithieux, L. Nivison-Smith, J. Rnjak, A. Waterhouse, S. G. Wise, A. S. Weiss, *Chem. Soc. Rev.* **2010**, *39*, 3371.

(87) J. G. Hardy, T. R. Scheibel, *Prog. Polym. Sci.* **2010**, *35*, 1093.

(88) J. Garnacho-Montero, C. Ortiz-Leyba, F. J. Jiménez-Jiménez, A. E. Barrero-Almodóvar, J. L. García-Garmendia, M. Bernabeu-Wittell, S. L. Gallego-Lara, J. Madrazo-Osuna, *Clin. Infect. Dis.* **2003**, *36*, 1111.

(89) J. Gu, Y. Su, P. Liu, P. Li, P. Yang, *ACS Appl. Mater. Interfaces* **2017**, *9*, 198.

(90) J. J. Amsden, P. Domachuk, A. Gopinath, R. D. White, L. D. Negro, D. L. Kaplan, F. G. Omenetto, *Adv. Mater.* **2010**, *22*, 1746.

(91) J. Luo, N. Porteous, Y. Sun, *ACS Appl. Mater. Interfaces* **2011**, *3*, 2895.

(92) J. M. Zuidema, C. J. Rivet, R. J. Gilbert, F. A. Morrison, *J. Biomed. Mater. Res. Part B Appl. Biomater.* **2013**, *102*, 1063.

(93) J. N. Renner, K. M. Cherry, R. S.-C. Su, J. C. Liu, *Biomacromolecules* **2012**, *13*, 3678.

(94) J. O. Anyango, J. Taylor, J. R. N. Taylor, *J. Agric. Food Chem.* **2011**, *59*, 12674.

(95) J. Park, K. Kim, M. Seo, *Chem. Commun.* **2018**, *54*, 7908.

(96) J. Raphel, J. Karlsson, S. Galli, A. Wennerberg, C. Lindsay, M. G. Haugh, J. Pajarinen, S. B. Goodman, R. Jimbo, M. Andersson, *Biomaterials* **2016**, *83*, 269.

(97) J. Raphel, M. Holodniy, S. B. Goodman, S. C. Heilshorn, *Biomaterials* **2016**, *84*, 301.

(98) J. Skopinska-Wisniewska, A. Sionkowska, A. Kaminska, A. Kaznica, R. Jachimiak, T. Drewa, *Appl. Surf. Sci.* **2009**, *255*, 8286.

(99) J. Su, Q. Guo, L. Mao, Y. Gao, F. Yuan, *Food Hydrocoll.* **2018**, *84*, 75.

(100) J. Sun, L. Yang, M. Jiang, Y. shi, B. Xu, H. Ma, *J. Chromatogr. B* **2017**, *1054*, 57.

(101) J. W. Costerton, P. S. Stewart, E. P. Greenberg, *Science* **1999**, *284*, 1318 LP.

(102) J. Zink, T. Wyrobnik, T. Prinz, M. Schmid, *Physical, Chemical and Biochemical Modifications of Protein-Based Films and Coatings: An Extensive Review*, **2016**.

(103) J.-W. Rhim, H.-M. Park, C.-S. Ha, *Prog. Polym. Sci.* **2013**, *38*, 1629.

(104) K. H. Smith, E. Tejeda-Montes, M. Poch, A. Mata, *Chem. Soc. Rev.* **2011**, *40*, 4563.

(105) K. Panduranga Rao, *J. Biomater. Sci. Polym. Ed.* **1996**, *7*, 623.

(106) K. R. Millington, H. Ishii, G. Maurdev, *Amino Acids* **2010**, *38*, 1395.

(107) K. S. Miller, M. T. Chiang, J. M. Krochta, *J. Food Sci.* **2006**, *62*, 1189.

(108) L. Chen, M.-L. Zhou, Z.-G. Qian, D. L. Kaplan, X.-X. Xia, *ACS Biomater. Sci. Eng.* **2017**, *3*, 335.

(109) L. D. Renner, D. B. Weibel, *MRS Bull.* **2011**, *36*, 347.

(110) L. J. Bastarrachea, J. M. Goddard, *J. Agric. Food Chem.* **2015**, *63*, 4243.

(111) L. L. C. Wong, P. M. Baiz Villafranca, A. Menner, A. Bismarck, *Langmuir* **2013**, *29*, 5952.

(112) L. Mei, Z. Teng, G. Zhu, Y. Liu, F. Zhang, J. Zhang, Y. Li, Y. Guan, Y. Luo, X. Chen, Q. Wang, *ACS Appl. Mater. Interfaces* **2017**, *9*, 35297.

(113) L. Meinel, S. Hofmann, V. Karageorgiou, L. Zichner, R. Langer, D. Kaplan, G. Vunjak-Novakovic, *Biotechnol. Bioeng.* **2004**, *88*, 379.

(114) L. Peng, L. Chang, X. Liu, J. Lin, H. Liu, B. Han, S. Wang, *ACS Appl. Mater. Interfaces* **2017**, *9*, 17688.

(115) L. Scheiterle, A. Ulmer, R. Birner, A. Pyka, *J. Clean. Prod.* **2018**, *172*, 3851.

(116) L. Timofeeva, N. Kleshcheva, *Appl. Microbiol. Biotechnol.* **2011**, *89*, 475

(117) L. Uebersax, T. Apfel, K. M. R. Nuss, R. Vogt, H. Y. Kim, L. Meinel, D. L. Kaplan, J. A. Auer, H. P. Merkle, B. von Rechenberg, *Eur. J. Pharm. Biopharm.* **2013**, *85*, 107.

(118) L. Xiao, S. Liu, D. Yao, Z. Ding, Z. Fan, Q. Lu, D. L. Kaplan, *Biomacromolecules* **2017**, *18*, 2073.

(119) L.-S. Wang, A. Gupta, B. Duncan, R. Ramanathan, M. Yazdani, V. M. Rotello, *ACS Biomater. Sci. Eng.* **2016**, *2*, 1862.

(120) L.-S. Wang, A. Gupta, V. M. Rotello, *ACS Infect. Dis.* **2016**, *2*, 3.

(121) L.-S. Wang, B. Duncan, R. Tang, Y.-W. Lee, B. Creran, S. G. Elci, J. Zhu, G. Yesilbag Tonga, J. Doble, M. Fessenden, M. Bayat, S. Nonnenmann, R. W. Vachet, V. M. Rotello, *ACS Appl. Mater. Interfaces* **2017**, *9*, 42.

(122) L.-S. Wang, S. Gopalakrishnan, Y.-W. Lee, J. Zhu, S. S. Nonnenmann, V. M. Rotello, *Mater. Horizons* **2018**, *5*, 268.

(123) M. A. Brenckle, B. Partlow, H. Tao, M. B. Applegate, A. Reeves, M. Paquette, B. Marelli, D. L. Kaplan, F. G. Omenetto, *Adv. Funct. Mater.* **2016**, *26*, 44.

(124) M. B. Pérez-Gago, P. Nadaud, J. M. Krochta, *J. Food Sci.* **2006**, *64*, 1034.

(125) M. Cloutier, D. Mantovani, F. Rosei, *Angew. Chemie Int. Ed.* **2017**, *56*, 4662.

(126) M. Cloutier, D. Mantovani, F. Rosei, *Trends Biotechnol.* **2015**, *33*, 637.

(127) M. G. A. Vieira, M. A. da Silva, L. O. dos Santos, M. M. Beppu, *Eur. Polym. J.* **2011**, *47*, 254.

(128) M. H. Lee, S. Y. Kim, H. J. Park, *Food Hydrocoll.* **2018**, *84*, 58.

(129) M. J. Gray, W.-Y. Wholey, U. Jakob, *Annu. Rev. Microbiol.* **2013**, *67*, 141.

(130) M. J. Roberts, N. Bhatt, C. M. Voge, E. R. Meshot, J. P. Stegemann, A. J. Hart, *J. Mater. Chem. B* **2013**, *1*, 4711.

(131) M. Joseph, W. T. J., B. Garima, *Med. Coatings Depos. Technol.* **2016**, DOI doi:10.1002/9781119308713.ch5.

(132) M. L. W. Knetsch, L. H. Koole, *Polym.* **2011**, *3*, 340

(133) M. Lejars, A. Margaillan, C. Bressy, *Chem. Rev.* **2012**, *112*, 4347.

(134) M. Li, M. J. Mondrinos, M. R. Gandhi, F. K. Ko, A. S. Weiss, P. I. Lelkes, *Biomaterials* **2005**, *26*, 5999.

(135) M. N. Yukuyama, P. L. F. Oseliero, E. T. M. Kato, R. Lobënberg, C. L. P. de Oliveira, G. L. B. de Araujo, N. A. Bou-Chacra, *Colloids Surfaces A Physicochem. Eng. Asp.* **2018**, *554*, 296.

(136) M. Oliviero, R. Rizvi, L. Verdolotti, S. Iannace, H. E. Naguib, E. Di Maio, H. C. Neitzert, G. Landi, *Adv. Funct. Mater.* **2017**, *27*, 1605142.

(137) M. Oussalah, S. Caillet, S. Salmiéri, L. Saucier, M. Lacroix, *J. Agric. Food Chem.* **2004**, *52*, 5598.

(138) M. Ray, Y.-W. Lee, J. Hardie, R. Mout, G. Yeşilbag Tonga, M. E. Farkas, V. M. Rotello, *Bioconjug. Chem.* **2018**, *29*, 445.

(139) M. Rezvanian, N. Ahmad, M. C. I. Mohd Amin, S.-F. Ng, *Int. J. Biol. Macromol.* **2017**, *97*, 131.

(140) M. S. Silverstein, *Prog. Polym. Sci.* **2014**, *39*, 199.

(142) M. S. Silverstein, *Polymer* **2014**, *55*, 304.

(143) M. Sarkari, I. Darrat, B. L. Knutson, *Biotechnol. Prog.*, **2003**, *19*, 448.

(144) M. Sato, K. Kojima, C. Sakuma, M. Murakami, Y. Tamada, H. Kitani, *Sci. Rep.* **2014**, *4*, 4080.

(145) M. T. Cicerone, M. J. Pikal, K. K. Qian, *Adv. Drug Deliv. Rev.* **2015**, *93*, 14.

(146) M. Wihodo, C. I. Moraru, *J. Food Eng.* **2013**, *114*, 292.

(147) M. Yu, D. You, J. Zhuang, S. Lin, L. Dong, S. Weng, B. Zhang, K. Cheng, W. Weng, H. Wang, *ACS Appl. Mater. Interfaces* **2017**, *9*, 19698.

(148) N. H. C. S. Silva, C. Vilela, I. M. Marrucho, C. S. R. Freire, C. Pascoal Neto, A. J. D. Silvestre, *J. Mater. Chem. B* **2014**, *2*, 3715.

(149) N. J. Greenfield, *Nat. Protoc.* **2006**, *1*, 2876.

(150) N. R. Cameron, D. C. Sherrington, *J. Mater. Chem.* **1997**, *7*, 2209.

(151) N. R. Cameron, *Polymer* **2005**, *46*, 1439.

(152) N. Rangavajhyala, V. Ghorpade, M. Hanna, *J. Agric. Food Chem.* **1997**, *45*, 4204.

(153) P. Hernández-Muñoz, A. López-Rubio, J. M. Lagarón, R. Gavara, *Biomacromolecules* **2004**, *5*, 415.

(154) P. Hernández-Muñoz, R. Villalobos, A. Chiralt, *Food Hydrocoll.* **2004**, *18*, 647.

(155) P. J. Nowatzki, D. A. Tirrell, *Biomaterials* **2004**, *25*, 1261.

(156) P. Krajnc, D. Štefanec, I. Pulko, *Macromol. Rapid Commun.* **2005**, *26*, 1289.

(157) Q. Wang, H. Ma, J. Chen, Z. Du, J. Mi, *J. Environ. Chem. Eng.* **2017**, *5*, 2807.

(158) Q. Wang, M. Jian, C. Wang, Y. Zhang, *Adv. Funct. Mater.* **2017**, *27,* 1605657.

(159) Q. Zhou, H. Kang, M. Bielec, X. Wu, Q. Cheng, W. Wei, H. Dai, *Carbohydr. Polym.* **2018**, *197*, 292.

(160) R. Craven, *Nat. Rev. Neurosci.* **2005**, *6*, 585.

(161) R. Güzel, A. Ersöz, İ. Dolak, R. Say, *Mater. Sci. Eng. C* **2017**, *79*, 336.

(162) R. M. Donlan, *Emerg. Infect. Dis.* **2001**, *7*, 277

(163) R. M. Klevens, J. R. Edwards, J. Chesley L. Richards, T. C. Horan, R. P. Gaynes, D. A. Pollock, D. M. Cardo, *Public Health Rep.* **2007**, *122*, 160.

(164) R. Moglia, M. Whitely, M. Brooks, J. Robinson, M. Pishko, E. Cosgriff-Hernandez, *Macromol. Rapid Commun.* **2014**, *35*, 1301.

(165) R. Murugan, P. Molnar, K. P. Rao, J. J. Hickman, *Int. J. Biomed. Eng. Technol.* **2009**, *2*, 104.

(166) R. S. Moglia, J. L. Holm, N. A. Sears, C. J. Wilson, D. M. Harrison, E. Cosgriff-Hernandez, *Biomacromolecules* **2011**, *12*, 3621.

(167) R. Wang, K. L. Chua, K. G. Neoh, *ACS Biomater. Sci. Eng.* **2015**, *1*, 405.

(168) R. Zhang, Y. Liu, M. He, Y. Su, X. Zhao, M. Elimelech, Z. Jiang, *Chem. Soc. Rev.* **2016**, *45*, 5888.

(169) R. Zhu, Y.-X. Chen, Q.-F. Ke, Y.-S. Gao, Y.-P. Guo, *J. Mater. Chem. B* **2017**, *5*, 5009.

(170) S. C. Gomes, I. B. Leonor, J. F. Mano, R. L. Reis, D. L. Kaplan, *Biomaterials* **2011**, *32*, 4255.

(171) S. Chen, L. Li, C. Zhao, J. Zheng, *Polymer.* **2010**, *51*, 5283.

(172) S. D. Kimmins, P. Wyman, N. R. Cameron, *Polymer* **2014**, *55*, 416.

(173) S. Gomes, I.B. Leonor, J. F. Mano, R. L. Reis, D. L. Kaplan, *Prog. Polym. Sci.* **2012**, *37*, 1.

(174) S. Hofmann, C. T. Wong Po Foo, F. Rossetti, M. Textor, G. Vunjak-Novakovic, D. L. Kaplan, H. P. Merkle, L. Meinel, *J. Control. Release* **2006**, *111*, 219.

(175) S. Javaherian, K. J. Li, A. P. McGuigan, *Biotechniques* **2013**, *55*, 21.

(176) S. Kim, B. Marelli, M. A. Brenckle, A. N. Mitropoulos, E.-S. Gil, K. Tsioris, H. Tao, D. L. Kaplan, F. G. Omenetto, *Nat. Nanotechnol.* **2014**, *9*, 306.

(177) S. L. Percival, L. Suleman, G. Donelli, *J. Med. Microbiol.* **2015**, *64*, 323.

(178) S. Liu, M. Jin, Y. Chen, H. Gao, X. Shi, W. Cheng, L. Ren, Y. Wang, *J. Mater. Chem. B* **2017**, *5*, 2671.

(179) S. Matsuda, H. Iwata, N. Se, Y. Ikada, *J. Biomed. Mater. Res.* **1999**, *45*, 20.

(180) S. R. Hynes, E. B. Lavik, *Graefe's Arch. Clin. Exp. Ophthalmol.* **2010**, *248*, 763.

(181) S. Saravanan, S. Nethala, S. Pattnaik, A. Tripathi, A. Moorthi, N. Selvamurugan, *Int. J. Biol. Macromol.* **2011**, *49*, 188.

(182) S. S. Magill, J. R. Edwards, W. Bamberg, Z. G. Beldavs, G. Dumyati, M. A. Kainer, R. Lynfield, M. Maloney, L. McAllister-Hollod, J. Nadle, S. M. Ray, D. L. Thompson, L. E. Wilson, S. K. Fridkin, *N. Engl. J. Med.* **2014**, *370*, 1198

(183) S. Toda, L. R. Blauch, S. K. Y. Tang, L. Morsut, W. A. Lim, *Science* **2018**. (doi: 10.1126/science.aat0271)

(184) S. Wang, J. Li, M. Qi, X. Gao, W.-J. Wang, *Langmuir* **2017**, *33*, 14295.

(185) S. Y. Chou, P. R. Krauss, P. J. Renstrom, *Science.* **1996**, *272*, 85.(1) S. H. Ahn, L. J. Guo, *ACS Nano* **2009**, *3*, 2304.

(186) T. B. Aigner, E. Desimone, T. Scheibel, *Adv. Mater.* **2018**, *1704636*, 1.

(187) T. Frieden, *Centres for Disease Control and Prevention* **2013**. Atlanta, Georgia U.S.A.

(188) T. K. Singh, S. K. Øiseth, L. Lundin, L. Day, *Food Funct.* **2014**, *5*, 2686.

(189) T. P. J. Knowles, T. W. Oppenheim, A. K. Buell, D. Y. Chirgadze, M. E. Welland, *Nat. Nanotechnol.* **2010**, *5*, 204.

(190) T. Xu, C. Gao, Y. Yang, X. Shen, M. Huang, S. Liu, X. Tang, *Food Hydrocoll.* **2018**, *84*, 84.

(191) T. Yang, Y. Hu, C. Wang, B. P. Binks, *ACS Appl. Mater. Interfaces* **2017**, *9*, 22950.

(192) V. Micard, R. Belamri, M.-H. Morel, S. Guilbert, *J. Agric. Food Chem.* **2000**, *48*, 2948.

(193) W. Hartleb, J. S. Saar, P. Zou, K. Lienkamp, *Macromol. Chem. Phys.* **2015**, *217*, 225.

(194) W. Zheng, W. Zhang, X. Jiang, *Adv. Healthc. Mater.* **2013**, *2*, 95.

(195) W. Zheng, Y. Jia, W. Chen, G. Wang, X. Guo, X. Jiang, *ACS Appl. Mater. Interfaces* **2017**, *9*, 21181.

(196) X. Fan, S. Zhang, Y. Zhu, J. Chen, *RSC Adv.* **2018**, *8*, 10141.

(197) X. Hu, P. Cebe, A. S. Weiss, F. Omenetto, D. L. Kaplan, *Mater. Today* **2012**, *15*, 208.

(198) X. L. Qi, C. Holt, D. Mcnulty, D. T. Clarke, S. Brownlow, G. R. Jones, *Biochem. J.* **1997**, *324*, 341 LP.

(199) X. Li, S. M. Robinson, A. Gupta, K. Saha, Z. Jiang, D. F. Moyano, A. Sahar, M. A. Riley, V. M. Rotello, *ACS Nano* **2014**, *8*, 10682.

(200) X. Li, Y.-C. Yeh, K. Giri, R. Mout, R. F. Landis, Y. S. Prakash, V. M. Rotello, *Chem. Commun.* **2015**, *51*, 282.

(201) X. Wang, X. Zhang, J. Castellot, I. Herman, M. Iafrati, D. L. Kaplan, *Biomaterials* **2008**, *29*, 894.

(202) X. Yang, L. Tan, L. Xia, C. D. Wood, B. Tan, *Macromol. Rapid Commun.* **2015**, *36*, 1553.

(203) Y. Har-el, J. A. Gerstenhaber, R. Brodsky, R. B. Huneke, P. I. Lelkes, *Wound Med.* **2014**, *5*, 9.

(204) Y. Jang, J. A. Champion, *Acc. Chem. Res.* **2016**, *49*, 2188.

(205) Y. Kambe, K. Kojima, Y. Tamada, N. Tomita, T. Kameda, *J. Biomed. Mater. Res. Part A* **2016**, *104*, 82.

(206) Y. Lin, K. Liu, C. Wang, L. Li, Y. Liu, *Anal. Chem.* **2015**, *87*, 8047.

(207) Y. S. Choi, S. R. Hong, Y. M. Lee, K. W. Song, M. H. Park, Y. S. Nam, *Biomaterials* **1999**, *20*, 409.

(208) Y. Shon, H. Kim, H. S. Hwang, E. S. Bae, T. Eom, E. J. Park, W.-S. Ahn, J. J. Wie, B. S. Shim, *Sensors Actuators B Chem.* **2017**, *244*, 1.

(209) Y. Sun, Y. Huang, *J. Mater. Chem. B* **2016**, *4*, 2768.

(210) Y. Wang, X. Mo, X. S. Sun, D. Wang, *J. Appl. Polym. Sci.* **2007**, *104*, 130.

(211) Y. Z. Zhang, J. Venugopal, Z.-M. Huang, C. T. Lim, S. Ramakrishna, *Polymer* **2006**, *47*, 2911.

(212) Y. Zhao, Q. Jiang, H. Xu, N. Reddy, L. Xu, Y. Yang, *J. Biomed. Mater. Res. Part B Appl. Biomater.* **2014**, *102*, 729.

(213) Y.-C. Chen, H.-C. Yu, C.-Y. Huang, W.-L. Chung, S.-L. Wu, Y.-K. Su, *Sci. Rep.* **2015**, *5*, 10022.

(214) Z. Al-Hamamre, M. Saidan, M. Hararah, K. Rawajfeh, H. E. Alkhasawneh, M. Al-Shannag, *Renew. Sustain. Energy Rev.* **2017**, *67*, 295.

(215) Z. Peles, M. Zilberman, *Acta Biomater.* **2012**, *8*, 209.

(216) Z. Ustunol, B. mert, *J. Food Sci.* **2006**, *69*, FEP129.